TARGETING AND INHIBITION OF TUMOR-ASSOCIATED MACROPHAGES IN BREAST CANCER

KARIN BINNEMARS-POSTMA

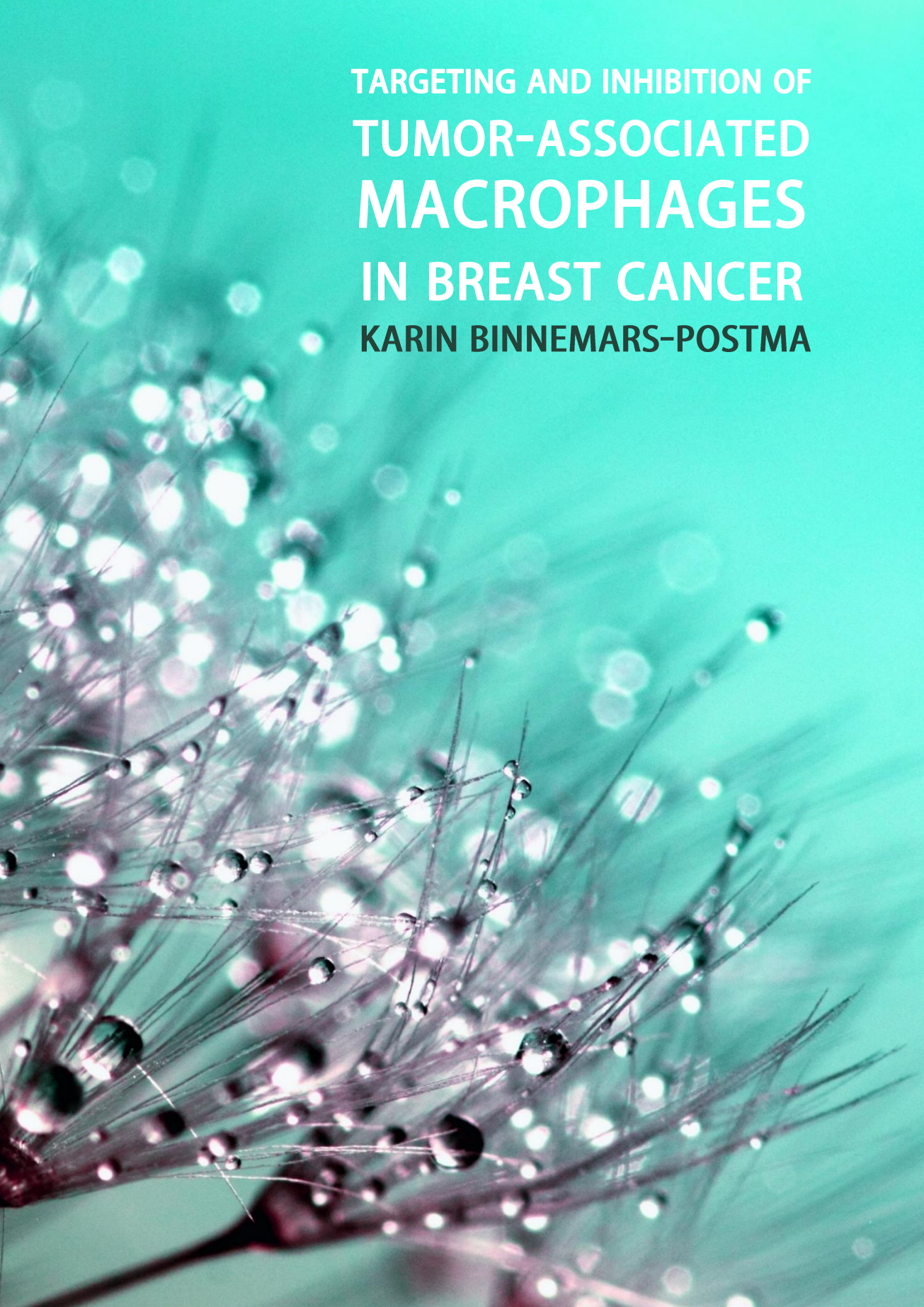

TARGETING AND INHIBITION OF TUMOR-ASSOCIATED MACROPHAGES IN BREAST CANCER

KARIN BINNEMARS-POSTMA

Samenstelling van de commissie

Voorzitter	Prof. Dr. Ir. J.W.M. Hilgenkamp	Universiteit Twente
Promotor	Prof. Dr. G. Storm	Universiteit Twente
Co-promotor	Dr. J. Prakash	Universiteit Twente
Leden:	Prof. Dr. H.B.J. Karperien	Universiteit Twente
	Prof. Dr. P.C.J.J. Passier	Universiteit Twente
	Prof. Dr. R. Schiffelers	Universitair Medisch Centrum Utrecht
	Prof. Dr. M.P.J. de Winther	Amsterdam Medisch Centrum
	Dr. P. van Hoogevest	Dir. Lipoid GmbH, Phospholipid Research center
	Dr. J.M. Metselaar	Algemeen Directeur Enceladus, Naarden

The research was supported by the University of Twente and this thesis has received funding from the Phospholipid Research Institute.

UNIVERSITY OF TWENTE.

Phospholipid
Forschungszentrum/Research Center
Heidelberg

The studies in this thesis have been carried out at University of Twente, MIRA Institute for Biomedical Technology and Technical Medicine.

UNIVERSITY OF TWENTE.

MIRA
BIOMEDICAL TECHNOLOGY
AND TECHNICAL MEDICINE

The printing of this thesis was financially supported by the Faculty of Science and Technology, University of Twente, Enschede, The Netherlands.

Title: Targeting and Inhibition of Tumor-Associated Macrophages in Breast Cancer
Author: Karin Antje Binnemars-Postma
ISBN: 978-90-365-4462-7
DOI: 10.3990/1.9789036544627

Cover design by Karin Binnemars-Postma and Inspiredimages
Printed by Ipskamp printing

TARGETING AND INHIBITION OF TUMOR-ASSOCIATED MACROPHAGES IN BREAST CANCER

PROEFSCHRIFT

Ter verkrijging van
de graad van doctor aan de Universiteit van Twente,
op gezag van de rector magnificus,
Prof. Dr. T.T.M. Palstra
volgens besluit van het College voor Promoties
in het openbaar te verdedigen
op donderdag 18 januari 2018 om 14.45 uur

door

Karin Antje Binnemars-Postma

geboren op 6 juni 1987
te Dantumadeel, Nederland

Dit proefschrift is goedgekeurd door:

Prof. Dr. G. Storm (Promotor)

Dr. J. Prakash (Co-promotor)

Voor mijn lieve man en zoontje

TABLE OF CONTENTS

Chapter 1

Introduction, Aim and Outline

1 Introduction

Breast cancer is the most occurring type of cancer and the leading cause of cancer-related deaths in women in Europe [1]. In 2012, 464.000 new cases of breast cancer were diagnosed, while 131.000 deaths were the result of this devastating disease [1]. As a result of the aging of the population, breast cancer occurrence and related mortality are expected to increase. Current therapies are aimed at the treatment of the primary tumor, by using cytotoxic agents, hormone treatment, radiation and small molecular inhibitors [2]. Tumor growth and metastasis depend strongly on the support of the tumor micro-environment (TME), where stromal cells, such as macrophages, fibroblasts, myeloid derived suppressor cells promote neo-angiogenesis and matrix remodeling, as well as cause suppression of the adaptive immune system [3, 4]. Macrophages play a major role in these processes.

Macrophages are phagocytic cells of the immune system and display a wide range of different functionalities. Monocytes are attracted from the circulation into tissues, where they become mature macrophages and display different phenotypes, depending on the stimuli they receive from the local environment [5, 6]. They may be described as 'classically activated' M1 macrophages or 'alternatively activated' M2 macrophages [7, 8]. M1 macrophages are involved in acute inflammation, where they are responsible for the detection and killing of pathogens [9, 10]. Activated by bacterial products (*e.g.* lipopolysaccharide (LPS)) and T-helper cell type 1 (Th1) cytokines (*e.g.* interferon-γ (IFN-γ)), they secrete pro-inflammatory cytokines (interleukin IL-12 and IL-23), release nitric oxide (NO) and reactive oxygen species (ROS), present antigens and stimulate the Th1 response. Due to these functions, M1 macrophages are not only proficient in the resolution of bacterial infections, but also effective in recognizing and eliminating tumor cells [6, 7, 11, 12]. In contrast, M2 macrophages are involved in wound healing, allergies and the removal of parasites [13]. IL-4 and IL-13, originating from Th2 cells, differentiate macrophages towards the M2 phenotype [14]. Upon differentiation, these cells release immunosuppressive cytokines (*e.g.* IL-10) and components necessary for collagen synthesis and cellular proliferation [15]. During tumor development, macrophages are attracted to the TME or differentiate from resident macrophages

(under influence of cytokines within the TME, *i.e.* IL-4 and IL-13) into M2-like tumor-associated macrophages (TAM). Due to their immunosuppressive and wound healing properties, they facilitate tumor growth and metastasis [6, 12, 16-18]. In tumors, high numbers of infiltrating TAM have been associated with increased risk of metastasis, as well as a decrease in disease-free and overall survival [19]. As indicated by the persuasive evidence on the adverse effects on tumor growth and metastasis, the selective targeting and treatment of TAM may prove to be an effective strategy in cancer therapy.

2 Aim and Outline

The aim of this thesis is to develop a novel nanoparticle-based strategy to target and inhibit TAM. Macrophages exist as different populations, such as Kupffer cells in the liver and microglia in the brain [20], which perform critical functions in homeostasis, and more importantly – in the context of this thesis – as M1 macrophages, which show anti-tumor activities [12]. To exploit the latter activities, it is necessary to selectively target TAM, in order to retain the beneficial functions of other macrophage populations. One way of selectively treating TAM, is to utilize mechanisms which are specifically active in this macrophage population. In **Chapter 2**, the role of TAM in tumor development is discussed in detail. We also provide an overview of the current literature on therapies used in the treatment of TAM.

Another method to selectively target TAM, is the use of nanomedicine. Since macrophages are a part of the mononuclear phagocyte system (MPS), they play a major role in the clearance of foreign particles from the body [21]. When nanoparticles are introduced into the circulation, macrophages will recognize, internalize and degrade them [22, 23]. Using the passive targeting approach, nanoparticles may be used to target macrophages. However, when using this approach, targeting specific macrophage populations remains a challenge. Active targeting, by using particles which are inherently recognized by TAM or are modified with ligands against TAM receptors, may increase targeting specificity. In chapter 2 we provide an overview of the current state of the art regarding nanoparticles and nanoparticle modifications used in TAM targeting.

In **Chapter 3**, we started to expand our knowledge on the intrinsic nature of macrophage populations to phagocytose nanoparticles. In

order to target specific macrophage populations, in this chapter, we investigated the uptake behavior of different macrophage populations, by changing particle size and incubation conditions. Here, the innate ability of M1 and M2 (TAM) macrophages to phagocytose different sizes of particles (silica, 50 – 1000 nm), under different conditions was studied. Moreover, the effect of serum proteins on nanoparticle uptake was evaluated. Using gene expression analysis, differences in expression of phagocytosis-related genes between M1 and M2 cells were investigated. These findings were subsequently linked to results derived from the analysis of the composition of the protein corona.

As shown in chapter 3, M2 macrophages displayed a number of upregulated phagocytic receptors. We observed that amongst these receptors, cluster of differentiation 36 (CD36), scavenger receptor class B1 (Scarb1) and collectin subfamily member 12 (Colec12) were involved in the recognition of oxidized lipids. Using this data, in **Chapter 4**, we explored the possibility of targeting these receptors using carboxylated lipids (CyPC) incorporated into liposomes. *In vitro*, the specific uptake of CyPC-containing liposomes was investigated in M1 and M2 macrophages. *In vivo*, tumor uptake and organ distribution (liver and spleen) were evaluated. Analysis of tumor tissues was performed to investigate co-localization of liposomes with M2 macrophage marker CD206 positive cells. Further analysis of the uptake mechanism was investigated by silencing specific genes and assessing their influence on the M2-macrophage specific uptake of CyPC-containing liposomes.

Next to targeting, we investigated in **Chapter 5** the novel drug AS1517499 for the treatment of TAM. After binding of IL-4 and IL-13 to their corresponding receptors, the signal transducer and activator of transcription 6 (Stat6) becomes activated and regulates the gene transcription of M2-associated genes [8, 24-26]. We investigated the role of Stat6 in macrophage polarization. Activation of Stat6 was investigated in different cell types and differentiation states. The effect of gene silencing of Stat6 on macrophage differentiation was evaluated. To pharmacologically inhibit Stat6 activation and subsequently TAM differentiation, the specific Stat6 inhibitor AS1517499 was used. *In vivo*, the effect and mechanism of action of this inhibitor on tumor growth and metastasis was investigated.

In chapter 5 we confirmed that the selective Stat6 inhibitor AS1517499 is effective in reducing tumor growth and metastasis. In **Chapter 6**, AS1517499 was incorporated into CyPC-containing liposomes (Figure 1). Pharmaceutical characteristics, such as drug loading, size distribution and stability were evaluated as well as effects on macrophage targeting and treatment *in vitro*. In this chapter, we take the first step to combining AS1517499 into a nanoparticle delivery vehicle for the effective targeting and modulation of TAM.

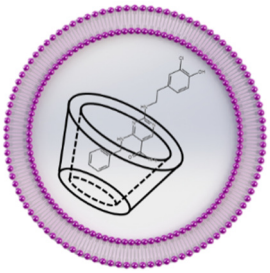

Figure 1: Graphical representation of AS1517499 incorporation into liposomes, facilitated by cyclodextrins

In **Chapter 7**, the results from all chapters are summarized and future perspectives are provided.

References

1. Ferlay, J., et al., Cancer incidence and mortality patterns in Europe: estimates for 40 countries in 2012. Eur J Cancer, 2013. **49**(6): p. 1374-403.
2. Robinson, A.G., C.M. Booth, and E.A. Eisenhauer, Progression-free survival as an end-point in solid tumours--perspectives from clinical trials and clinical practice. Eur J Cancer, 2014. **50**(13): p. 2303-8.
3. Quail, D.F. and J.A. Joyce, Microenvironmental regulation of tumor progression and metastasis. Nat Med, 2013. **19**(11): p. 1423-37.
4. Mantovani, A., et al., Cancer-related inflammation. Nature, 2008. **454**(7203): p. 436-44.
5. Sica, A., et al., Macrophage polarization in pathology. Cell Mol Life Sci, 2015. **72**(21): p. 4111-26.
6. Sica, A., et al., Tumour-associated macrophages are a distinct M2 polarised population promoting tumour progression: potential targets of anti-cancer therapy. Eur J Cancer, 2006. **42**(6): p. 717-27.
7. Biswas, S.K. and A. Mantovani, Macrophage plasticity and interaction with lymphocyte subsets: cancer as a paradigm. Nat Immunol, 2010. **11**(10): p. 889-96.
8. Sica, A. and A. Mantovani, Macrophage plasticity and polarization: in vivo veritas. J Clin Invest, 2012. **122**(3): p. 787-95.
9. Martinez, F.O. and S. Gordon, The M1 and M2 paradigm of macrophage activation: time for reassessment. F1000Prime Rep, 2014. **6**: p. 13.
10. Nau, G.J., et al., Human macrophage activation programs induced by bacterial pathogens. Proc Natl Acad Sci U S A, 2002. **99**(3): p. 1503-8.
11. Mills, C.D., M1 and M2 Macrophages: Oracles of Health and Disease. Crit Rev Immunol, 2012. **32**(6): p. 463-88.
12. Allavena, P. and A. Mantovani, Immunology in the clinic review series; focus on cancer: tumour-associated macrophages: undisputed stars of the inflammatory tumour microenvironment. Clin Exp Immunol, 2012. **167**(2): p. 195-205.
13. Mantovani, A., et al., Macrophage plasticity and polarization in tissue repair and remodelling. J Pathol, 2013. **229**(2): p. 176-85.
14. Heusinkveld, M. and S.H. van der Burg, Identification and manipulation of tumor associated macrophages in human cancers. J Transl Med, 2011. **9**: p. 216.

15. Hao, N.B., et al., Macrophages in tumor microenvironments and the progression of tumors. Clin Dev Immunol, 2012. **2012**: p. 948098.
16. Sica, A., et al., Autocrine production of IL-10 mediates defective IL-12 production and NF-kappa B activation in tumor-associated macrophages. J Immunol, 2000. **164**(2): p. 762-7.
17. Biswas, S.K., P. Allavena, and A. Mantovani, Tumor-associated macrophages: functional diversity, clinical significance, and open questions. Semin Immunopathol, 2013. **35**(5): p. 585-600.
18. Qian, B.Z. and J.W. Pollard, Macrophage diversity enhances tumor progression and metastasis. Cell, 2010. **141**(1): p. 39-51.
19. Yuan, Z.Y., et al., High infiltration of tumor-associated macrophages in triple-negative breast cancer is associated with a higher risk of distant metastasis. Onco Targets Ther, 2014. **7**: p. 1475-80.
20. Epelman, S., K.J. Lavine, and G.J. Randolph, Origin and functions of tissue macrophages. Immunity, 2014. **41**(1): p. 21-35.
21. Flannagan, R.S., V. Jaumouille, and S. Grinstein, The cell biology of phagocytosis. Annu Rev Pathol, 2012. **7**: p. 61-98.
22. Alexis, F., et al., Factors affecting the clearance and biodistribution of polymeric nanoparticles. Molecular Pharmaceutics, 2008. **5**(4): p. 505-15.
23. Haniffa, M., V. Bigley, and M. Collin, Human mononuclear phagocyte system reunited. Semin Cell Dev Biol, 2015.
24. Nelms, K., et al., The IL-4 receptor: signaling mechanisms and biologic functions. Annu Rev Immunol, 1999. **17**: p. 701-38.
25. Wang, N., H. Liang, and K. Zen, Molecular mechanisms that influence the macrophage m1-m2 polarization balance. Front Immunol, 2014. **5**: p. 614.
26. Pauleau, A.L., et al., Enhancer-mediated control of macrophage-specific arginase I expression. J Immunol, 2004. **172**(12): p. 7565-73.

CHAPTER 2

NANOMEDICINE STRATEGIES TO TARGET TUMOR-ASSOCIATED MACROPHAGES

Published: Int J Mol Sci. 2017 May 4;18(5)

Abstract

In recent years, the influence of the tumor microenvironment (TME) on cancer progression has been better understood. Macrophages, one of the most important cell types in the TME, exist in different subtypes, each of which has a different function. While classically activated M1 macrophages are involved in inflammatory and malignant processes, activated M2 macrophages are more involved in the wound-healing processes occurring in tumors. Tumor-associated macrophages (TAM) display M2 macrophage characteristics and support tumor growth and metastasis by matrix remodeling, neo-angiogenesis, and suppressing local immunity. Due to their detrimental role in tumor growth and metastasis, selective targeting of TAM for the treatment of cancer may prove to be beneficial in the treatment of cancer. Due to the plastic nature of macrophages, their activities may be altered to inhibit tumor growth. In this review, we will discuss the therapeutic options for the modulation and targeting of TAM. Different therapeutic strategies to deplete, inhibit recruitment of, or re-educate TAM will be discussed. Current strategies for the targeting of TAM using nanomedicine are reviewed. Passive targeting using different nanoparticle systems is described. Since TAM display a number of upregulated surface proteins compared to non-TAM, specific targeting using targeting ligands coupled to nanoparticles is discussed in detail.

1 Introduction

As long ago as 1863, Rudolf Virchow noticed leukocytic infiltration in neoplastic regions; he was the first to link inflammation to cancer [1]. During tumor progression, not only are the malignant cells characterized by genetic mutations, but the tumor stroma, consisting of the extracellular matrix (ECM) and cells within it, is also known to play a crucial role in this process [2,3]. Due to the resemblance of tumor stroma to the granulation tissue formed during wound healing, tumors were described as "wounds that never heal" by Hal Dvorak [4]. In recent years, our understanding of the cross-talk between malignant cells and the tumor stroma has greatly increased. The inflammatory process caused by the tumor cells and the surrounding stroma has been shown to promote tumor growth and progression [2,3,5]. Since the tumor stroma cells are more genetically stable than malignant cells, they represent promising targets for therapeutic intervention. This review provides a summary of state-of-the-art technologies for the treatment and nanoparticle-based targeting of tumor-associated macrophages (TAM).

2 Stromal inflammation

A major drive for tumor progression is the inflammatory process that can originate from intrinsic or extrinsic pathways. In the intrinsic pathway, genetic mutations cause oncogene activation, while the extrinsic pathway includes external stimuli, such as infection or chemical insult. Chronic inflammation creates an environment that increases malignant transformation, either by causing DNA damage and impeding DNA repair, or by inducing mutations and proliferation of already mutated cells [6]. These inflammatory processes can take place at specific sites of the body, for example in the colon, where inflammatory bowel disease increases the risk of developing malignancies. Studies have suggested that inhibition of the inflammatory process may reduce the risk of developing cancer [7,8,9].

The course of immune cell infiltration and activation of stromal cells leading to cancer-related inflammation is intricate. Many different cell types (mainly macrophages, dendritic cells, neutrophils, fibroblasts, and T-cells), and tumor cells themselves, play crucial roles in regulating this process. In solid tumors, tumor cells produce

transcription factors like NF-κB, signal transducer and activator of transcription 3 (STAT3), and hypoxia-inducible factor 1α (HIF-1α), all of which have a profound effect on the recruitment, differentiation, and maturation of infiltrating leukocytes [10]. Moreover, tumor cells produce chemokines (such as chemokine C–C motif 2 (CCL2), -7 and -8) and cytokines, which attract inflammatory cells to the tumor site [11]. Macrophages, whether resident or recruited, due to the local cytokine environment, acquire the TAM phenotype, stimulating tumor survival, growth, and metastasis [10,11,12,13]. Macrophage and TAM biology will be discussed in more detail below.

Only in the last few years has the role of neutrophils in tumor progression been illustrated, although the relationship between circulating neutrophil numbers and poor prognosis has been established for years [14]. There are different phenotypes for neutrophils: the antitumor N1 phenotype and the protumoral N2 phenotype [15]. During early tumor development, N2 neutrophils promote angiogenesis and subsequently support tumor growth and invasion by remodeling the ECM [15,16,17,18].

3 Macrophage polarization

Macrophages are commonly known phagocytic cells that can display various kinds of functional activities depending on their polarization state. They are one of the most plastic cell types known so far. Resident macrophages in tissues can display a high range of phenotypes, such as Kupffer cells in the liver, microglia in brain, alveolar macrophages in lungs, and peritoneal macrophages in the gut [19,20,21]. During inflammation, infiltrated monocytes derived from the bloodstream transform into mature macrophages in specific tissues. These macrophages may transform into either classically activated (M1) macrophages, which have pro-inflammatory properties in general, or become alternatively activated (M2) macrophages, which show anti-inflammatory and tumor-promoting capabilities [13]. The polarization state is largely dependent on the cues they receive from the local microenvironment [22]. The M1 and M2 nomenclature mirrors that of T helper cell type 1 and T helper cell type 2 (Th1 and Th2), since these cells differentially produce interferon-γ (IFN-γ) and intereukin (IL)-4, cytokines that are important in the polarization of M1 and M2 types, respectively [20]. Macrophages are often classified as either M1 or M2

cells, but these represent extremes in a system of continuous functional states. They usually display a phenotype somewhere in between M1 or M2, and for this reason they are more correctly described as either M1-like or M2-like macrophages. Here, for the sake of simplicity we will refer to them as M1 or M2 macrophages. Below, we discuss the M1 and M2 phenotypes in more detail.

3.1 M1 macrophages

Classically activated or M1 macrophages are involved in the resolution of bacterial infection and exert anti-tumor activities. These macrophages display pattern recognition receptors, such as toll-like receptors (TLRs), which are able to recognize bacterial patterns, including lipopolysaccharide (LPS), muramyl peptide, and lipoteichoic acid [23,24]. Macrophages can become polarized by these bacterial products, but also by cytokines secreted by Th1 cells (*e.g.*, IFN-γ). Following activation, M1 macrophages stimulate the adaptive immune response by releasing the pro-inflammatory cytokines IL-1, IL-6, IL-12, IL-23, and tumor necrosis factor-α (TNF-α). M1 macrophages can also be recognized by their different metabolism, *e.g.*, arginine is metabolized by inducible nitric oxide synthase (iNOS), producing nitric oxide (NO), which has cytotoxic effects [12,25]. There are no characteristic receptors that are able to mark macrophages as the M1 phenotype, but they do overexpress certain receptors, *e.g.*, cluster of differentiation (CD) 16, CD86, CD80, IL-1R I, major histocompatibility complex class II (MHC II), TLR2, and TLR4 [26]. They are sometimes characterized by the cytokines which they secrete, marking them by their IL-10^{low}, IL-12^{high} profile [27]. M1 macrophages, either activated by bacterial products or IFN-γ, display high antigen presentation and high pro-inflammatory cytokine (*e.g.*, IL-12 and IL-23) production, which stimulates the Th1 response. Moreover, they are able to produce high amounts of toxic intermediates (NO) and reactive oxygen species (ROS)), which allows M1 macrophages to be potent effector cells in killing microbes and tumor cells [13,28,29,30].

3.2 M2 macrophages

Unlike M1 macrophages, alternatively activated or M2 macrophages are involved in the wound healing process, allergies, and the killing of parasites, and they display pro-tumoral activities. Th2 cells elicit the stimuli (*e.g.*, IL-4, IL-13) that are needed to polarize macrophages

towards M2 phenotype. Upon differentiation, M2 cells display many receptors that are rather specific, *e.g.*, decoy IL-1R II receptor, the macrophage scavenging receptor I (CD204), the mannose receptor (CD206), and the hemoglobin scavenger receptor (CD163) [26]. Also, because of the presence of arginase in these cells, arginine is not metabolized towards NO but to ornithine and polyamines, which are necessary for collagen synthesis and cellular proliferation [27]. M2 cells generally have a low production of pro-inflammatory cytokines, while they produce large amounts of IL-10 (IL-10^{high}, IL-12^{low}) [13,31,32].

Besides the normal M2 macrophages, there are also macrophages that have an "M2d state" following stimulation by immune complexes, LPS, or glucocorticosteroids [20,23]. These cells share some of the characteristics of M2 macrophages, but also produce cytokines such as IL-1 and IL-6, normally seen in M1 cells [20,23].

4 Tumor-associated macrophages

Tumor-associated macrophages (TAM) are key tumor stromal cell types and play a critical role in tumor survival, growth, and metastasis [10]. TAM may either originate from resident macrophages or are attracted from the bone marrow and spleen to the tumor site by the CCL2 (also known as monocyte chemoattractant protein-1 (MCP-1)). TAM are often compared to M2 macrophages. Indeed, they display characteristics of the M2 phenotype, sharing functions such as matrix remodeling, promoting angiogenesis, suppressing inflammation, and secreting growth factors [13]. Numerous investigations have shown a positive correlation between macrophage numbers and prognosis, both in human and murine malignancies [33,34,35]. The cytokine profile (macrophage colony stimulating factor (M-CSF), IL-4, IL-13, IL-10, Prostaglandin E2 (PGE2)) that is present in the tumor microenvironmentTME polarizes these macrophages and as a result they display pro-tumoral functions. Recently it has been shown that lactic acid, a byproduct of anaerobic glycolysis in tumor cells under hypoxic conditions, induces the gene expression of Vegf and Arg-1 in TAM. This effect was mediated by HIF-1α. The lactate-induced expression of Arginase-1 was shown to induce tumor growth [36]. Following acquisition of the TAM phenotype, these macrophages

display a number of functions that generally lead to pro-tumoral effects, as detailed below.

4.1 Suppression of adaptive immunity

Suppression of the adaptive immune system is achieved by TAM through various mechanisms. TAM lack the proper ability for antigen presentation, making them unsuitable for eliciting an immune response by other immune cells. TAM also secrete anti-inflammatory cytokines such as IL-10 and TGF-β, while being unable to secrete the pro-inflammatory cytokine IL-12, a lack of which leads to induction of T-regulatory (Treg) cells. This in turn suppresses the activity of effector T-cells and other immune cells such as monocytes [13,37]. A possible regulator in these processes is STAT3, which is overactivated in TAM [38]. ROS have also been shown to play a critical role in macrophage differentiation. Recently, it has been shown that pretreatment of monocytes with the antioxidant butylated hydroxyanisole inhibits polarization of monocytes towards the M2 type, but not the M1 type, suggesting that ROS are necessary for the polarization of monocytes towards the M2 type [39]. Following differentiation, monocytes produce superoxide (O^{2-}), which is needed for the biphasic activation of the ERK pathway, a critical pathway in macrophage differentiation [39].

4.2 Matrix remodeling, tumor invasion and metastasis

The prognosis of patients with high numbers of infiltrating macrophages in primary tumors is unfavorable: in triple negative breast cancer, TAM infiltration was quantified using immunohistochemical staining for CD68. High numbers of infiltrating macrophages are associated with a significantly higher risk of distant metastasis, as well as a decreased disease-free and overall survival [40]. In endometrial adenocarcinoma, the presence of TAM was associated with advanced disease staging, high tumor grade, increased lymph vessel density, lymphovascular space invasion, and lymph node metastasis [41]. There is mounting evidence that TAM play a critical role in tumor invasion and metastasis [12,42,43]. In the mouse mammary tumor virus-driven polyomavirus middle T antigen (MMTV–PyMT) model of mammary carcinogenesis, in macrophage-deficient mice, tumor progression and metastasis were significantly delayed [44].

One of the most important mechanisms of tumor cell migration, induced by macrophages, has been elucidated in the past: it was shown that in *in vivo* experiments macrophages and tumor cells were both able to migrate to stimuli specific for only one of the cell types (*i.e.*, colony-stimulating factor-1 (CSF-1) for macrophages and epidermal growth factor (EGF) for tumor cells), indicating the existence of a paracrine loop, leading to a synergistic relationship between migration of both macrophages and tumor cells [45]. Indeed, tumor cells produce CSF-1, which induces migration of macrophages. Macrophages in turn, produce EGF, which leads to tumor cell migration [45,46]. An important biological barrier in invasion and metastasis is the basement membrane. During cancer progression, this membrane is degraded by proteolytic enzymes. Matrix metalloproteinases (MMPs) are a class of proteases that play an important role in this process. Macrophages are able to produce a variety of MMPs, such as MMP-1, -2, -7, -9, and -12 in a TNF-α-dependent manner [47]. The ECM also plays an important role in tumor cell invasion. During mammary gland development, macrophages have been shown to promote collagen fibrillogenesis [48]. Fibrillar collagen 1 facilitates the movement of macrophages and tumor cells, at up to 10 times the speed at which they would move through the tumor stroma [49]. As these collagenous fibrils anchor easily to blood vessels, tumor cells are guided towards them, making it possible for tumor cells to escape via the vasculature [43,49].

4.3 Neo-angiogenesis

HIF play an important role in macrophage recruitment and angiogenesis. Due to rapid growth, tumors are prone to develop hypoxic areas. In an HIF-dependent manner, vascular endothelial growth factor (VEGF), C–X–C motif chemokine ligand-12 (CXCL12) and C–X–C chemokine receptor-4 (CXCR4) attract macrophages to these hypoxic areas [10]. This leads to the activation of a pro-angiogenic program: increased expression of VEGF, basic fibroblast growth factor (bFGF), and CXCL8, also regulated by HIF-1 and 2 [13]. Although macrophages themselves can be a source of VEGF, it is also released from the ECM by ECM degradation caused by macrophage-derived MMP-9 [50]. Casazza *et al.* showed that hypoxia-induced Sema3A acts as a chemo attractant for TAM through the neuropilin-1 (Nrp-1) and PlexinA1/PlexinA4 receptor complex. They demonstrated that Nrp-1 is downregulated in hypoxic areas, but stop signals were still

produced via signaling by Sema3A through the PlexinA1/PlexinA4 complex. This resulted in trapping of the recruited TAM in the hypoxic tumor regions. Interestingly, deletion of the Nrp-1 gene in macrophages resulted in the retention of macrophages in normoxic areas, subsequently leading to diminished pro-angiogenic and immunosuppressive functions. This study concluded that localization of macrophages, regulated by Sema3A/Nrp-1 signaling, plays an important role in their functional states [51]. In addition to degrading the basement membranes and ECM, TAM provide activated endothelial cells with an environment (via increased availability of VEGF and production of CXLC-1, -2, and -8), in which they can migrate, proliferate, and form new blood vessels [52,53,54].

5 Targeting strategies and active agents

Proximity of TAM to the TME is necessary for TAM to maintain their tumor-promoting functions. Several strategies have been proposed in literature to reduce the tumor-promoting functions of TAM:

- Inhibiting macrophage recruitment;
- Reprogramming TAM towards a more anti-tumoral phenotype;
- Initiation of immune response;
- Blocking the tumor-promoting functions of TAM;
- Depletion of TAM.

5.1 Inhibiting macrophage recruitment

Inhibition of macrophage infiltration can be accomplished at two levels: (1) preventing chemo-attractants secreted by the tumor cells to recruit macrophages; or (2) blocking of macrophage surface receptors, thereby effectively preventing signal transduction or adhesion to be established.

CCL2 is involved in the recruitment of monocytes to the tumor site. Several small molecular inhibitors and antibodies against this protein have been used in various types of cancer. The small molecule inhibitor Bindarit has been reported to be effective in reducing tumor growth and macrophage recruitment in CCL2-positive melanoma [55]. Another approach is to block the receptor for CCL2, *i.e.*, the C–C motif chemokine receptor 2 (CCR2). A small molecule inhibitor (RS102895) was found to be effective in inhibiting macrophage migration. In addition, two monoclonal antibodies (Carlumab and MLN1202)

directed against CCL2/CCR2 are currently under investigation for their effectiveness in treating cancer [56,57,58]. Furthermore, an antibody against CD11b was used in a mouse squamous cell carcinoma xenograft model [59]. CD11b is the α-subunit of the CD18 integrin, which is expressed on both granulocytes and macrophages. This subunit has been shown to be involved in the adhesion, migration, and chemotaxis of myeloid cells [60]. In this study, the authors showed that, by administering CD11b antibodies, they inhibited the recruitment of myeloid cells into the xenografts and improved the response to irradiation [59]. A recent development for preventing macrophage recruitment is the use of inhibitors for the colony-stimulating factor receptor-1 (CSF-1R): PLX3397, BLZ945, and GW2580 [61,62,63,64]. PLX3397 showed reduction in macrophage infiltration in tumors in mouse models for neurofibroma, melanoma, gastrointestinal stromal tumors and malignant peripheral nerve sheath tumors, thereby reducing tumor growth [61,65,66,67]. The inhibitor BLZ945 was tested in a mouse model for glioblastoma multiforme. Surprisingly, TAMs were not depleted, but their survival was facilitated by IFN-γ and granulocyte macrophage colony stimulating factor (GM-CSF), while M2 markers decreased in surviving TAMs [64]. A third CSF-1R antagonist GW2580 was tested in combination therapy. Simultaneous treatment with gemcitabine augmented the effect of chemotherapy [63]. Next to small molecular inhibitors, the monoclonal antibody RG7155 has also been found to profoundly affect tumor macrophage populations. In a phase I clinical trial of patients suffering non-diffuse giant cell tumors, dose escalation studies have shown a compelling decline in $CSF\text{-}1R^{+}/CD163^{+}$ macrophages, which translated into clinical objective responses [68]. Currently, this antibody is investigated in phase 1a/1b clinical trials as monotherapy or in combination with other cancer immunotherapy agents [69].

5.2 Reprogramming and blocking tumor-promoting functions of TAM and initiating immune response

Even though TAM exhibit tumor-promoting M2 characteristics, studies have shown that, depending on the cytokines present, they can be reprogrammed towards the tumoricidal M1-like phenotype [64,70]. Introducing Th1-cytokines or interfering in the transcription pathway leading to M2 macrophages are promising ways to modulate macrophage polarization. Another way for reprogramming is

activation of the NF-κB pathway via the introduction of TLR-agonists [71]. These receptors play a major role in the innate immune system via pattern recognition of pathogens and inducing a Th1 response. In addition to introducing Th1 cytokines or ligands for TLRs, stimulating the immune response by activating co-stimulatory proteins such as CD40 has shown promising results [72,73,74]. Recently, a clinical trial using the fully humanized CD40 agonist antibody in combination with gemcitabine treatment in advanced pancreatic cancer was completed [72]. In this trial, the authors observed a partial clinical effect, the mechanism of which was later elucidated in a murine model for pancreatic cancer, where they found a modified macrophage phenotype, with increased MHC class II and CD86 expression [72]. In another study, CD40 agonist antibodies were combined with immunostimulatory CpG oligodeoxynucleotides in a model for murine multiple melanoma. Here, due to co-stimulation, macrophages were activated towards the M1 phenotype and a strong increase in IL-12 production was observed [75]. Indeed, restoring M1 macrophage functionality in tumors relieves the immunosuppressive environment and allows other effector immune cells to be recruited [76].

Other than monoclonal antibodies, Tasquinimod, a small molecule inhibitor of S100A9 and HDAC4, both important signaling molecules in the TME, used in the treatment of prostate cancer was investigated for its effects on TAM [77]. This inhibitor was found to increase the secreted amount of intra-tumoral IL-12, which resulted in a decrease of neo-vascularization and TAM infiltration as well as an increase in M1 macrophages. Furthermore, another study showed that a combination of Tasquinimod with an immunotherapy resulted in decreased M2-polarized macrophages and increased immune response [78]. Another molecule which inhibits macrophage polarization is 4-iodo-6-phenylpyrimidine (4-IPP), an inhibitor of macrophage migration inhibitory factor (MIF). MIF, both excreted by tumor cells and macrophages, has been linked to tumor promotion in paracrine and autocrine manners [79,80,81]. In melanoma-bearing mice, administration of 4-IPP led to attenuated TAM polarization, immunosuppression, neo-angiogenesis and melanoma outgrowth, offering MIF inhibition as an interesting target for further investigation [81].

In addition to preventing macrophage recruitment and reprogramming towards the tumoricidal phenotype, the prevention of M2 TAM formation has been investigated. One of the signaling pathways that, upon activation, causes M2 differentiation is the STAT3 pathway. The role of STAT3 in TAM as an important target for cancer immunotherapy was first described by Cheng *et al.* They showed that the disruption of the STAT3 pathway restored the responsiveness of immunotolerant T-cells from tumor-bearing mice [82]. Since then, many drugs have been used to inhibit the STAT3 pathway, including the clinically used kinase inhibitors sorafenib and sunitinib [83,84].

Another pathway involved in the differentiation towards M2 macrophages is the STAT6 pathway. Following binding of the M2-inducing cytokines IL-4 and IL-13 to their receptors, STAT6 becomes phosphorylated via Janus kinases (JAKs) and translocates to the nucleus, where it acts as a transcription factor [85]. Currently identified STAT6 inhibitors include AS1517499, TMC-264 and the active metabolite of Leflunomide (A771726) [71]. Binnemars-Postma *et al.* showed they could inhibit STAT6 phosphorylation and macrophage polarization towards the M2 phenotype using AS1517499. Tumor growth was significantly inhibited in the murine 4T1 mammary tumor model. Moreover, genetic markers for TAM infiltration (measured by F4/80 and YM-1) and pro-metastatic markers (matrix metalloproteinase-2 (MMP-2), Periostin and CD34) were significantly inhibited in the livers of treated mice, suggesting STAT6 is involved in the formation of the pre-metastatic niche [86].

5.3 Depletion of TAM

The most radical way of blocking TAM activity in tumors is to deplete them altogether. Currently, the most effective way of achieving this is by adding compounds that are toxic specifically to macrophages. Frequently used agents are bisphosphonates, including clodronate and zoledronic acid, but more recently trabectedin as well [71,87].

Bisphosphonates are classically used to inhibit osteoclast function and thus bone resorption in the treatment of osteoporosis, bone metastasis and Paget's disease. Their mode of action is based upon the inhibition prenylation of proteins such as Ras, causing apoptotic cell death. Upon administration, bisphosphonates have a high binding affinity for hydroxyapatite and are therefore readily distributed to the bone, where

they are taken up by the highly endocytic osteoclasts. In macrophages, bisphosphonates have been found to affect proliferation and motility and induce apoptosis [88]. Due to their extremely short half-life, most bisphosphonates by themselves do not reach sufficient tissue concentrations to exert any effect on macrophages [89]. However, when using clodronate-loaded liposomes, van Rooijen *et al.* found a transient decrease in spleen macrophages as soon as one day after injection [90]. In subsequent studies, the inhibition of tumor growth via macrophage depletion was established [91,92]. In a recent study using a murine xenograft model for cutaneous T-cell lymphoma, the administration of clodronate-loaded liposomes led to a reduction in tumor growth [93]. In the tumor tissue, the authors showed a decrease in pSTAT3 and total macrophage count, suggesting that clodronate-loaded liposomes caused a decrease in TAM and thereby a decrease in tumor cell growth [93]. Combinations of the various ways of targeting macrophages have also been investigated, using the combination of zoledronic acid with the previously mentioned STAT3 inhibitor sorafenib [94]. In a nude mouse xenograft model of hepatocellular carcinoma, the combination of drugs (rather than the individual drugs) was shown to significantly reduce tumor growth, metastasis, and angiogenesis [94]. More recently, nitrogen-containing bisphosphonates were found to be effective without the aid of a carrier. In this study, risedronate was able to bind to micro-calcifications, which were subsequently taken up by macrophages, but not by tumor cells [95].

Trabectedin, isolated from the sea squirt Ecteinascidia turbinata, is used in the treatment of soft tissue sarcoma, breast, and ovarian cancer [96]. This compound has been shown to induce apoptosis in macrophages as well. Its mechanism of action is complex and not fully understood. It is able to bind to DNA in the minor groove, bending it towards the major groove, severely influencing DNA structure. Additionally, it induces non-p53-induced apoptosis and blocks the cell cycle in the late S and G_2–M phase [97,98,99,100]. Trabectedin has also been found to inhibit cancer cell proliferation, and modulate the TME, acting as an anti-angiogenic and anti-TAM agent [87,101,102,103].

6 Passive and active targeting

Up until now, few studies have investigated the drug targeting of TAM. Below, we will report on the studies that have investigated TAM targeting using specific carriers or targeting moieties. Figure 1 shows the effect of targeted nanomedicines on TAM.

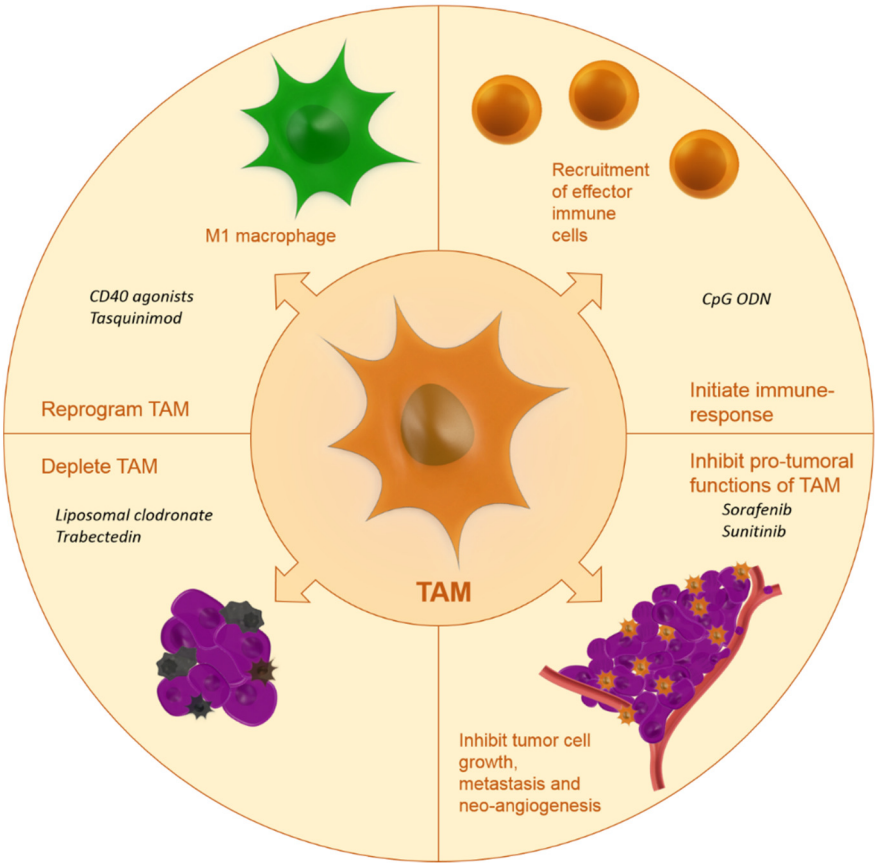

Figure 1. Anti-tumoral effects by targeting TAM using nanocarriers including examples of TAM-modulating therapies (in italics). Abbreviations: CD40: cluster of differentiation 40, CpG ODN: oligodeoxynucleotides containing CpG motifs.

6.1 Passive Targeting

Macrophages are part of the mononuclear phagocyte system (MPS). This system, mostly present in the liver, spleen, and lungs, is responsible for the clearance for foreign matter from the body [104]. As a consequence, nanoparticles that come into contact with macrophages will be rapidly recognized, internalized, and degraded [105,106,107,108]. This intrinsic mechanism of particle uptake by macrophages may be employed to target them. However, reaching certain tissues or specific cell types using passive targeting remains a challenge. Nanoparticle-based therapies, which are being used to target tumor tissues, often rely on the passive enhanced permeation and retention (EPR effect). Due to leaky vasculature and impaired drainage from the tumor site, nanoparticles tend to accumulate in the tumor near the blood vessels [109]. However, penetration of these nanoparticles inside the tumor tissue is often very poor. Moreover, following clinical experience, the EPR effect in humans seems highly variable and limited, possibly due to slow tumor growth, high interstitial fluid pressure, irregular vascular distribution and poor intra-tumoral blood flow [110,111,112]. This issue, together with degree of TAM infiltration, was addressed by imaging of magnetic nanoparticle distribution in tumors and the TME. Magnetic nanoparticles showed clear co-localization with model PLGA–PEG particles, making it possible to identify patients which would be able to benefit from nanoparticle-based therapies [113]. However, even when the EPR effect is limited, macrophages are able to migrate deeper inside tumor tissue, driven by oxygen gradients, towards the hypoxic areas [10,13]. Macrophages may also act as a drug depot, which accumulates drug-loaded nanoparticles and releases them over time [114]. Macrophages may even act as carriers themselves. In this approach, macrophages are loaded with therapeutics ex vivo, after which they will be reintroduced and act as “Trojan Horses” when recruited into the TME. As this strategy has already been reviewed elsewhere, we will not discuss it here [115]. Altogether, due to the EPR effect and the ability of macrophages to phagocytose particles and migrate into tumor areas, nanomedicine may be used to target macrophages and indirectly treat tumor cells. In the sections below, we will discuss a number of nanocarriers used to passively target TAM. A summary of the described studies is displayed in Table 1.

6.1.1 Liposomes

Liposomes are one of the most studied and frequently used carriers in the nanomedicine field. Perhaps the most well-known example of macrophage targeting by liposomes is their depletion by bisphosphonate-loaded liposomes, as mentioned in the "Depletion of TAM" (Section 5.3). Other examples of liposome-based macrophage targeting are described in the section on Active Targeting (Section 6.2). Indeed, due to their composition, enabling encapsulation of hydrophobic, as well as hydrophilic compounds, liposomes have been shown to be excellent carriers for a multitude of different active ingredients, including DNA and siRNA [116]. A nice example of the versatility of liposomes is a study in which pegylated liposomes were loaded with the anti-cancer drug doxorubicin and the bisphosphonate alendronate [117]. Compared to encapsulated doxorubicin, the combination led to superior inhibition of tumor growth in lung and breast cancer mouse models. The authors attribute this enhanced effect to the possible TAM reprogramming by alendronate and heightened immune response due to increased expression of phosphoantigens in tumor cells after exposure to aminobisphosphonates [117]. Another notable example of liposomes as a carrier for the delivery of agents to the TME is the delivery of simvastatin. At high doses, statins have been shown to exert anti-tumor effects [118]. In this study, in order to increase the concentration of simvastatin at the active site, a liposomal delivery system containing simvastatin was used, which was found to inhibit tumor growth, possibly due to the reduction in oxidative stress caused by macrophages, via the inhibition of intra-tumoral HIF-1α [119].

6.1.2 Polymeric nanoparticles

Polymeric nanoparticles are polymer-based nanoparticles that may take different forms: solid capsules/particles (polymeric nanoparticles), highly branched structures (dendrimers), or amphiphilic assemblies (micelles). Advantages of using polymers are the ability to highly tune nanoparticle properties as well as a high drug-loading capacity [120]. Poly(lactic-co-glycolic acid) (PLGA) is a biodegradable copolymer that has been approved for the delivery of therapeutics via sustained release devices and microparticle formulations [121]. Furthermore, next to a wide range of other applications, nanoparticle formulations containing PLGA as a carrier

are now being investigated as a delivery mechanism to target TAM. In a recent attempt to reach glioma cells in the brain, rabies virus glycoproteins (RVG), specifically designed to cross the blood brain barrier (BBB), were conjugated to mixed-lipid covered PLGA cores. Although no specific targeting ligand is present on these particles, using *in vitro* cultured bone marrow derived macrophages the authors were able to show macrophage targeting, which did not occur with neural cells. *In vivo* results show particle brain accumulation, but specific TAM targeting needs to be confirmed [122].

In a different approach, nanoparticles were prepared using acetylated carboxymethylcellulose. Docetaxel and PEG were coupled via ester linkage (Cellax-DTX). The resulting 120-nm particles were used in different animal models for pancreatic cancer, where specific accumulation in the tumor stroma (specifically fibroblasts and macrophages) was observed, resulting in stromal depletion. However, macrophage populations were able to recover after 2–3 weeks, suggesting that depletion was based on the neutropenic effects of docetaxel rather than macrophage targeting [123].

Linear cyclodextrin polymers have been employed in the preparation of self-assembling nanoparticles. One of the best examples, currently under investigation in clinical trials, is CRLX101. This cyclodextrin-based polymer conjugate is loaded with camptothecin for the treatment of multiple tumor types [124]. Using particles similar to this platform, other applications of cyclodextrin-based polymer–drug conjugates have been investigated as well. One such example is the targeting of intracranial glioma tissues using rhodamine-labeled nanoparticles. Particles that were administered i.v. were predominantly found at the edges of gliomas, internalized by macrophages and microglia. By injecting directly into the tumors, migration of nanoparticle-positive cells was observed into circulation and distant tumor sites, indicating the ability of macrophages and microglia to carry nanoparticles from the injection site towards other affected areas [125].

In an attempt to cross the BBB for the treatment of glioblastoma, hydroxyl-functionalized, generation-4 poly(amidoamine) (PAMAM) dendrimer nanoparticles were intravenously administered to gliosarcoma-bearing rats. Investigators found homogenous distribution of the dendrimers throughout the tumor within 15 minutes

after administration, after which retention in microglia and macrophages was observed. The authors propose that dendrimers hold great promise for the delivery of immunomodulatory drugs to TAM across the BBB [126].

6.1.3 Iron oxide nanoparticles

Ferumoxytol is an ultrasmall superparamagnetic iron oxide (USPIO) nanoparticle that has been approved for the treatment of anemia due to chronic renal failure. More recently, it has been investigated as a contrast agent in magnetic resonance imaging (MRI). Particles are cleared from the system by the reticuloendothelial system (RES) and macrophages. Due to the uptake of these particles by macrophages, iron oxide nanoparticles have been the subject of investigation in macrophage targeting and imaging [127]. Apart from their favorable imaging properties, plain USPIO have been found to inhibit tumor growth by inducing pro-inflammatory macrophage polarization. In a recent study by Zanganeh *et al.*, *in vitro* incubation of femuroxytol with co-cultures of macrophages and tumor cells induced tumor cell apoptosis and enhanced macrophage M1 polarization. *In vivo*, co-implantation of MMTV–PyMT tumor cells with ferumoxytol led to significant inhibition of tumor growth. Analysis of TAM showed an increased presence of pro-inflammatory M1 macrophages in tumor tissues. Moreover, pre-treatment with iron particles prevented liver metastasis after i.v. tumor cell challenge [128]. Considering the available data, USPIO nanoparticles themselves may prove to be promising, not only for imaging, but also for the treatment of TAM.

6.1.4 Biological carriers

Next to synthetic carriers, biological carriers, mainly due to their favorable immunological functions, may be employed in the targeting and treatment of TAM. Red blood cells (RBCs) have been used as carriers and loaded with various active agents. In one of the earliest studies, prolonged survival was observed after treatment with methotrexate-loaded RBCs in a mouse model of hepatoma ascites tumors [129]. Several other studies have demonstrated the successful loading of bisphosphonates into RBCs for the depletion of macrophages [130,131]. However, these therapies were not tested in disease models. Loaded RBCs in the targeting and treatment of TAM therefore remains to be investigated. High-density lipoprotein (HDL)

is another class of biological particles, used in carriers, which, in contrast to RBCs has been shown to be specifically taken up by macrophages, mainly in models for atherosclerosis [132,133]. More recently, these particles, by radioactive labeling, have been used for the imaging of TAM [134]; however, although targeting has been achieved, treatment of TAM using HDL-based carriers has not been attempted yet.

6.1.5 Viral particles

In line with non-synthetic carriers, a striking article on the use of plant virus particles, specifically interacting with M2 macrophage populations, was published. In this paper, cowpea mosaic virus (CPMV), which is known to interact with vimentin on tumor cells, was prepared as a nanoparticle and the authors demonstrated enhanced uptake by M2-differentiated macrophages [135]. In subsequent studies, however, distinct differences in uptake between M1 and M2 cells were less pronounced, possibly due to different experimental conditions [136].

6.1.6 Carbon nanotubes

Over the years, carbon nanotubes (CNTs) have received a lot of attention for their use as a biological vector. Moreover, they have been shown to be able to penetrate cells, making them interesting carriers for cell specific targeting [137]. In one of the earliest studies using CNTs to treat brain tumors, after intra-tumoral injection, particles were found to specifically accumulate in TAM, associated with gliomas in mice. Furthermore, no significant toxicities were observed, accompanied by minor changes in tumor cytokine levels [138]. In a study investigating immunotherapy, CpG deoxyoligonucleotides (CpGs) were conjugated to CNTs and injected intratumorally in glioma-bearing mice. Conjugated CpGs were found to be more effective than free CpGs, showing enhanced uptake in TAM. Not only were intracranial gliomas eradicated, but treated mice proved to be immune to subsequent intracranial or systemic tumor challenges, suggesting an induction in systemic anti-tumor immunity [139]. In subsequent studies investigating the effect of CpG-CNT-conjugates on the brain metastasis of primary melanomas, investigators found only a modest inhibition of intracranial melanoma tumors when treating the primary subcutaneous tumor. Intracranial treatment, however, halted both

brain and subcutaneous tumor growth. This effect was accompanied by a strong immune response, with increased effector cell infiltration and cytotoxicity. Further investigation into this altered response showed an increase in retention of particles and an increase in infiltration of TLR-9 positive microglia. In contrast, treated subcutaneous tumors showed abundant myeloid-derived suppressor cells. The authors concluded that intracranial delivery of CpG-CNT conjugates is more effective in stimulating immune responses that affect both the brain and subcutaneous melanomas [140].

6.1.7 Albumin nanoparticles

In addition to other biological carriers, proteins may function as carriers for therapeutics as well. The advantages of using proteins as carrier molecules are their biodegradability (when derived from natural proteins) and their amphiphilic nature, which allows them to interact with drug molecules but also makes them soluble in aqueous environments [141]. The FDA-approved nanoparticle-albumin-bound paclitaxel (nab-paclitaxel, Abraxane) is a good example of this. It is registered for the treatment of advanced breast cancer, advanced non-small cell lung cancer, and advanced pancreatic cancer. Treatment using this conjugate, compared to the free drug, led to a decrease in side effects, increased tumor cell toxicity, and higher overall response rates [142]. Originally, these improved effects were attributed to the higher intra-tumoral concentrations of paclitaxel, due to the binding of albumin to endothelial 60-kDa glycoprotein receptor (gp60), facilitating vascular transcytosis and the binding of albumin to the tumor cell surface receptor secreted protein, acidic and rich in cysteine (SPARC) [143,144,145]. Most recently, an additional mechanism for improved effectiveness was discovered by Cullis *et al.* [146]. They found that nab-paclitaxel was internalized by macrophages via macropinocytosis. This led to immunostimulatory cytokine and inducible nitric oxide (iNOS) expression. *In vivo*, nab-paclitaxel was internalized by TAM, leading to increased $MHCII^+$ $CD80^+$ $CD86^+$ M1 macrophage populations. The authors conclude that albumin nanoparticles may be used in the delivery of macrophage-activating agents in the treatment of cancer types with high amounts of M2 macrophage infiltration [146].

6.1.8 Silica nanoparticles

Although nab-paclitaxel particles have shown potent anti-tumor effects on their own, recently these particles were incorporated into multistage nanovectors (MSVs), consisting of mesoporous silicon nanoparticles, loaded with nab-paclitaxel [147]. By loading nab-paclitaxel into mesoporous silicon nanoparticles, the authors propose a redirection of particles to the liver. In liver metastasis, originating from breast or lung cell lines, authors found decreased liver weights and increased survival of animals treated with loaded MSVs, compared to nab-paclitaxel alone. In subsequent *in vitro* experiments, macrophages incubated with loaded MSVs were found to form a paclitaxel depot, which was slowly released from the macrophages. The authors conclude that this approach increases therapeutic efficacy without increasing the chance of developing systemic side effects [147]. Since loading into mesoporous silicon nanoparticles dramatically increases the size of the particles, the effect on splenic uptake would be interesting to investigate as well. Indeed, nanoparticle characteristics greatly influence their uptake by different subtypes of macrophages [148]. In a recent study, we investigated the uptake of silica nanoparticles by differentiated macrophages. We found that, with increasing size, the presence of serum proteins greatly influenced the uptake of particles, which was most pronounced in M2 (TAM-like) macrophages. This study indicates that targeting may be achieved by tuning nanoparticle properties, specifically size, in such a way that they are preferentially taken up by specific macrophage populations [149].

Table 1: Examples of studies using nanocarriers to passively target TAM

Carrier type	Cargo	Model	Purpose	Ref.
Liposomes	Simvastatin	B16.F10 murine melanoma	Improve efficacy of statins using a tumor targeted delivery system	[119]
	Alendronate and doxorubicin	Multiple murine cancer models	Increase anti-tumor efficacy by co-delivery of alendronate and doxorubicin	[117]

Acetylated CMC	Docetaxel	PAN02 pancreatic cancer xenograft	Targeted depletion of stroma	[123]
Linear cyclodextrin-based nanoparticle	Fluorescent label	Murine GL261 glioma	Macrophage and microglia targeting	[125]
Iron oxide nanoparticle	-	Murine breast cancer using MMTV-PyMT cells	Evaluate intrinsic therapeutic effects of USPIO	[128]
Red blood cells	Bisphos-phonates	Normal Swiss, C57BL/6 and Balb/C mice	Macrophage depletion	[130, 131]
High density lipoprotein-based nanoparticle	Radiolabel	Murine 4T1 breast cancer	Imaging of TAM	[134]
Cowpea mosaic virus	Fluorescent label, Photo-sensitizer	RAW264.7 macrophages and B16F10 tumor cells	TAM and tumor cell targeting	[135, 136]
PAMAM dendrimers	Fluorescent dye	Rat 9L gliosarcoma	Cross BBB and achieve homogenous tumor distribution	[126]
Carbon nano-tubes	Fluorescent dye	Murine GL261 glioma	Study uptake and toxicity	[138]
	CpGs	Murine GL261 glioma	Evaluate CNT as a delivery vehicle	[139, 140]
Albumin-paclitaxel conjugate	Paclitaxel	Murine KPC pancreatic ductal adeno-carcinoma	Investigate new mechanism for Abraxane effectiveness	[146]
Mesoporous silicon particles loaded with albumin-paclitaxel conjugate	Paclitaxel	Murine 4T1 breast cancer and murine 3LL lung cancer	Redirect nab-paclitaxel to liver metastasis	[147]

Abbreviations: BBB: Blood Brain Barrier, CMC: carboxymethylcellulose, USPIO: Ultrasmall Superparamagnetic Iron Oxide, PAMAM: poly(amidoamine), CNT: Carbon nanotubes

6.2 Active targeting

In recent years, various nanocarriers have been developed. Many of these particles end up in macrophages via endocytosis. Specific targeting of TAM without affecting other macrophage populations is a field of ongoing research. TAMs overexpress different surface receptors, which are exploited for the targeted therapy against these macrophages. Different surface receptors and other proteins that are overexpressed by TAM are discussed below. A summary of the described studies is displayed in Table 2. Figure 2 shows examples of surface proteins that can be targeted using nanoparticles.

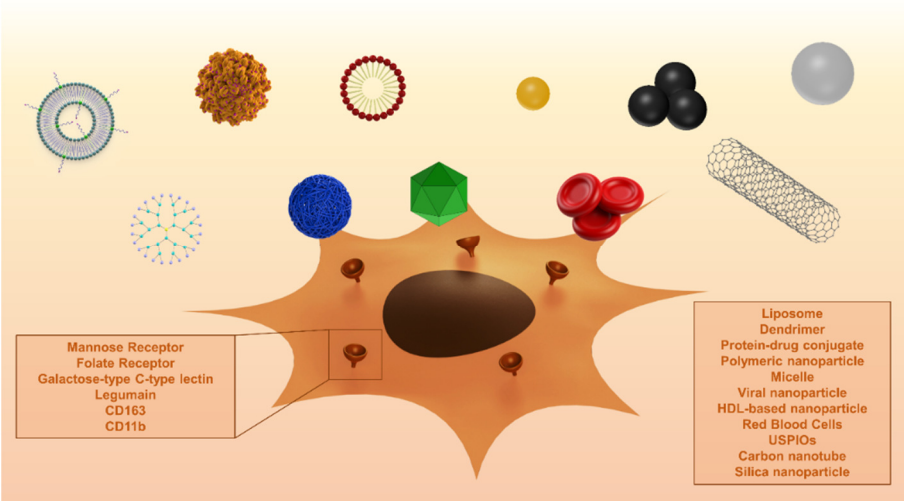

Figure 2. Graphical presentation of surface proteins and different nanoparticles used in TAM targeting. Names of nanoparticles are displayed in their order of appearance, left to right. Abbreviations: HDL: High density lipoproteins, CD: cluster of differentiation, USPIO: ultrasmall superparamagnetic iron oxides.

6.2.1 Mannose receptor

The mannose receptor 1 (MRC1, also called CD206) is a scavenger receptor that is overexpressed on the surface of TAMs. Mannose-modified nanoparticles have been used for macrophage targeting to achieve various goals: boosting of the immune responses, imaging, depletion of macrophages, and anti-tumor therapy.

In early studies, mannose-modified cationic liposomes were used for the targeted delivery of genes to enhance the immune response [150,151,152,153]. Hattori *et al.* compared the delivery of the model gene for ovalbumin encapsulated in normal liposomes and mannosylated liposomes and showed they could increase the immune response by using mannose as a targeting ligand [154]. In subsequent studies, mannose was used for specific TAM targeting and treatment. Locke *et al.* investigated the accumulation of mannosylated ^{64}Cu-loaded liposomes in a mouse model for pulmonary adenocarcinoma using PET imaging and fluorescence microscopy [155]. They compared mannosylated and non-mannosylated liposomes labeled with fluorescent dyes and showed that the mannosylated liposomes accumulated at the tumor regions, while the normal liposomes were distributed throughout the entire lung tissue. Subsequent confocal microscopy confirmed the uptake of the mannosylated liposomes in macrophages expressing MRC1, confirming that mannosylation is a viable approach for targeting TAMs [155]. Similar to the latter study, the polysaccharide mannan, a ligand for the mannose receptor, has been used in several studies for the delivery of nanoparticles to macrophages [156,157]. In a study by Zhan *et al.*, a glucomannan polysaccharide from Bletilla striata was employed to target the mannose receptor [158]. The polysaccharide was coupled to the bisphosphonate alendronate for the depletion of macrophages. They showed that a conjugate of the polysaccharide and alendronate preferentially accumulated in macrophages and induced apoptosis *in vitro*. Furthermore, in a mouse tumor model they showed that depletion of TAM led to inhibition of angiogenesis, recovered local immune surveillance, and suppression of tumor growth [158]. Mannose has also been used in the targeting of polymeric nanoparticles towards TAM. In the past, PEG-sheddable, acid-sensitive, mannose-modified PLGA carriers have been developed and tested for their macrophage targeting potential [159]. In subsequent studies by different investigators, these particles have been tested for their efficacy in cancer treatment [160,161]. One such example is the delivery of acid-sensitive, sheddable, PEGylated, mannose-modified doxorubicin nanoparticles to TAM. In this study, targeted nanoparticles formulations were more effective in reducing tumor growth than non-targeted formulations. Using the targeted

formulation, compared to doxorubicin alone, a reduction in the intratumoral CD206+ cell populations was observed [161].

In another approach using polymers, elegant tri-block copolymer nanoparticles were developed for the delivery of siRNA. In these particles, the core consists of a hydrophobic pH sensitive block, which triggers endosomal escape and enables cytoplasmatic delivery of siRNA. The second block consists of cationic DMAEMA polymers, which are able to condense anionic oligonucleotides within the particle, thus carrying and protecting the cargo. The third block is the azide-presenting block, which enables the particles to be functionalized with targeting molecules, in this case, mannose. Using this functionalized particle, the authors showed the effective transfection of TAM *in vitro* and *in vivo*. In primary mammary tumors, the effective delivery of labeled nucleotides was confirmed. Enhanced delivery of labeled nucleotides by targeted particles was established in ovarian tumors, compared to non-targeted particles. Furthermore, *in vivo*, no significant toxicity was observed [162]. Having established successful targeting of TAM in several mouse models for cancer, investigators then incorporated siRNA for manipulation of the NF-κB pathway. *In vitro*, the potent induction of cytotoxicity and immunostimulatory functions of TAM was confirmed. In upcoming studies, the authors plan to investigate the effects of this gene silencing *in vivo* [163,164].

6.2.2 Folate Receptor

Another surface receptor is folate receptor (FR), a glycoprotein that binds to folic acid with high affinity. Initially FR was found to be overexpressed on cancer types of epithelial origin and was thus used for targeted delivery of therapeutics to tumor cells. However, Turk *et al.* found that FR was also expressed on activated macrophages. In an experimental mouse model of ovarian cancer, they showed a 10-fold higher uptake of folate-conjugated liposomes in TAMs compared to tumor cells, where endocytosis via FR was responsible for 50% of the total uptake [165]. Additional experiments by other groups have shown the presence of the FR-β subtype on the surface of TAMs [166], and the possibility of targeting TAMs using this receptor [167]. In this study, Pseudomonas exotoxin A was coupled to an antibody directed against FR-β and injected into C6 glioma xenografts in nude mice. This treatment led to a significant reduction in tumor growth and depletion of TAM. Using this study, the authors concluded that the depletion of

FR-β positive macrophages might be a suitable option for immunotherapy of human glioblastoma [167]. Hattori *et al.* investigated zoledronic-acid-loaded folate modified liposomes for selective TAM depletion. TAM-mediated uptake was observed; however, due to severe toxicity of both conjugated and unconjugated liposomes, no additional anti-tumoral effect could be detected [168].

Folate has also been used in the targeting of USPIO towards TAM. An example is the imaging of TAM in the PyMT mouse mammary tumor model i.v. injected USPIO enhanced MRI signaling in tumor tissues. Upon further investigation, iron oxide nanoparticles were associated with intra-tumoral TAM. In addition, by decorating USPIO nanoparticles with folate, the authors showed increased macrophage uptake [169].

6.2.3 CD163

CD163 is a member of the scavenger receptor cysteine-rich (SRCR) superfamily. It is expressed in most mature macrophages and plays a role in the resolution of inflammation [170,171]. Moreover, it is involved in homeostasis by binding to hemoglobin–haptoglobin complexes [171]. Gordon *et al.* reported high expression of this receptor in alternatively activated, *i.e.*, M2-like macrophages [172].

Although it is well established that the CD163 receptor is overexpressed on TAM, there is a lack of studies exploiting this receptor for TAM targeting. However, one study attempted to target monocytes by coupling an anti-CD163 antibody via a PEG linker to long circulating liposomes [173]. *In vitro*, greater uptake in CD163 transfected cells was observed compared to non-transfected cells. When using doxorubicin as a therapeutic agent, cell viability in peripheral blood mononuclear cells was greatly decreased using the targeted construct. The authors conclude that CD163 targeted stealth liposomes may be used to target macrophages in inflammatory and malignant processes.

6.2.4 Legumain

Legumain is a member of the asparaginyl endopeptidase family. It functions as a stress protein, induced by hypoxia, and is overexpressed in TAM, tumor vascular cells, and tumor cells, but not in normal tissues [174,175]. Using a DNA-based vaccine against legumain as a tool, mice were immunized against legumain, leading to depletion of TAM in

tumor tissues of 4T1 breast tumor-bearing mice. Depletion of TAM led to a pronounced reduction of TGF-β, TNF-α, MMP-9, and VEGF, resulting in the suppression of angiogenesis, tumor growth, and metastasis. Moreover, vaccination after i.v. tumor cell challenge led to survival of 75% of injected mice, while 62% of them were found to be completely tumor-free [176]. In a nanoparticle-based approach, the small molecular inhibitor for legumain RR-11a was coupled to liposomes. Loading of these particles with doxorubicin led to complete inhibition of tumor growth [177]. In a follow-up study, the legumain-targeted nanoparticle was used for the treatment of TAM. In order to re-educate TAM, hydrazinocurcumin, a synthetic analogue of curcumin able to inhibit the STAT3 pathway, was encapsulated and delivered to TAM. By changing the M2 phenotype of TAM from IL-10^{high}/IL-12^{low}/TGF-β^{high} to M1 phenotype IL-10^{low}/IL-12^{high}/TGF-β^{low}, authors were able to show TAM re-education *in vitro*. *In vivo*, suppressed tumor growth, metastasis, and angiogenesis were observed [178]. Most recently, using an elegant liposomal modification for the simultaneous targeting of TAM, endothelial cells, and tumor cells, the cyclic RGD peptide (iRGD) was combined with a substrate for legumain, alanine-alanine-asparagine (AAN), yielding nRGD [179]. nRGD could specifically bind to legumain, present on tumor endothelial cells, tumor cells, and TAM. Once cleaved by legumain, the remaining nRGD would then be able to bind to $\alpha v\beta_3/\beta_5$ integrin receptors, where it would be cleaved again. The remaining peptide would then bind to neuropilin-1 on tumor cells. The targeted nanoparticle was loaded with doxorubicin and subsequently used in the treatment of 4T1 tumor-bearing mice. Specific interaction with tumor vasculature and efficient tumor penetration were observed. Furthermore, the TME was modulated by depletion of TAM. Overall, the attachment of nRGD to doxorubicin-loaded liposomes led to excellent anti-tumor efficacy, increasing doxorubicin efficacy and low toxicity [179].

6.2.5 Galactose-type C-type lectins

In a novel approach to target TAM for the specific delivery of oligonucleotides, specifically CpG, anti-IL-10, and anti-IL-10R, Huang *et al.* have developed an acid-sensitive (PEG-histidine modified alginate) nanoparticle, using galactosylated cationic dextran (gal-C-dextran) to form stable nanoplexes able to incorporate and protect

oligonucleotides. TAM express high levels of macrophage galactose-type lectin (MGL), making it a suitable target for galactose [180]. In an allograft hepatoma murine model, authors found accumulation of nucleic acids in TAM after i.v. injection. Treatment using the nanoparticles led to significant reduction in tumor growth. Moreover, in TAM isolated from tumor tissues, pro-tumor functions were suppressed and anti-tumor activities were stimulated [181].

6.2.6 CD11b

In another approach to delivering siRNA to macrophages, a glucan-based carrier was developed. Glucans display pathogen-associated molecular patterns (PAMPS), which are recognized and internalized by macrophages. In previous studies, the authors developed water-soluble variants of glucan: β-(1→3)-(1→4)-glucan (BG34). This glucan was found to be internalized by primary monocytes via the CD11b receptor [182]. In a follow-up study, siRNA against MIF was incorporated into this glucan, resulting in 80–120 nm nanoparticles. An i.v. injection of these nanoparticles led to specific tumor accumulation in 4T1 mammary tumor-bearing mice. FACS analysis of TAM isolated from tumor tissues showed a sustained reduction in MIF expression [183].

6.2.7 Peptides

A different way of selectively targeting TAM is the use of peptides. This new approach for targeting TAMs was investigated by Cieslewicz *et al.* They identified a murine M2 macrophage specific peptide, called M2pep, using subtractive phage biopanning. They showed that this peptide was able to preferentially bind to M2 macrophages, compared to other leukocytes, and they confirmed the accumulation in TAMs *in vivo*. By fusing M2pep with a pro-apoptotic peptide, they were able to show delayed mortality and a decrease in M2 TAM population in a murine model for colon carcinoma [184].

Table 2. Examples of studies using nanocarriers to actively target TAM.

Ligand/Target	Carrier	Cargo	Model	Purpose	Ref.
AAN/Legumain	Liposome	Doxorubicin	Murine 4T1 breast cancer	TAM depletion	[179]
CD163 antibody/CD163	Liposome	Fluorescent label, Doxorubicin	*In vitro* HEK293, CHO K1	TAM depletion	[173]

			cells and PBMC's		
Folate receptor	USPIO	-	MMTV-PyMT murine mammary carcinoma model	Imaging	[169]
	Liposome	Radio- and fluorescent label	Murine IGROV ovarian cancer	Imaging	[165]
		Fluorescent label, zoledronic acid	Several tumor types	TAM depletion	[168]
	FR Antibody	Pseudo-monas exotoxin A	Human and rat C6 glioma xenografts in mice	TAM depletion	[167]
Galactose/MGL	Alginate-based nano-particles	CpG, anti-IL-10 and anti-IL-10R oligo-nucleotides	Hepa 1-6 murine hepatoma	Inhibit pro-tumoral functions and repro-gram TAM, initiate immune response	[181]
M2pep/M2 macrophages	Peptide-based nano-particle	Fluorescent label, proapoptotic peptide	Colon carcinoma	Imaging	[184]
Mannose/MR	PLGA	Doxorubicin	Murine M-Wnt triple-negative mammary tumors	TAM depletion	[161]
	BMA-PAA-DMAEMA micelles	siRNA	Multiple tumor types	Repro-gram TAM	[162-164]
	Liposomes				

		Radiolabel, fluorescent dye	Urethane-FVB pulmonary adeno-carcinoma	Imaging	[155]
Polysaccharide from *Bletilla striata*/MR	Polysaccharide from *Bletilla striata*-drug conjugate	Alendronate	Murine S180 sarcoma	TAM depletion	[158]
Rabies virus glycoprotein	PLGA-core with mixed-lipid coating	Paclitaxel	U87 glioma xenograft	TAM depletion	[122]
RR-11a/Legumain	Liposomes	Hydrazino-curcumin	Murine 4T1 breast cancer	Reprogramming of TAM	[178]
β-(1→3)-(1→4)-glucan/CD11b	Glucan-based nano-particle	MIF siRNA	Murine 4T1 breast cancer	Inhibit recruit-ment and reprogramming TAM	[182, 183]

Abbreviations: PLGA: poly(lactic-co-glycolic acid), MR: Mannose Receptor, BBB: Blood Brain Barrier, BMA: butyl methacrylate , PAA: 2-propylacrylic acid , DMAEMA: 2-(dimethylamino)ethyl methacrylate, CMC: carboxymethylcellulose, FR: Folate Receptor, USPIO: Ultrasmall Superparamagnetic Iron Oxide, CNT: Carbon nanotubes, MHC class I: major histocompatibility complex class I, PBMC: Peripheral blood mononuclear cell, MGL: Macrophage galactose-type C-type lectin, MIF: Macrophage migration inhibitory factor

7 Future perspectives

Specific targeting of TAM is a very recent field of investigation and many hurdles are still remaining. Even though some research has been done to achieve specific targeting of TAM, the expression of the specific markers on other cell types remains a major obstacle. Most active targeting strategies are based on the targeting to upregulated receptors in TAM, but as a matter of fact macrophages often display intermediate states (in between M1 and M2 phenotypes) and other cell types may display these receptors as well [42,185]. Therefore, targeting specificity remains a key challenge. A lack of specificity may lead to treatment of tissue-specific macrophages, such as red pulp macrophages in the

spleen or Kupffer cells in the liver. Effects on other macrophage types or receptor-expressing cells should be investigated as well. Moreover, acute toxicity has been observed when administering liposomal zoledronic acid, most likely caused by increased cytokine production [168,186]. Furthermore, the long-term effects of macrophage depletion have yet to be investigated, as there are indications that macrophage depletion may aggravate liver lesions in liver injury and impair skeletal muscle repair after muscle injury [187,188]. However, targeting macrophages seems to be a more effective strategy than identifying tumor specific antigens, as these may change over the course of tumor development and expression may vary between different groups of patients [189]. Recent advances have shown that the EPR effect is not as pronounced in human cancers as in mouse models. Screening of patients in terms of EPR effect and TAM infiltration may increase the number of responders to nanoparticle-based treatments [113,114]. Combining therapy with diagnostics (theranostics), which has been employed in the evaluation of the effectiveness of the targeting and treatment of TAM, might be another useful approach [190].

Production and characterization of complex nanoformulations in GMP conditions may make the translation to the clinic difficult. Production scale-up from the laboratory to the clinic will become more complicated when the particles are prepared in a multi-step process. Therefore, straightforward particles and targeting ligands would be preferable. As shown in several studies, by simply tuning particle characteristics TAM specificity may be increased [149,191]. Preparing them in a single step may make scaling up easier.

8 Conclusions

TAM prove to be an interesting therapeutic target for the inhibition of tumor growth and metastasis. Currently, many lines of research are being investigated for the effective delivery of TAM-modulating therapies. A large number of successful attempts have been reported to target TAM via cell-specific surface receptors either to deplete, re-educate, or initiate anti-tumor immune responses. Moreover, the combination of TAM-targeted therapies with conventional medication, directed against the tumor and metastatic sites, holds great promise for effective cancer therapy in the future. Although there are still some

hurdles to be overcome, the many preclinical studies reviewed herein show promising results and warrant the further translation of TAM targeting technologies towards the clinic.

References

1. Balkwill, F.; Mantovani, A., Inflammation and cancer: back to Virchow? Lancet 2001, 357, (9255), 539-45.
2. Brigati, C.; Noonan, D. M.; Albini, A.; Benelli, R., Tumors and inflammatory infiltrates: friends or foes? Clinical & experimental metastasis 2002, 19, (3), 247-58.
3. Liotta, L. A.; Kohn, E. C., The microenvironment of the tumour-host interface. Nature 2001, 411, (6835), 375-9.
4. Dvorak, H. F., Tumors: wounds that do not heal. Similarities between tumor stroma generation and wound healing. The New England journal of medicine 1986, 315, (26), 1650-9.
5. Hagerling, C.; Casbon, A. J.; Werb, Z., Balancing the innate immune system in tumor development. Trends in cell biology 2014.
6. Elinav, E.; Nowarski, R.; Thaiss, C. A.; Hu, B.; Jin, C.; Flavell, R. A., Inflammation-induced cancer: crosstalk between tumours, immune cells and microorganisms. Nature reviews. Cancer 2013, 13, (11), 759-71.
7. Mantovani, A.; Allavena, P.; Sica, A.; Balkwill, F., Cancer-related inflammation. Nature 2008, 454, (7203), 436-44.
8. Koehne, C. H.; Dubois, R. N., COX-2 inhibition and colorectal cancer. Seminars in oncology 2004, 31, (2 Suppl 7), 12-21.
9. Flossmann, E.; Rothwell, P. M., Effect of aspirin on long-term risk of colorectal cancer: consistent evidence from randomised and observational studies. Lancet 2007, 369, (9573), 1603-13.
10. Sica, A.; Allavena, P.; Mantovani, A., Cancer related inflammation: the macrophage connection. Cancer letters 2008, 267, (2), 204-15.
11. Pollard, J. W., Tumour-educated macrophages promote tumour progression and metastasis. Nature reviews. Cancer 2004, 4, (1), 71-8.
12. Allavena, P.; Mantovani, A., Immunology in the clinic review series; focus on cancer: tumour-associated macrophages: undisputed stars of the inflammatory tumour microenvironment. Clinical and experimental immunology 2012, 167, (2), 195-205.
13. Sica, A.; Schioppa, T.; Mantovani, A.; Allavena, P., Tumour-associated macrophages are a distinct M2 polarised population promoting tumour progression: potential targets of anti-cancer therapy. Eur J Cancer 2006, 42, (6), 717-27.
14. Shoenfeld, Y.; Tal, A.; Berliner, S.; Pinkhas, J., Leukocytosis in non hematological malignancies--a possible tumor-associated marker. Journal of cancer research and clinical oncology 1986, 111, (1), 54-8.

15. Fridlender, Z. G.; Albelda, S. M., Tumor-associated neutrophils: friend or foe? Carcinogenesis 2012, 33, (5), 949-55.
16. Pillay, J.; Tak, T.; Kamp, V. M.; Koenderman, L., Immune suppression by neutrophils and granulocytic myeloid-derived suppressor cells: similarities and differences. Cellular and molecular life sciences : CMLS 2013, 70, (20), 3813-27.
17. Dumitru, C. A.; Lang, S.; Brandau, S., Modulation of neutrophil granulocytes in the tumor microenvironment: mechanisms and consequences for tumor progression. Seminars in cancer biology 2013, 23, (3), 141-8.
18. Brandau, S.; Moses, K.; Lang, S., The kinship of neutrophils and granulocytic myeloid-derived suppressor cells in cancer: cousins, siblings or twins? Seminars in cancer biology 2013, 23, (3), 171-82.
19. Okabe, Y.; Medzhitov, R., Tissue-specific signals control reversible program of localization and functional polarization of macrophages. Cell 2014, 157, (4), 832-44.
20. Locati, M.; Mantovani, A.; Sica, A., Macrophage activation and polarization as an adaptive component of innate immunity. Advances in immunology 2013, 120, 163-84.
21. Epelman, S.; Lavine, K. J.; Randolph, G. J., Origin and functions of tissue macrophages. Immunity 2014, 41, (1), 21-35.
22. Sica, A.; Erreni, M.; Allavena, P.; Porta, C., Macrophage polarization in pathology. Cellular and molecular life sciences : CMLS 2015, 72, (21), 4111-26.
23. Martinez, F. O.; Gordon, S., The M1 and M2 paradigm of macrophage activation: time for reassessment. F1000prime reports 2014, 6, 13.
24. Nau, G. J.; Richmond, J. F.; Schlesinger, A.; Jennings, E. G.; Lander, E. S.; Young, R. A., Human macrophage activation programs induced by bacterial pathogens. Proceedings of the National Academy of Sciences of the United States of America 2002, 99, (3), 1503-8.
25. Mantovani, A.; Sica, A.; Sozzani, S.; Allavena, P.; Vecchi, A.; Locati, M., The chemokine system in diverse forms of macrophage activation and polarization. Trends in immunology 2004, 25, (12), 677-86.
26. Heusinkveld, M.; van der Burg, S. H., Identification and manipulation of tumor associated macrophages in human cancers. Journal of translational medicine 2011, 9, 216.
27. Hao, N. B.; Lu, M. H.; Fan, Y. H.; Cao, Y. L.; Zhang, Z. R.; Yang, S. M., Macrophages in tumor microenvironments and the progression of tumors. Clinical & developmental immunology 2012, 2012, 948098.

28. Biswas, S. K.; Mantovani, A., Macrophage plasticity and interaction with lymphocyte subsets: cancer as a paradigm. Nature immunology 2010, 11, (10), 889-96.
29. Mills, C. D., M1 and M2 Macrophages: Oracles of Health and Disease. Critical reviews in immunology 2012, 32, (6), 463-88.
30. Mills, C. D.; Shearer, J.; Evans, R.; Caldwell, M. D., Macrophage arginine metabolism and the inhibition or stimulation of cancer. J Immunol 1992, 149, (8), 2709-14.
31. Heusinkveld, M.; de Vos van Steenwijk, P. J.; Goedemans, R.; Ramwadhdoebe, T. H.; Gorter, A.; Welters, M. J.; van Hall, T.; van der Burg, S. H., M2 macrophages induced by prostaglandin E2 and IL-6 from cervical carcinoma are switched to activated M1 macrophages by CD4+ Th1 cells. J Immunol 2011, 187, (3), 1157-65.
32. Fujiwara, Y.; Komohara, Y.; Kudo, R.; Tsurushima, K.; Ohnishi, K.; Ikeda, T.; Takeya, M., Oleanolic acid inhibits macrophage differentiation into the M2 phenotype and glioblastoma cell proliferation by suppressing the activation of STAT3. Oncology reports 2011, 26, (6), 1533-7.
33. Oishi, K.; Sakaguchi, T.; Baba, S.; Suzuki, S.; Konno, H., Macrophage density and macrophage colony-stimulating factor expression predict the postoperative prognosis in patients with intrahepatic cholangiocarcinoma. Surgery today 2014.
34. Ding, T.; Xu, J.; Wang, F.; Shi, M.; Zhang, Y.; Li, S. P.; Zheng, L., High tumor-infiltrating macrophage density predicts poor prognosis in patients with primary hepatocellular carcinoma after resection. Human pathology 2009, 40, (3), 381-9.
35. Mantovani, A.; Allavena, P.; Sica, A., Tumour-associated macrophages as a prototypic type II polarised phagocyte population: role in tumour progression. Eur J Cancer 2004, 40, (11), 1660-7.
36. Colegio, O. R.; Chu, N. Q.; Szabo, A. L.; Chu, T.; Rhebergen, A. M.; Jairam, V.; Cyrus, N.; Brokowski, C. E.; Eisenbarth, S. C.; Phillips, G. M.; Cline, G. W.; Phillips, A. J.; Medzhitov, R., Functional polarization of tumour-associated macrophages by tumour-derived lactic acid. Nature 2014.
37. Sica, A.; Saccani, A.; Bottazzi, B.; Polentarutti, N.; Vecchi, A.; van Damme, J.; Mantovani, A., Autocrine production of IL-10 mediates defective IL-12 production and NF-kappa B activation in tumor-associated macrophages. J Immunol 2000, 164, (2), 762-7.
38. Rebe, C.; Vegran, F.; Berger, H.; Ghiringhelli, F., STAT3 activation: A key factor in tumor immunoescape. Jak-Stat 2013, 2, (1), e23010.

39. Zhang, Y.; Choksi, S.; Chen, K.; Pobezinskaya, Y.; Linnoila, I.; Liu, Z. G., ROS play a critical role in the differentiation of alternatively activated macrophages and the occurrence of tumor-associated macrophages. Cell research 2013, 23, (7), 898-914.
40. Yuan, Z. Y.; Luo, R. Z.; Peng, R. J.; Wang, S. S.; Xue, C., High infiltration of tumor-associated macrophages in triple-negative breast cancer is associated with a higher risk of distant metastasis. OncoTargets and therapy 2014, 7, 1475-80.
41. Kubler, K.; Ayub, T. H.; Weber, S. K.; Zivanovic, O.; Abramian, A.; Keyver-Paik, M. D.; Mallmann, M. R.; Kaiser, C.; Serce, N. B.; Kuhn, W.; Rudlowski, C., Prognostic significance of tumor-associated macrophages in endometrial adenocarcinoma. Gynecologic oncology 2014.
42. Biswas, S. K.; Allavena, P.; Mantovani, A., Tumor-associated macrophages: functional diversity, clinical significance, and open questions. Seminars in immunopathology 2013, 35, (5), 585-600.
43. Qian, B. Z.; Pollard, J. W., Macrophage diversity enhances tumor progression and metastasis. Cell 2010, 141, (1), 39-51.
44. Lin, E. Y.; Nguyen, A. V.; Russell, R. G.; Pollard, J. W., Colony-stimulating factor 1 promotes progression of mammary tumors to malignancy. J Exp Med 2001, 193, (6), 727-40.
45. Wyckoff, J.; Wang, W.; Lin, E. Y.; Wang, Y.; Pixley, F.; Stanley, E. R.; Graf, T.; Pollard, J. W.; Segall, J.; Condeelis, J., A paracrine loop between tumor cells and macrophages is required for tumor cell migration in mammary tumors. Cancer research 2004, 64, (19), 7022-9.
46. Wyckoff, J. B.; Wang, Y.; Lin, E. Y.; Li, J. F.; Goswami, S.; Stanley, E. R.; Segall, J. E.; Pollard, J. W.; Condeelis, J., Direct visualization of macrophage-assisted tumor cell intravasation in mammary tumors. Cancer research 2007, 67, (6), 2649-56.
47. Hagemann, T.; Robinson, S. C.; Schulz, M.; Trumper, L.; Balkwill, F. R.; Binder, C., Enhanced invasiveness of breast cancer cell lines upon co-cultivation with macrophages is due to TNF-alpha dependent up-regulation of matrix metalloproteases. Carcinogenesis 2004, 25, (8), 1543-9.
48. Ingman, W. V.; Wyckoff, J.; Gouon-Evans, V.; Condeelis, J.; Pollard, J. W., Macrophages promote collagen fibrillogenesis around terminal end buds of the developing mammary gland. Dev Dyn 2006, 235, (12), 3222-9.
49. Condeelis, J.; Segall, J. E., Intravital imaging of cell movement in tumours. Nature reviews. Cancer 2003, 3, (12), 921-30.
50. Du, R.; Lu, K. V.; Petritsch, C.; Liu, P.; Ganss, R.; Passegue, E.; Song, H.; Vandenberg, S.; Johnson, R. S.; Werb, Z.; Bergers, G.,

HIF1alpha induces the recruitment of bone marrow-derived vascular modulatory cells to regulate tumor angiogenesis and invasion. Cancer cell 2008, 13, (3), 206-20.

51. Casazza, A.; Laoui, D.; Wenes, M.; Rizzolio, S.; Bassani, N.; Mambretti, M.; Deschoemaeker, S.; Van Ginderachter, J. A.; Tamagnone, L.; Mazzone, M., Impeding macrophage entry into hypoxic tumor areas by Sema3A/Nrp1 signaling blockade inhibits angiogenesis and restores antitumor immunity. Cancer cell 2013, 24, (6), 695-709.
52. Guruvayoorappan, C., Tumor versus tumor-associated macrophages: how hot is the link? Integrative cancer therapies 2008, 7, (2), 90-5.
53. Mantovani, A.; Savino, B.; Locati, M.; Zammataro, L.; Allavena, P.; Bonecchi, R., The chemokine system in cancer biology and therapy. Cytokine & growth factor reviews 2010, 21, (1), 27-39.
54. Lazennec, G.; Richmond, A., Chemokines and chemokine receptors: new insights into cancer-related inflammation. Trends Mol Med 2010, 16, (3), 133-44.
55. Gazzaniga, S.; Bravo, A. I.; Guglielmotti, A.; van Rooijen, N.; Maschi, F.; Vecchi, A.; Mantovani, A.; Mordoh, J.; Wainstok, R., Targeting tumor-associated macrophages and inhibition of MCP-1 reduce angiogenesis and tumor growth in a human melanoma xenograft. The Journal of investigative dermatology 2007, 127, (8), 2031-41.
56. Pienta, K. J.; Machiels, J. P.; Schrijvers, D.; Alekseev, B.; Shkolnik, M.; Crabb, S. J.; Li, S.; Seetharam, S.; Puchalski, T. A.; Takimoto, C.; Elsayed, Y.; Dawkins, F.; de Bono, J. S., Phase 2 study of carlumab (CNTO 888), a human monoclonal antibody against CC-chemokine ligand 2 (CCL2), in metastatic castration-resistant prostate cancer. Invest New Drugs 2013, 31, (3), 760-8.
57. Sandhu, S. K.; Papadopoulos, K.; Fong, P. C.; Patnaik, A.; Messiou, C.; Olmos, D.; Wang, G.; Tromp, B. J.; Puchalski, T. A.; Balkwill, F.; Berns, B.; Seetharam, S.; de Bono, J. S.; Tolcher, A. W., A first-in-human, first-in-class, phase I study of carlumab (CNTO 888), a human monoclonal antibody against CC-chemokine ligand 2 in patients with solid tumors. Cancer Chemother Pharmacol 2013, 71, (4), 1041-50.
58. ClinicalTrials.gov, N. L. o. H. MLN1202 in Treating Patients With Bone Metastases. https://clinicaltrials.gov/ct2/show/NCT01015560 (2017 03 07),
59. Ahn, G. O.; Tseng, D.; Liao, C. H.; Dorie, M. J.; Czechowicz, A.; Brown, J. M., Inhibition of Mac-1 (CD11b/CD18) enhances tumor response to radiation by reducing myeloid cell

recruitment. Proceedings of the National Academy of Sciences of the United States of America 2010, 107, (18), 8363-8.
60. Arnaout, M. A., Structure and function of the leukocyte adhesion molecules CD11/CD18. Blood 1990, 75, (5), 1037-50.
61. Prada, C. E.; Jousma, E.; Rizvi, T. A.; Wu, J.; Dunn, R. S.; Mayes, D. A.; Cancelas, J. A.; Dombi, E.; Kim, M. O.; West, B. L.; Bollag, G.; Ratner, N., Neurofibroma-associated macrophages play roles in tumor growth and response to pharmacological inhibition. Acta neuropathologica 2013, 125, (1), 159-68.
62. Strachan, D. C.; Ruffell, B.; Oei, Y.; Bissell, M. J.; Coussens, L. M.; Pryer, N.; Daniel, D., CSF1R inhibition delays cervical and mammary tumor growth in murine models by attenuating the turnover of tumor-associated macrophages and enhancing infiltration by CD8 T cells. Oncoimmunology 2013, 2, (12), e26968.
63. Weizman, N.; Krelin, Y.; Shabtay-Orbach, A.; Amit, M.; Binenbaum, Y.; Wong, R. J.; Gil, Z., Macrophages mediate gemcitabine resistance of pancreatic adenocarcinoma by upregulating cytidine deaminase. Oncogene 2014, 33, (29), 3812-9.
64. Pyonteck, S. M.; Akkari, L.; Schuhmacher, A. J.; Bowman, R. L.; Sevenich, L.; Quail, D. F.; Olson, O. C.; Quick, M. L.; Huse, J. T.; Teijeiro, V.; Setty, M.; Leslie, C. S.; Oei, Y.; Pedraza, A.; Zhang, J.; Brennan, C. W.; Sutton, J. C.; Holland, E. C.; Daniel, D.; Joyce, J. A., CSF-1R inhibition alters macrophage polarization and blocks glioma progression. Nature medicine 2013, 19, (10), 1264-72.
65. Sluijter, M.; van der Sluis, T. C.; van der Velden, P. A.; Versluis, M.; West, B. L.; van der Burg, S. H.; van Hall, T., Inhibition of CSF-1R supports T-cell mediated melanoma therapy. PloS one 2014, 9, (8), e104230.
66. Kim, T. S.; Cavnar, M. J.; Cohen, N. A.; Sorenson, E. C.; Greer, J. B.; Seifert, A. M.; Crawley, M. H.; Green, B. L.; Popow, R.; Pillarsetty, N.; Veach, D. R.; Ku, A. T.; Rossi, F.; Besmer, P.; Antonescu, C. R.; Zeng, S.; Dematteo, R. P., Increased KIT inhibition enhances therapeutic efficacy in gastrointestinal stromal tumor. Clinical cancer research : an official journal of the American Association for Cancer Research 2014, 20, (9), 2350-62.
67. Patwardhan, P. P.; Surriga, O.; Beckman, M. J.; de Stanchina, E.; Dematteo, R. P.; Tap, W. D.; Schwartz, G. K., Sustained inhibition of receptor tyrosine kinases and macrophage depletion by PLX3397 and rapamycin as a potential new approach for the treatment of MPNSTs. Clinical cancer

research : an official journal of the American Association for Cancer Research 2014, 20, (12), 3146-58.

68. Ries, C. H.; Cannarile, M. A.; Hoves, S.; Benz, J.; Wartha, K.; Runza, V.; Rey-Giraud, F.; Pradel, L. P.; Feuerhake, F.; Klaman, I.; Jones, T.; Jucknischke, U.; Scheiblich, S.; Kaluza, K.; Gorr, I. H.; Walz, A.; Abiraj, K.; Cassier, P. A.; Sica, A.; Gomez-Roca, C.; de Visser, K. E.; Italiano, A.; Le Tourneau, C.; Delord, J. P.; Levitsky, H.; Blay, J. Y.; Ruttinger, D., Targeting tumor-associated macrophages with anti-CSF-1R antibody reveals a strategy for cancer therapy. Cancer cell 2014, 25, (6), 846-59.
69. Roche Investor update. http://www.roche.com/investors/updates/inv-update-2014-06-01.htm (2017 01 24),
70. Duluc, D.; Corvaisier, M.; Blanchard, S.; Catala, L.; Descamps, P.; Gamelin, E.; Ponsoda, S.; Delneste, Y.; Hebbar, M.; Jeannin, P., Interferon-gamma reverses the immunosuppressive and protumoral properties and prevents the generation of human tumor-associated macrophages. International journal of cancer. Journal international du cancer 2009, 125, (2), 367-73.
71. Tang, X.; Mo, C.; Wang, Y.; Wei, D.; Xiao, H., Anti-tumour Strategies Aiming to Target Tumour-associated Macrophages. Immunology 2012.
72. Beatty, G. L.; Chiorean, E. G.; Fishman, M. P.; Saboury, B.; Teitelbaum, U. R.; Sun, W.; Huhn, R. D.; Song, W.; Li, D.; Sharp, L. L.; Torigian, D. A.; O'Dwyer, P. J.; Vonderheide, R. H., CD40 agonists alter tumor stroma and show efficacy against pancreatic carcinoma in mice and humans. Science 2011, 331, (6024), 1612-6.
73. Buhtoiarov, I. N.; Lum, H.; Berke, G.; Paulnock, D. M.; Sondel, P. M.; Rakhmilevich, A. L., CD40 ligation activates murine macrophages via an IFN-gamma-dependent mechanism resulting in tumor cell destruction in vitro. J Immunol 2005, 174, (10), 6013-22.
74. Buhtoiarov, I. N.; Lum, H. D.; Berke, G.; Sondel, P. M.; Rakhmilevich, A. L., Synergistic activation of macrophages via CD40 and TLR9 results in T cell independent antitumor effects. J Immunol 2006, 176, (1), 309-18.
75. Jensen, J. L.; Rakhmilevich, A.; Heninger, E.; Broman, A. T.; Hope, C.; Phan, F.; Miyamoto, S.; Maroulakou, I.; Callander, N.; Hematti, P.; Chesi, M.; Bergsagel, P. L.; Sondel, P.; Asimakopoulos, F., Tumoricidal Effects of Macrophage-Activating Immunotherapy in a Murine Model of Relapsed/Refractory Multiple Myeloma. Cancer immunology research 2015, 3, (8), 881-90.

76. Mantovani, A.; Marchesi, F.; Malesci, A.; Laghi, L.; Allavena, P., Tumour-associated macrophages as treatment targets in oncology. Nat Rev Clin Oncol 2017.
77. Olsson, A.; Nakhle, J.; Sundstedt, A.; Plas, P.; Bauchet, A. L.; Pierron, V.; Bruetschy, L.; Deronic, A.; Torngren, M.; Liberg, D.; Schmidlin, F.; Leanderson, T., Tasquinimod triggers an early change in the polarization of tumor associated macrophages in the tumor microenvironment. J Immunother Cancer 2015, 3, 53.
78. Shen, L.; Sundstedt, A.; Ciesielski, M.; Miles, K. M.; Celander, M.; Adelaiye, R.; Orillion, A.; Ciamporcero, E.; Ramakrishnan, S.; Ellis, L.; Fenstermaker, R.; Abrams, S. I.; Eriksson, H.; Leanderson, T.; Olsson, A.; Pili, R., Tasquinimod Modulates Suppressive Myeloid Cells and Enhances Cancer Immunotherapies in Murine Models. Cancer immunology research 2014.
79. White, E. S.; Flaherty, K. R.; Carskadon, S.; Brant, A.; Iannettoni, M. D.; Yee, J.; Orringer, M. B.; Arenberg, D. A., Macrophage migration inhibitory factor and CXC chemokine expression in non-small cell lung cancer: role in angiogenesis and prognosis. Clinical cancer research : an official journal of the American Association for Cancer Research 2003, 9, (2), 853-60.
80. White, E. S.; Strom, S. R.; Wys, N. L.; Arenberg, D. A., Non-small cell lung cancer cells induce monocytes to increase expression of angiogenic activity. J Immunol 2001, 166, (12), 7549-55.
81. Yaddanapudi, K.; Putty, K.; Rendon, B. E.; Lamont, G. J.; Faughn, J. D.; Satoskar, A.; Lasnik, A.; Eaton, J. W.; Mitchell, R. A., Control of tumor-associated macrophage alternative activation by macrophage migration inhibitory factor. J Immunol 2013, 190, (6), 2984-93.
82. Cheng, F.; Wang, H. W.; Cuenca, A.; Huang, M.; Ghansah, T.; Brayer, J.; Kerr, W. G.; Takeda, K.; Akira, S.; Schoenberger, S. P.; Yu, H.; Jove, R.; Sotomayor, E. M., A critical role for Stat3 signaling in immune tolerance. Immunity 2003, 19, (3), 425-36.
83. Xin, H.; Zhang, C.; Herrmann, A.; Du, Y.; Figlin, R.; Yu, H., Sunitinib inhibition of Stat3 induces renal cell carcinoma tumor cell apoptosis and reduces immunosuppressive cells. Cancer research 2009, 69, (6), 2506-13.
84. Edwards, J. P.; Emens, L. A., The multikinase inhibitor sorafenib reverses the suppression of IL-12 and enhancement of IL-10 by PGE(2) in murine macrophages. International immunopharmacology 2010, 10, (10), 1220-8.

85. Hebenstreit, D.; Wirnsberger, G.; Horejs-Hoeck, J.; Duschl, A., Signaling mechanisms, interaction partners, and target genes of STAT6. Cytokine & growth factor reviews 2006, 17, (3), 173-88.
86. Binnemars-Postma, K.; Bansal, R.; Storm, G.; Prakash, J., 355 Targeting the STAT6 pathway to inhibit tumor-associated macrophages-induced tumor growth and metastasis in breast cancer. European Journal of Cancer 51, S72-S73.
87. Germano, G.; Frapolli, R.; Belgiovine, C.; Anselmo, A.; Pesce, S.; Liguori, M.; Erba, E.; Uboldi, S.; Zucchetti, M.; Pasqualini, F.; Nebuloni, M.; van Rooijen, N.; Mortarini, R.; Beltrame, L.; Marchini, S.; Fuso Nerini, I.; Sanfilippo, R.; Casali, P. G.; Pilotti, S.; Galmarini, C. M.; Anichini, A.; Mantovani, A.; D'Incalci, M.; Allavena, P., Role of macrophage targeting in the antitumor activity of trabectedin. Cancer cell 2013, 23, (2), 249-62.
88. Rogers, T. L.; Holen, I., Tumour macrophages as potential targets of bisphosphonates. Journal of translational medicine 2011, 9, 177.
89. Fleisch, H., Bisphosphonates: a new class of drugs in diseases of bone and calcium metabolism. Recent Results Cancer Res 1989, 116, 1-28.
90. van Rooijen, N.; van Nieuwmegen, R., Elimination of phagocytic cells in the spleen after intravenous injection of liposome-encapsulated dichloromethylene diphosphonate. An enzyme-histochemical study. Cell Tissue Res 1984, 238, (2), 355-8.
91. Brown, H. K.; Holen, I., Anti-tumour effects of bisphosphonates--what have we learned from in vivo models? Current cancer drug targets 2009, 9, (7), 807-23.
92. Zeisberger, S. M.; Odermatt, B.; Marty, C.; Zehnder-Fjallman, A. H.; Ballmer-Hofer, K.; Schwendener, R. A., Clodronate-liposome-mediated depletion of tumour-associated macrophages: a new and highly effective antiangiogenic therapy approach. Br J Cancer 2006, 95, (3), 272-81.
93. Wu, X.; Schulte, B. C.; Zhou, Y.; Haribhai, D.; Mackinnon, A. C.; Plaza, J. A.; Williams, C. B.; Hwang, S. T., Depletion of M2-Like Tumor-Associated Macrophages Delays Cutaneous T-Cell Lymphoma Development In Vivo. The Journal of investigative dermatology 2014.
94. Zhang, W.; Zhu, X. D.; Sun, H. C.; Xiong, Y. Q.; Zhuang, P. Y.; Xu, H. X.; Kong, L. Q.; Wang, L.; Wu, W. Z.; Tang, Z. Y., Depletion of tumor-associated macrophages enhances the effect of sorafenib in metastatic liver cancer models by antimetastatic and antiangiogenic effects. Clinical cancer

research : an official journal of the American Association for Cancer Research 2010, 16, (13), 3420-30.
95. Junankar, S.; Shay, G.; Jurczyluk, J.; Ali, N.; Down, J.; Pocock, N.; Parker, A.; Nguyen, A.; Sun, S.; Kashemirov, B.; McKenna, C. E.; Croucher, P. I.; Swarbrick, A.; Weilbaecher, K.; Phan, T. G.; Rogers, M. J., Real-time intravital imaging establishes tumor-associated macrophages as the extraskeletal target of bisphosphonate action in cancer. Cancer Discov 2015, 5, (1), 35-42.
96. Guan, Y.; Sakai, R.; Rinehart, K. L.; Wang, A. H., Molecular and crystal structures of ecteinascidins: potent antitumor compounds from the Caribbean tunicate Ecteinascidia turbinata. J Biomol Struct Dyn 1993, 10, (5), 793-818.
97. Allavena, P.; Signorelli, M.; Chieppa, M.; Erba, E.; Bianchi, G.; Marchesi, F.; Olimpio, C. O.; Bonardi, C.; Garbi, A.; Lissoni, A.; de Braud, F.; Jimeno, J.; D'Incalci, M., Anti-inflammatory properties of the novel antitumor agent yondelis (trabectedin): inhibition of macrophage differentiation and cytokine production. Cancer research 2005, 65, (7), 2964-71.
98. Pommier, Y.; Kohlhagen, G.; Bailly, C.; Waring, M.; Mazumder, A.; Kohn, K. W., DNA sequence- and structure-selective alkylation of guanine N2 in the DNA minor groove by ecteinascidin 743, a potent antitumor compound from the Caribbean tunicate Ecteinascidia turbinata. Biochemistry 1996, 35, (41), 13303-9.
99. Zewail-Foote, M.; Hurley, L. H., Ecteinascidin 743: a minor groove alkylator that bends DNA toward the major groove. J Med Chem 1999, 42, (14), 2493-7.
100. Erba, E.; Bergamaschi, D.; Bassano, L.; Damia, G.; Ronzoni, S.; Faircloth, G. T.; D'Incalci, M., Ecteinascidin-743 (ET-743), a natural marine compound, with a unique mechanism of action. Eur J Cancer 2001, 37, (1), 97-105.
101. D'Incalci, M.; Zambelli, A., Trabectedin for the treatment of breast cancer. Expert Opin Investig Drugs 2016, 25, (1), 105-15.
102. Germano, G.; Frapolli, R.; Simone, M.; Tavecchio, M.; Erba, E.; Pesce, S.; Pasqualini, F.; Grosso, F.; Sanfilippo, R.; Casali, P. G.; Gronchi, A.; Virdis, E.; Tarantino, E.; Pilotti, S.; Greco, A.; Nebuloni, M.; Galmarini, C. M.; Tercero, J. C.; Mantovani, A.; D'Incalci, M.; Allavena, P., Antitumor and anti-inflammatory effects of trabectedin on human myxoid liposarcoma cells. Cancer research 2010, 70, (6), 2235-44.
103. Atmaca, H.; Uzunoglu, S., Anti-angiogenic effects of trabectedin (Yondelis; ET-743) on human breast cancer cells. Eur Cytokine Netw 2014, 25, (1), 1-7.

104. Flannagan, R. S.; Jaumouille, V.; Grinstein, S., The cell biology of phagocytosis. Annu Rev Pathol 2012, 7, 61-98.
105. Alexis, F.; Pridgen, E.; Molnar, L. K.; Farokhzad, O. C., Factors affecting the clearance and biodistribution of polymeric nanoparticles. Molecular pharmaceutics 2008, 5, (4), 505-15.
106. Haniffa, M.; Bigley, V.; Collin, M., Human mononuclear phagocyte system reunited. Semin. Cell Dev. Biol. 2015.
107. Liu, T.; Choi, H.; Zhou, R.; Chen, I. W., Quantitative evaluation of the reticuloendothelial system function with dynamic MRI. PloS one 2014, 9, (8), e103576.
108. Owens, D. E., 3rd; Peppas, N. A., Opsonization, biodistribution, and pharmacokinetics of polymeric nanoparticles. Int. J. Pharm. 2006, 307, (1), 93-102.
109. Maeda, H.; Nakamura, H.; Fang, J., The EPR effect for macromolecular drug delivery to solid tumors: Improvement of tumor uptake, lowering of systemic toxicity, and distinct tumor imaging in vivo. Adv Drug Deliv Rev 2013, 65, (1), 71-9.
110. Nichols, J. W.; Bae, Y. H., EPR: Evidence and fallacy. Journal of controlled release : official journal of the Controlled Release Society 2014, 190, 451-64.
111. Shi, J.; Kantoff, P. W.; Wooster, R.; Farokhzad, O. C., Cancer nanomedicine: progress, challenges and opportunities. Nature reviews. Cancer 2017, 17, (1), 20-37.
112. Anchordoquy, T. J.; Barenholz, Y.; Boraschi, D.; Chorny, M.; Decuzzi, P.; Dobrovolskaia, M. A.; Farhangrazi, Z. S.; Farrell, D.; Gabizon, A.; Ghandehari, H.; Godin, B.; La-Beck, N. M.; Ljubimova, J.; Moghimi, S. M.; Pagliaro, L.; Park, J. H.; Peer, D.; Ruoslahti, E.; Serkova, N. J.; Simberg, D., Mechanisms and Barriers in Cancer Nanomedicine: Addressing Challenges, Looking for Solutions. ACS nano 2017, 11, (1), 12-18.
113. Miller, M. A.; Gadde, S.; Pfirschke, C.; Engblom, C.; Sprachman, M. M.; Kohler, R. H.; Yang, K. S.; Laughney, A. M.; Wojtkiewicz, G.; Kamaly, N.; Bhonagiri, S.; Pittet, M. J.; Farokhzad, O. C.; Weissleder, R., Predicting therapeutic nanomedicine efficacy using a companion magnetic resonance imaging nanoparticle. Sci Transl Med 2015, 7, (314), 314ra183.
114. Miller, M. A.; Zheng, Y. R.; Gadde, S.; Pfirschke, C.; Zope, H.; Engblom, C.; Kohler, R. H.; Iwamoto, Y.; Yang, K. S.; Askevold, B.; Kolishetti, N.; Pittet, M.; Lippard, S. J.; Farokhzad, O. C.; Weissleder, R., Tumour-associated macrophages act as a slow-release reservoir of nano-therapeutic Pt(IV) pro-drug. Nat Commun 2015, 6, 8692.
115. Si, J.; Shao, S.; Shen, Y.; Wang, K., Macrophages as Active Nanocarriers for Targeted Early and Adjuvant Cancer Chemotherapy. Small 2016, 12, (37), 5108-5119.

116. Allen, T. M.; Cullis, P. R., Liposomal drug delivery systems: from concept to clinical applications. Adv Drug Deliv Rev 2013, 65, (1), 36-48.
117. Shmeeda, H.; Amitay, Y.; Gorin, J.; Tzemach, D.; Mak, L.; Stern, S. T.; Barenholz, Y.; Gabizon, A., Coencapsulation of alendronate and doxorubicin in pegylated liposomes: a novel formulation for chemoimmunotherapy of cancer. Journal of drug targeting 2016, 24, (9), 878-889.
118. Qi, X. F.; Kim, D. H.; Yoon, Y. S.; Kim, S. K.; Cai, D. Q.; Teng, Y. C.; Shim, K. Y.; Lee, K. J., Involvement of oxidative stress in simvastatin-induced apoptosis of murine CT26 colon carcinoma cells. Toxicol Lett 2010, 199, (3), 277-87.
119. Alupei, M. C.; Licarete, E.; Patras, L.; Banciu, M., Liposomal simvastatin inhibits tumor growth via targeting tumor-associated macrophages-mediated oxidative stress. Cancer letters 2015, 356, (2 Pt B), 946-52.
120. Perez-Herrero, E.; Fernandez-Medarde, A., Advanced targeted therapies in cancer: Drug nanocarriers, the future of chemotherapy. Eur J Pharm Biopharm 2015, 93, 52-79.
121. Peres, C.; Matos, A. I.; Conniot, J.; Sainz, V.; Zupancic, E.; Silva, J. M.; Graca, L.; Sa Gaspar, R.; Preat, V.; Florindo, H. F., Poly(lactic acid)-based particulate systems are promising tools for immune modulation. Acta biomaterialia 2017, 48, 41-57.
122. Zou, L.; Tao, Y.; Payne, G.; Do, L.; Thomas, T.; Rodriguez, J.; Dou, H., Targeted delivery of nano-PTX to the brain tumor-associated macrophages. Oncotarget 2016.
123. Ernsting, M. J.; Hoang, B.; Lohse, I.; Undzys, E.; Cao, P.; Do, T.; Gill, B.; Pintilie, M.; Hedley, D.; Li, S. D., Targeting of metastasis-promoting tumor-associated fibroblasts and modulation of pancreatic tumor-associated stroma with a carboxymethylcellulose-docetaxel nanoparticle. Journal of controlled release : official journal of the Controlled Release Society 2015, 206, 122-30.
124. Cerulean Pharma Inc. Platform & Pipeline CRLX101. http://ceruleanrx.com/platform-pipeline/crlx101.php (2017 01 23),
125. Alizadeh, D.; Zhang, L.; Hwang, J.; Schluep, T.; Badie, B., Tumor-associated macrophages are predominant carriers of cyclodextrin-based nanoparticles into gliomas. Nanomedicine 2010, 6, (2), 382-90.
126. Zhang, F.; Mastorakos, P.; Mishra, M. K.; Mangraviti, A.; Hwang, L.; Zhou, J.; Hanes, J.; Brem, H.; Olivi, A.; Tyler, B.; Kannan, R. M., Uniform brain tumor distribution and tumor associated macrophage targeting of systemically administered dendrimers. Biomaterials 2015, 52, 507-16.

127. Bashir, M. R.; Bhatti, L.; Marin, D.; Nelson, R. C., Emerging applications for ferumoxytol as a contrast agent in MRI. J Magn Reson Imaging 2015, 41, (4), 884-98.
128. Zanganeh, S.; Hutter, G.; Spitler, R.; Lenkov, O.; Mahmoudi, M.; Shaw, A.; Pajarinen, J. S.; Nejadnik, H.; Goodman, S.; Moseley, M.; Coussens, L. M.; Daldrup-Link, H. E., Iron oxide nanoparticles inhibit tumour growth by inducing pro-inflammatory macrophage polarization in tumour tissues. Nat Nanotechnol 2016, 11, (11), 986-994.
129. Kruse, C. A.; Freehauf, C. L.; Patel, K. R.; Baldeschwieler, J. D., Mouse erythrocyte carriers osmotically loaded with methotrexate. Biotechnol Appl Biochem 1987, 9, (2), 123-40.
130. Rossi, L.; Serafini, S.; Antonelli, A.; Pierige, F.; Carnevali, A.; Battistelli, V.; Malatesta, M.; Balestra, E.; Calio, R.; Perno, C. F.; Magnani, M., Macrophage depletion induced by clodronate-loaded erythrocytes. Journal of drug targeting 2005, 13, (2), 99-111.
131. Sabatino, R.; Antonelli, A.; Battistelli, S.; Schwendener, R.; Magnani, M.; Rossi, L., Macrophage depletion by free bisphosphonates and zoledronate-loaded red blood cells. PloS one 2014, 9, (6), e101260.
132. Duivenvoorden, R.; Tang, J.; Cormode, D. P.; Mieszawska, A. J.; Izquierdo-Garcia, D.; Ozcan, C.; Otten, M. J.; Zaidi, N.; Lobatto, M. E.; van Rijs, S. M.; Priem, B.; Kuan, E. L.; Martel, C.; Hewing, B.; Sager, H.; Nahrendorf, M.; Randolph, G. J.; Stroes, E. S.; Fuster, V.; Fisher, E. A.; Fayad, Z. A.; Mulder, W. J., A statin-loaded reconstituted high-density lipoprotein nanoparticle inhibits atherosclerotic plaque inflammation. Nat Commun 2014, 5, 3065.
133. Tang, J.; Lobatto, M. E.; Hassing, L.; van der Staay, S.; van Rijs, S. M.; Calcagno, C.; Braza, M. S.; Baxter, S.; Fay, F.; Sanchez-Gaytan, B. L.; Duivenvoorden, R.; Sager, H.; Astudillo, Y. M.; Leong, W.; Ramachandran, S.; Storm, G.; Perez-Medina, C.; Reiner, T.; Cormode, D. P.; Strijkers, G. J.; Stroes, E. S.; Swirski, F. K.; Nahrendorf, M.; Fisher, E. A.; Fayad, Z. A.; Mulder, W. J., Inhibiting macrophage proliferation suppresses atherosclerotic plaque inflammation. Sci Adv 2015, 1, (3).
134. Perez-Medina, C.; Tang, J.; Abdel-Atti, D.; Hogstad, B.; Merad, M.; Fisher, E. A.; Fayad, Z. A.; Lewis, J. S.; Mulder, W. J.; Reiner, T., PET Imaging of Tumor-Associated Macrophages with 89Zr-Labeled High-Density Lipoprotein Nanoparticles. Journal of nuclear medicine : official publication, Society of Nuclear Medicine 2015, 56, (8), 1272-7.
135. Agrawal, A.; Manchester, M., Differential uptake of chemically modified cowpea mosaic virus nanoparticles in macrophage

subpopulations present in inflammatory and tumor microenvironments. Biomacromolecules 2012, 13, (10), 3320-6.
136. Wen, A. M.; Lee, K. L.; Cao, P.; Pangilinan, K.; Carpenter, B. L.; Lam, P.; Veliz, F. A.; Ghiladi, R. A.; Advincula, R. C.; Steinmetz, N. F., Utilizing Viral Nanoparticle/Dendron Hybrid Conjugates in Photodynamic Therapy for Dual Delivery to Macrophages and Cancer Cells. Bioconjug Chem 2016, 27, (5), 1227-35.
137. Klumpp, C.; Kostarelos, K.; Prato, M.; Bianco, A., Functionalized carbon nanotubes as emerging nanovectors for the delivery of therapeutics. Biochimica et biophysica acta 2006, 1758, (3), 404-12.
138. VanHandel, M.; Alizadeh, D.; Zhang, L.; Kateb, B.; Bronikowski, M.; Manohara, H.; Badie, B., Selective uptake of multi-walled carbon nanotubes by tumor macrophages in a murine glioma model. J Neuroimmunol 2009, 208, (1-2), 3-9.
139. Zhao, D.; Alizadeh, D.; Zhang, L.; Liu, W.; Farrukh, O.; Manuel, E.; Diamond, D. J.; Badie, B., Carbon nanotubes enhance CpG uptake and potentiate antiglioma immunity. Clinical cancer research : an official journal of the American Association for Cancer Research 2011, 17, (4), 771-82.
140. Fan, H.; Zhang, I.; Chen, X.; Zhang, L.; Wang, H.; Da Fonseca, A.; Manuel, E. R.; Diamond, D. J.; Raubitschek, A.; Badie, B., Intracerebral CpG immunotherapy with carbon nanotubes abrogates growth of subcutaneous melanomas in mice. Clinical cancer research : an official journal of the American Association for Cancer Research 2012, 18, (20), 5628-38.
141. Lohcharoenkal, W.; Wang, L.; Chen, Y. C.; Rojanasakul, Y., Protein nanoparticles as drug delivery carriers for cancer therapy. Biomed Res Int 2014, 2014, 180549.
142. Kundranda, M. N.; Niu, J., Albumin-bound paclitaxel in solid tumors: clinical development and future directions. Drug Des Devel Ther 2015, 9, 3767-77.
143. Desai, N.; Trieu, V.; Yao, Z.; Louie, L.; Ci, S.; Yang, A.; Tao, C.; De, T.; Beals, B.; Dykes, D.; Noker, P.; Yao, R.; Labao, E.; Hawkins, M.; Soon-Shiong, P., Increased antitumor activity, intratumor paclitaxel concentrations, and endothelial cell transport of cremophor-free, albumin-bound paclitaxel, ABI-007, compared with cremophor-based paclitaxel. Clinical cancer research : an official journal of the American Association for Cancer Research 2006, 12, (4), 1317-24.
144. Desai, N. P.; Trieu, V.; Hwang, L. Y.; Wu, R.; Soon-Shiong, P.; Gradishar, W. J., Improved effectiveness of nanoparticle albumin-bound (nab) paclitaxel versus polysorbate-based

docetaxel in multiple xenografts as a function of HER2 and SPARC status. Anticancer Drugs 2008, 19, (9), 899-909.
145. Desai, N.; Trieu, V.; Damascelli, B.; Soon-Shiong, P., SPARC Expression Correlates with Tumor Response to Albumin-Bound Paclitaxel in Head and Neck Cancer Patients. Transl Oncol 2009, 2, (2), 59-64.
146. Cullis, J.; Siolas, D.; Avanzi, A.; Barui, S.; Maitra, A.; Bar-Sagi, D., Macropinocytosis of Nab-paclitaxel Drives Macrophage Activation in Pancreatic Cancer. Cancer immunology research 2017, 5, (3), 182-190.
147. Tanei, T.; Leonard, F.; Liu, X.; Alexander, J. F.; Saito, Y.; Ferrari, M.; Godin, B.; Yokoi, K., Redirecting Transport of Nanoparticle Albumin-Bound Paclitaxel to Macrophages Enhances Therapeutic Efficacy against Liver Metastases. Cancer research 2016, 76, (2), 429-39.
148. Verma, A.; Stellacci, F., Effect of surface properties on nanoparticle-cell interactions. Small 2010, 6, (1), 12-21.
149. Binnemars-Postma, K. A.; Ten Hoopen, H. W.; Storm, G.; Prakash, J., Differential uptake of nanoparticles by human M1 and M2 polarized macrophages: protein corona as a critical determinant. Nanomedicine (Lond) 2016, 11, (22), 2889-2902.
150. Perrie, Y.; Frederik, P. M.; Gregoriadis, G., Liposome-mediated DNA vaccination: the effect of vesicle composition. Vaccine 2001, 19, (23-24), 3301-10.
151. Ishii, N.; Fukushima, J.; Kaneko, T.; Okada, E.; Tani, K.; Tanaka, S. I.; Hamajima, K.; Xin, K. Q.; Kawamoto, S.; Koff, W.; Nishioka, K.; Yasuda, T.; Okuda, K., Cationic liposomes are a strong adjuvant for a DNA vaccine of human immunodeficiency virus type 1. AIDS Res Hum Retroviruses 1997, 13, (16), 1421-8.
152. Tanaka, M.; Kaneda, Y.; Fujii, S.; Yamano, T.; Hashimoto, K.; Huang, S. K.; Hoon, D. S., Induction of a systemic immune response by a polyvalent melanoma-associated antigen DNA vaccine for prevention and treatment of malignant melanoma. Mol Ther 2002, 5, (3), 291-9.
153. Toda, S.; Ishii, N.; Okada, E.; Kusakabe, K. I.; Arai, H.; Hamajima, K.; Gorai, I.; Nishioka, K.; Okuda, K., HIV-1-specific cell-mediated immune responses induced by DNA vaccination were enhanced by mannan-coated liposomes and inhibited by anti-interferon-gamma antibody. Immunology 1997, 92, (1), 111-7.
154. Hattori, Y.; Kawakami, S.; Suzuki, S.; Yamashita, F.; Hashida, M., Enhancement of immune responses by DNA vaccination through targeted gene delivery using mannosylated cationic liposome formulations following intravenous administration in

mice. Biochemical and biophysical research communications 2004, 317, (4), 992-9.
155. Locke, L. W.; Mayo, M. W.; Yoo, A. D.; Williams, M. B.; Berr, S. S., PET imaging of tumor associated macrophages using mannose coated 64Cu liposomes. Biomaterials 2012, 33, (31), 7785-93.
156. Kaur, A.; Jain, S.; Tiwary, A. K., Mannan-coated gelatin nanoparticles for sustained and targeted delivery of didanosine: in vitro and in vivo evaluation. Acta Pharm 2008, 58, (1), 61-74.
157. Yu, W.; Liu, C.; Liu, Y.; Zhang, N.; Xu, W., Mannan-modified solid lipid nanoparticles for targeted gene delivery to alveolar macrophages. Pharmaceutical research 2010, 27, (8), 1584-96.
158. Zhan, X.; Jia, L.; Niu, Y.; Qi, H.; Chen, X.; Zhang, Q.; Zhang, J.; Wang, Y.; Dong, L.; Wang, C., Targeted depletion of tumour-associated macrophages by an alendronate-glucomannan conjugate for cancer immunotherapy. Biomaterials 2014, 35, (38), 10046-57.
159. Zhu, S.; Niu, M.; O'Mary, H.; Cui, Z., Targeting of tumor-associated macrophages made possible by PEG-sheddable, mannose-modified nanoparticles. Molecular pharmaceutics 2013, 10, (9), 3525-30.
160. Niu, M.; Naguib, Y. W.; Aldayel, A. M.; Shi, Y. C.; Hursting, S. D.; Hersh, M. A.; Cui, Z., Biodistribution and in vivo activities of tumor-associated macrophage-targeting nanoparticles incorporated with doxorubicin. Molecular pharmaceutics 2014, 11, (12), 4425-36.
161. Niu, M.; Valdes, S.; Naguib, Y. W.; Hursting, S. D.; Cui, Z., Tumor-Associated Macrophage-Mediated Targeted Therapy of Triple-Negative Breast Cancer. Molecular pharmaceutics 2016, 13, (6), 1833-42.
162. Ortega, R. A.; Barham, W. J.; Kumar, B.; Tikhomirov, O.; McFadden, I. D.; Yull, F. E.; Giorgio, T. D., Biocompatible mannosylated endosomal-escape nanoparticles enhance selective delivery of short nucleotide sequences to tumor associated macrophages. Nanoscale 2014, 7, (2), 500-10.
163. Ortega, R. A.; Barham, W.; Sharman, K.; Tikhomirov, O.; Giorgio, T. D.; Yull, F. E., Manipulating the NF-kappaB pathway in macrophages using mannosylated, siRNA-delivering nanoparticles can induce immunostimulatory and tumor cytotoxic functions. International journal of nanomedicine 2016, 11, 2163-77.
164. Yu, S. S.; Lau, C. M.; Barham, W. J.; Onishko, H. M.; Nelson, C. E.; Li, H.; Smith, C. A.; Yull, F. E.; Duvall, C. L.; Giorgio, T. D., Macrophage-specific RNA interference targeting via "click",

mannosylated polymeric micelles. Molecular pharmaceutics 2013, 10, (3), 975-87.
165. Turk, M. J.; Waters, D. J.; Low, P. S., Folate-conjugated liposomes preferentially target macrophages associated with ovarian carcinoma. Cancer letters 2004, 213, (2), 165-72.
166. Puig-Kroger, A.; Sierra-Filardi, E.; Dominguez-Soto, A.; Samaniego, R.; Corcuera, M. T.; Gomez-Aguado, F.; Ratnam, M.; Sanchez-Mateos, P.; Corbi, A. L., Folate receptor beta is expressed by tumor-associated macrophages and constitutes a marker for M2 anti-inflammatory/regulatory macrophages. Cancer research 2009, 69, (24), 9395-403.
167. Nagai, T.; Tanaka, M.; Tsuneyoshi, Y.; Xu, B.; Michie, S. A.; Hasui, K.; Hirano, H.; Arita, K.; Matsuyama, T., Targeting tumor-associated macrophages in an experimental glioma model with a recombinant immunotoxin to folate receptor beta. Cancer immunology, immunotherapy : CII 2009, 58, (10), 1577-86.
168. Hattori, Y.; Yamashita, J.; Sakaida, C.; Kawano, K.; Yonemochi, E., Evaluation of antitumor effect of zoledronic acid entrapped in folate-linked liposome for targeting to tumor-associated macrophages. Journal of liposome research 2014, 1-10.
169. Daldrup-Link, H. E.; Golovko, D.; Ruffell, B.; Denardo, D. G.; Castaneda, R.; Ansari, C.; Rao, J.; Tikhomirov, G. A.; Wendland, M. F.; Corot, C.; Coussens, L. M., MRI of tumor-associated macrophages with clinically applicable iron oxide nanoparticles. Clinical cancer research : an official journal of the American Association for Cancer Research 2011, 17, (17), 5695-704.
170. Tang, X., Tumor-associated macrophages as potential diagnostic and prognostic biomarkers in breast cancer. Cancer Lett 2013, 332, (1), 3-10.
171. Fabriek, B. O.; Dijkstra, C. D.; van den Berg, T. K., The macrophage scavenger receptor CD163. Immunobiology 2005, 210, (2-4), 153-60.
172. Gordon, S., Alternative activation of macrophages. Nat Rev Immunol 2003, 3, (1), 23-35.
173. Etzerodt, A.; Maniecki, M. B.; Graversen, J. H.; Moller, H. J.; Torchilin, V. P.; Moestrup, S. K., Efficient intracellular drug-targeting of macrophages using stealth liposomes directed to the hemoglobin scavenger receptor CD163. Journal of controlled release : official journal of the Controlled Release Society 2012, 160, (1), 72-80.
174. Liu, C.; Sun, C.; Huang, H.; Janda, K.; Edgington, T., Overexpression of legumain in tumors is significant for

invasion/metastasis and a candidate enzymatic target for prodrug therapy. Cancer research 2003, 63, (11), 2957-64.
175. Murthy, R. V.; Arbman, G.; Gao, J.; Roodman, G. D.; Sun, X. F., Legumain expression in relation to clinicopathologic and biological variables in colorectal cancer. Clinical cancer research : an official journal of the American Association for Cancer Research 2005, 11, (6), 2293-9.
176. Luo, Y.; Zhou, H.; Krueger, J.; Kaplan, C.; Lee, S. H.; Dolman, C.; Markowitz, D.; Wu, W.; Liu, C.; Reisfeld, R. A.; Xiang, R., Targeting tumor-associated macrophages as a novel strategy against breast cancer. The Journal of clinical investigation 2006, 116, (8), 2132-2141.
177. Liao, D.; Liu, Z.; Wrasidlo, W.; Chen, T.; Luo, Y.; Xiang, R.; Reisfeld, R. A., Synthetic enzyme inhibitor: a novel targeting ligand for nanotherapeutic drug delivery inhibiting tumor growth without systemic toxicity. Nanomedicine 2011, 7, (6), 665-73.
178. Zhang, X.; Tian, W.; Cai, X.; Wang, X.; Dang, W.; Tang, H.; Cao, H.; Wang, L.; Chen, T., Hydrazinocurcumin Encapsuled nanoparticles "re-educate" tumor-associated macrophages and exhibit anti-tumor effects on breast cancer following STAT3 suppression. PloS one 2013, 8, (6), e65896.
179. Song, X.; Wan, Z.; Chen, T.; Fu, Y.; Jiang, K.; Yi, X.; Ke, H.; Dong, J.; Yang, L.; Li, L.; Sun, X.; Gong, T.; Zhang, Z., Development of a multi-target peptide for potentiating chemotherapy by modulating tumor microenvironment. Biomaterials 2016, 108, 44-56.
180. Raes, G.; Brys, L.; Dahal, B. K.; Brandt, J.; Grooten, J.; Brombacher, F.; Vanham, G.; Noel, W.; Bogaert, P.; Boonefaes, T.; Kindt, A.; Van den Bergh, R.; Leenen, P. J.; De Baetselier, P.; Ghassabeh, G. H., Macrophage galactose-type C-type lectins as novel markers for alternatively activated macrophages elicited by parasitic infections and allergic airway inflammation. Journal of leukocyte biology 2005, 77, (3), 321-7.
181. Huang, Z.; Zhang, Z.; Jiang, Y.; Zhang, D.; Chen, J.; Dong, L.; Zhang, J., Targeted delivery of oligonucleotides into tumor-associated macrophages for cancer immunotherapy. Journal of controlled release : official journal of the Controlled Release Society 2012, 158, (2), 286-92.
182. Zhang, M.; Kim, J. A., Effect of molecular size and modification pattern on the internalization of water soluble beta-(1 --> 3)-(1 --> 4)-glucan by primary murine macrophages. Int J Biochem Cell Biol 2012, 44, (6), 914-27.

183. Zhang, M.; Gao, Y.; Caja, K.; Zhao, B.; Kim, J. A., Non-viral nanoparticle delivers small interfering RNA to macrophages in vitro and in vivo. PloS one 2015, 10, (3), e0118472.
184. Cieslewicz, M.; Tang, J.; Yu, J. L.; Cao, H.; Zavaljevski, M.; Motoyama, K.; Lieber, A.; Raines, E. W.; Pun, S. H., Targeted delivery of proapoptotic peptides to tumor-associated macrophages improves survival. Proceedings of the National Academy of Sciences of the United States of America 2013, 110, (40), 15919-24.
185. Cook, J.; Hagemann, T., Tumour-associated macrophages and cancer. Current opinion in pharmacology 2013, 13, (4), 595-601.
186. Shmeeda, H.; Amitay, Y.; Tzemach, D.; Gorin, J.; Gabizon, A., Liposome encapsulation of zoledronic acid results in major changes in tissue distribution and increase in toxicity. Journal of controlled release : official journal of the Controlled Release Society 2013, 167, (3), 265-75.
187. Golbar, H. M.; Izawa, T.; Wijesundera, K. K.; Bondoc, A.; Tennakoon, A. H.; Kuwamura, M.; Yamate, J., Depletion of Hepatic Macrophages Aggravates Liver Lesions Induced in Rats by Thioacetamide (TAA). Toxicol Pathol 2016, 44, (2), 246-58.
188. Liu, X.; Liu, Y.; Zhao, L.; Zeng, Z.; Xiao, W.; Chen, P., Macrophage depletion impairs skeletal muscle regeneration: The roles of regulatory factors for muscle regeneration. Cell Biol Int 2017, 41, (3), 228-238.
189. Mosser, D. M.; Edwards, J. P., Exploring the full spectrum of macrophage activation. Nat Rev Immunol 2008, 8, (12), 958-69.
190. Patel, S. K.; Janjic, J. M., Macrophage targeted theranostics as personalized nanomedicine strategies for inflammatory diseases. Theranostics 2015, 5, (2), 150-72.
191. Hoppstadter, J.; Seif, M.; Dembek, A.; Cavelius, C.; Huwer, H.; Kraegeloh, A.; Kiemer, A. K., M2 polarization enhances silica nanoparticle uptake by macrophages. Front Pharmacol 2015, 6, 55.

Chapter 3

Differential Uptake of Nanoparticles by Human M1 and M2 Polarized Macrophages: Protein Corona as a Critical Determinant

Published: Nanomedicine (Lond). 2016 Nov;11(22):2889-2902

Abstract

Aim: To investigate the interaction behavior of M1- and M2-type macrophages with nanoparticles of different sizes with/without the presence of serum. Materials/Methods: THP-1 human monocytes were differentiated into M1 and M2 macrophages and the uptake of silica nanoparticle (50-1000 nm) was studied using flow cytometry and different microscopies. Results: Without serum, higher uptake of all sized nanoparticles was observed by M1 compared to M2. With serum, uptake of nanoparticles (200-1000 nm) was dramatically increased by M2. Furthermore, serum proteins adsorbed (corona) by nanoparticles were found to be the ligands for receptors expressed by M2, as revealed by SDS-PAGE and gene profiling analyses. Conclusion: The observed differential uptake by M1 and M2 macrophages will help understand the fate of nanoparticles *in vivo*.

1 Introduction

Nanoscale particles are increasingly used for *in vivo* applications for diagnostics and therapeutics [1-3]. *In vivo*, the fate of nanoparticles is determined by their interaction with the immune system. Macrophages, the professional phagocytic immune cells, are responsible for the clearance of foreign particles and are largely localized in liver, lungs and spleen [4]. Once exposed to the foreign particles, macrophages rapidly engulf and degrade them [5-8]. Interaction between macrophages and particles remains a key topic of research, impacting various fields of nanomaterials, nanomedicine and nanotoxicology [9-11].

Cellular interaction and uptake of nanoparticles by macrophages is a dynamic and intricate process in which physicochemical characteristics of nanoparticles, including size, shape, charge and elasticity influence their interaction and uptake by macrophages. Large-sized nanoparticles are shown to be more efficiently taken up by macrophages than smaller-sized nanoparticles [7, 12]. Champion and Mitragotri demonstrated that elongated nanoparticles compared to spherical ones are engulfed by macrophages at much slower rate [13]. Furthermore, other studies showed that charged particles were taken up to higher extent by macrophages compared to neutral particles [14, 15]. Recently, particle elasticity was shown by Anselmo *et al* to influence particle uptake by immune cells and other cell types [16]. However, in these studies, macrophages were considered as a single cell population, despite the fact that macrophages are not a homogenous cell population, but rather exist in different phenotypes *i.e.* M1 and M2 types, depending on the local microenvironment and stimuli therein [17].

M1 are 'classically-activated' pro-inflammatory macrophages, stimulating the adaptive immune response and are present during acute inflammation. On the other hand, M2 are 'alternatively-activated' macrophages which attenuate inflammation by secreting anti-inflammatory cytokines (*e.g.* Interleukin 10 (IL-10)) and stimulate the wound-healing process [18]. M2 macrophages are key players in chronic diseases such as fibrosis, atherosclerosis and cancer [19-21]. In cancer, tumor-associated macrophages (TAMs) exhibiting the M2 phenotype are not only crucial for inducing tumor growth, survival and

metastasis, but are also key players in nanoparticle uptake and drug release [21-25]. The disease-driven polarization of macrophages into M1 and M2 also modulates their phagocytic activities. For example, M1 are shown to be more prone to phagocytosis of *S. Aureus* [26], whereas M2 macrophages are more phagocytic towards myelin [27], latex beads and apoptotic cells [28]. These differences in phagocytic potential consequently may have an influence on their nanoparticle uptake capability. Although nanoparticle uptake by macrophages has been studied for many years, there is a lack of data comprehensively addressing the factors influencing potential differences in nanoparticle uptake by M1 and M2 macrophages.

In the present study, we therefore aimed to investigate the nanoparticle uptake by M1 and M2 macrophages in detail and understand the impact of particle size, functional groups and presence of serum on nanoparticle uptake by macrophages. To investigate that, we generated M1 and M2 polarized human macrophage populations and determined cellular uptake of different sizes (50, 100, 200, 500, 1000 nm) fluorescent silica nanoparticles with/without the presence of serum, using fluorescence microscopy, flow cytometry and Scanning Electron Microscopy (SEM). To understand the differential uptake, on one hand we examined the differences in the protein corona adsorbed on the nanoparticles using gel electrophoresis and on the other hand, we examined the phagocytic receptors and pathways in M1 and M2 which could be responsible for the observed differential uptake behavior, using phagocytosis gene array studies.

2 Materials & Methods

2.1 Cell culture

Monocytic human THP-1 cells (ATCC, Rockville, MD) were cultured in suspension in RPMI-1640 medium supplemented with 10% FBS (Lonza, Basel, Switzerland), 100 U/ml penicillin, 0.1 mg/ml streptomycin (Sigma Aldrich, St Louis, MO) and 2 mM L-glutamine (GE Healthcare, Little Chalfont, UK) in a CO2 incubator at 37°C.

2.2 Macrophage differentiation

THP-1 cells were treated for 24 h with 100 ng/ml of phorbol 12-myristate 13-acetate (PMA, Cayman Chemicals, Ann Arbor, MI) to allow their attachment. Then the medium was replaced by medium containing 20 ng/ml IL-4 and IL-13 (Peprotech, London, UK) for M2 differentiation, or 20 ng/ml IFN-γ (Peprotech) and 100 ng/ml LPS (Sigma Aldrich) for M1 differentiation. Cells were incubated with cytokines for 6 h (gene expression on differentiation), 24 h (phagocytosis array gene expression), 72 h (morphology analysis) and 120 h (nanoparticle uptake experiments).

2.3 Quantitative Real Time PCR

0.5 x 106 cells were plated in 12-well plates and differentiated, as described above. Cells were washed with PBS and then lysed using lysis buffer and total RNA was isolated using SV Total RNA Isolation System (Promega, Madison, WI). cDNA was prepared by using iScript cDNA synthesis kit (Bio-Rad, Hercules, CA) and qRT-PCR was performed with 10 ng of cDNA per reaction mixture using SYBR green assay (Bioline, London, UK). Primer sequences are listed in Table 1. Reactions were measured using the CFX384 Real-Time PCR detection system (Bio-Rad). The threshold cycles (Ct) values were calculated and relative gene expression (ddCt method) was analyzed after normalization using the RSP18 house-keeping gene.

2.4 eSEM

For the imaging of differentiated cells and cellular uptake of nanoparticles, 0.25 x 10^6 cells were plated on a 12 mm glass coverslip placed in a 12-well plate and differentiated as described earlier. After 72 h of the cytokine incubations, cells were washed 3 times with PBS and fixed in 4% formalin for 20 min. Subsequently, cells were washed

3x in PBS, then dehydrated using increasing concentrations of ethanol. After dehydration, cells on coverslips were dried at the critical point using the Balzers CPD 030. Coverslips were mounted on a stub and gold sputtered. Cells were then imaged using the Philips XL30 ESEM-FEG (Philips, Amsterdam, Netherlands). Overview images of cells (50x) were taken and used for calculation of the elongation factor, where the length and width of the cell were measured (using ImageJ software) perpendicularly across the nucleus and the ratio between length and width was determined.

Gene	Forward (5'→ 3')	Reverse (3'→ 5')	Accession
RPS18	TGAGGTGGAACGTGTGATCA	CCTCTATGGGCCCGAATCTT	NM_022551.2
DC-SIGN	GAACTGGCACGACTCCATCA	CTGGAAGACTGCTCCTCAGC	NM_001144897.1
DECTIN-1	ATGGCTCTGGGAGGATGGAT	GGGCACACTACACAGTTGGT	NM_197947.2
TNF-α	CTTCTGCCTGCTGCACTTTG	GTCACTCGGGGTTCGAGAAG	NM_000594.3
IL-1β	CAGAAGTACCTGAGCTCGCC	AGATTCGTAGCTGGATGCCG	NM_000576.2

Table 1: Primer sequences of selected human genes

2.5 Nanoparticle analysis

Different sized plain (50, 100, 200, 500 and 1000 nm), amine-conjugated (50 nm and 1000 nm), non-porous red fluorescent silica nanoparticles were purchased (Micromod, Rostock, Germany). Nanoparticle size (in PBS) and zeta potential (in 0.1 mM potassium chloride solution) were measured using Dynamic light scattering (DLS, Zetasizer Nano ZS, Malvern, Malvern, UK). Silica nanoparticle shapes were visualized using eSEM.

2.6 Nanoparticle uptake

Silica nanoparticles were diluted to a concentration of 25 μg/ml in culture medium either without serum, 10% human serum (Sigma Aldrich), 10% heat inactivated human serum (by heating to 56 °C for 30 min) or 4.5 mg/ml human albumin (Sigma Aldrich) and added to the differentiated macrophages and incubated at 37°C. After incubation, cells were vigorously washed, immediately placed on ice and then detached using Accutase cell detachment solution (Sigma Aldrich) and gentle scraping. Cells were then collected and particle uptake was assessed by measuring mean fluorescence intensities in the FL-2 channel for at least 10,000 gated cells, using flow cytometry (BD FACSCalibur, Becton Dickinson, Franklin Lakes, NJ). Gates were set in the FSC vs SSC plot, using untreated control cell populations. For all experiments, identical settings were used. Data was analyzed using Flowing Software 2.5.0. For microscopic analysis of particle uptake,

cells were treated as described above. Cells were fixed in 4% formalin for 20 min at RT. Cells were mounted in Fluoroshield™ with DAPI (Sigma Aldrich). Images were taken using the EVOS Fl inverted microscope (Life Technologies, Carlsbad, CA), using DAPI and RFP filters.

2.7 Phagocytosis gene array

For analysis of phagocytic receptors, recognition and engulfment, phagosome maturation, phagosome processing and signal transduction, cells were cultured and differentiated as described in macrophage differentiation. After 24 h of cytokine incubation, cells were lysed and RNA was isolated as described above. Gene expression was analyzed using the RT2 Profiler PCR Array for human phagocytosis (Qiagen, Venlo, Netherlands). Samples were measured using the CFX96 Real-Time PCR detection system (Bio-Rad). Results were analyzed using software (SABioscience) specifically designed for the analysis of Qiagen PCR arrays. Results were normalized using GAPDH and expression threshold was set to 3.0.

2.8 Protein corona analysis

Different sizes silica nanoparticles (25 μg/ml) were incubated for 30 min in 10% human serum at 37 °C. Nanoparticles were centrifuged for 30 min at 20,000 rcf (14,000 rpm) at 4 °C. Supernatant was removed and particles were resuspended in 750 μl of filtered PBS. Particles were centrifuged again. Washing was repeated twice more. After the final centrifugation step, particles were resuspended in 20 μl SDS sample buffer containing DTT and frozen overnight at -20 °C. The next morning, particles were sonicated for 10 min in a waterbath, boiled for 5 min at 95 °C and then centrifuged at 20,000 rcf (14,000 rpm) for 5 min at 20 °C. Equal volumes of sample or sample corrected for the surface area of the particles were loaded and ran in a NuPAGE 4-12% Bis-Tris gel (Thermo Fisher Scientific, Waltham, MA). The gel was subsequently stained using the Pierce Silver staining kit (Thermo Fisher Scientific). Protein bands were quantified using ImageJ (1.46r) software. Total protein concentrations were determined for each particle size and separated into different protein sizes according to the protein ladder. Using this data, the percentage of each protein size fraction per particle was calculated and compared between the different particle sizes.

2.9 Statistical analysis

Data are presented as mean + standard error of the mean (SEM). All graphs were created and statistical analysis were performed using Graphpad Prism (Graphpad, La Jolla, CA) using two-sided unpaired student's t-test. Statistical tests were performed with a minimum significance level of $p<0.05$.

3 Results

3.1 Differentiation of macrophages into M1 and M2

To generate M1 and M2 macrophages *in vitro*, we treated human monocytes (THP-1) with specific cytokines (Interferon-γ (IFN-γ)/ Lipopolysaccharide (LPS) for M1 and Interleukin 4 (IL-4)/ IL-13 for M2. The macrophage polarization was confirmed at the transcriptional level, using the validated M1-specific markers (*i.e. TNF-α* and *IL-1β*) and M2-specific markers (*i.e. DC-SIGN* (*CD209*) and Dectin-1 (*CLEC7A*)), as shown in Figure 1A and 1B.

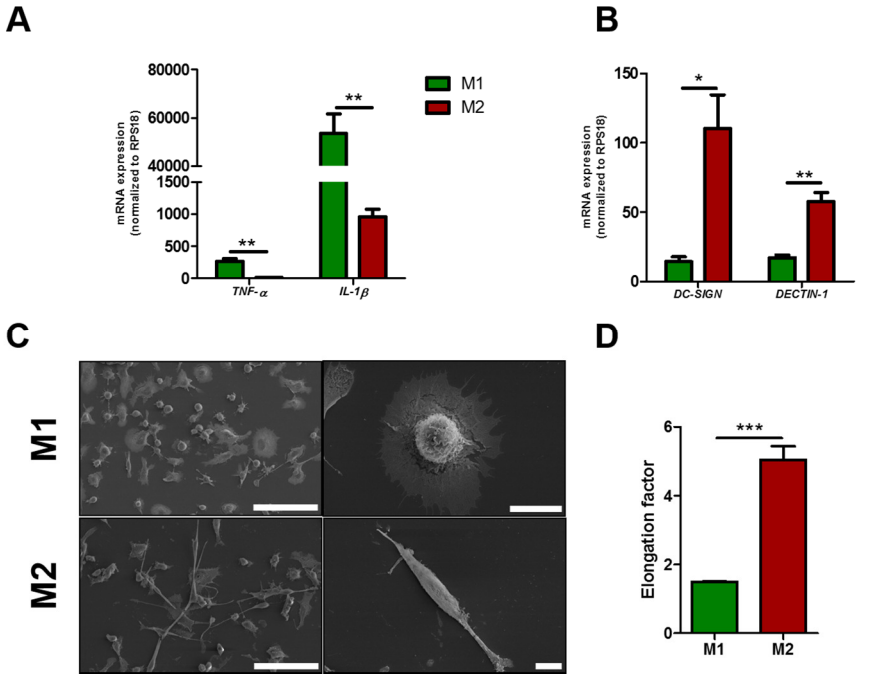

Figure 1: THP-1 cells were treated with PMA for 24 h and then with cytokines for M1 differentiation (IFNγ and LPS) or M2 differentiation (IL-4 and IL-13) for 6 h (gene expression) or 72 h (morphology analysis). The mRNA expression levels showing upregulation of M1 markers (**A**) and M2 markers (**B**) in IFNγ/LPS and IL-4/IL-13 treated cells, respectively. Panel **C** shows eSEM images depicting the morphological changes after M1 and M2 differentiation (scale bar = 100 µm, left images) and typical elongation or rounding for M1 and M2 cells, respectively (scale bar = 10 µm, right images). **(D)** Quantitative analysis for the elongation factor of M2 versus M1 cells. Values are shown as mean + SEM for 3 independent experiments. *p<0.05 and **p<0.01, ***p<0.001. Abbreviations: LPS: Lipopolysaccharide; PMA: Phorbol 12-myristate 13-acetate; eSEM: Environmental scanning electron microscopy

Both M2 markers *DC-SIGN* and *Dectin-1* showed significant upregulation in M2 compared to M1, while *TNF-α* and *IL-1β* were significantly upregulated in M1. Next, we also found the morphological differences between M1 and M2 types, as shown with scanning electron microscopy. M2 macrophages had an elongated appearance, whereas M1 macrophages attained a flat and rounded morphology (Figure 1C). These microscopic observations were confirmed by quantifying the elongation factor *i.e.* cell length divided by cell width, measured across the nucleus (Figure 1D). In addition, we performed immunocytochemical staining for CD80 (marker for M1) and CD206 (marker for M2) after 96h of differentiation (Figure S1). These data showed that CD80 is only expressed by M1 but not by M2 whereas CD206 is strongly expressed by M2 compared to M1 (Figure S1). These data confirm that human M1 and M2 phenotypes were successfully attained by macrophages to study the uptake of nanoparticles.

Expected mean size and type of surface modification	**Z-average (nm)**	**PDI (nm)**	**Zeta-potential (mV)**
50 nm	45	0.07	-38
100 nm	108	0.06	-50
200 nm	190	0.02	-45
500 nm	461	0.04	-52
1000 nm	1103	0.11	-63
1000 nm (amine functionalized)	1255	0.2	-7

Table 2: Characterization of silica nanoparticles. The nanoparticle size was calculated using intensity weighted mean hydrodynamic size by DLS in PBS and zeta potential was measured in 0.1mM KCl. Abbreviations: PDI: Polydispersity index; DLS: Dynamic light scattering; PBS: Phosphate buffered saline

3.2 Characterization of silica nanoparticles

To investigate the uptake of differently sized nanoparticles by M1 and M2 macrophages, we chose fluorescent silica nanoparticles. The sizes (50, 100, 200, 500 and 1000 nm) were confirmed using Dynamic Light Scattering (DLS), as shown in Figure 2 and Table 2. In addition, the zeta potential on the particles was highly negative due to free silanol groups on the nanoparticles surface (Table 2). Amine functionalized 1000 nm sized nanoparticles had a lower negative charge. Since shape is an important parameter for nanoparticles, we confirmed that all particles had spherical shape (Figure 2).

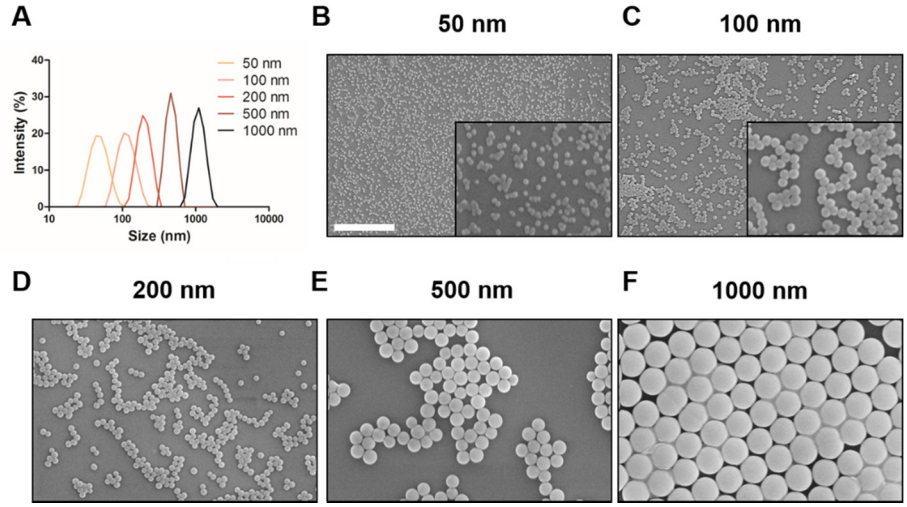

Figure 2: Nanoparticle size and characterization. (A) Nanoparticles size distribution, as measured by DLS. SEM images of 50 nm (B), 100 nm (C), 200 nm (D), 500 nm (E) and 1000 nm (F) particles.

3.3 Uptake of silica nanoparticles by M1 and M2 macrophages.

To study the differences in uptake between M1 and M2 macrophages, nanoparticles were incubated with these cells for different time points (30 min, 2h and 6h) with or without serum and the uptake was analyzed using flow cytometry. We found that under the serum-free conditions, all nanoparticles were increasingly taken up by both cell types with the increase of time (Figure 3). Interestingly, we found that 100 and 200 nm nanoparticles were significantly more taken up by M1 macrophages compared to M2 macrophages, either at all or specific time points. These data indicated that M1 and M2 possess different uptake behavior towards different sized nanoparticles. Representative flow cytometry histograms of uptake without serum are shown in Figure S2.

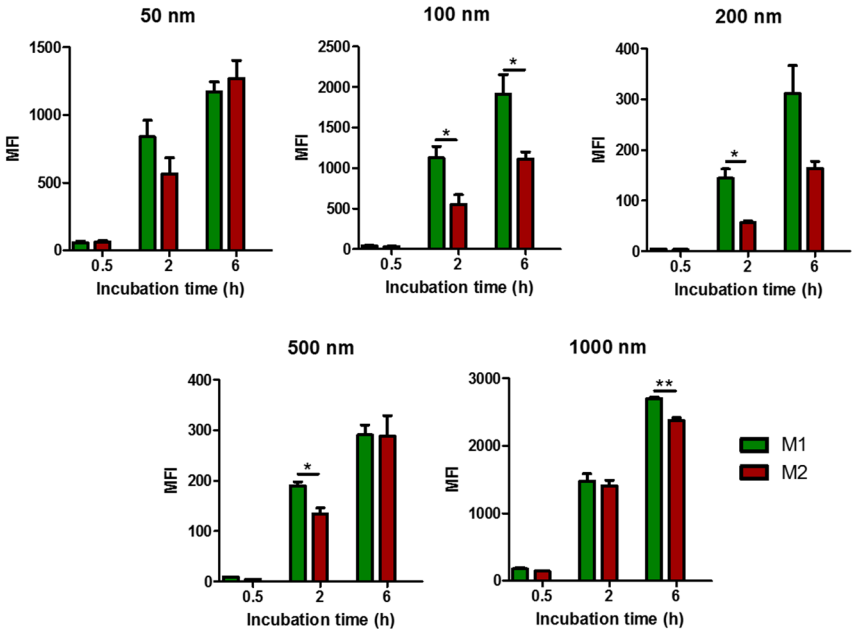

Figure 3: Quantitative uptake of differently sized nanoparticles by M1 and M2 macrophages without serum. Quantitative analysis of the uptake of silica nanoparticles (50 – 1000 nm) by differentiated macrophages at different time points, measured using flow cytometry. Identical settings were maintained at all time points. MFI: Mean Fluorescence Intensity. Values are shown as mean + SEM, of a minimum of 3 independent experiments. *p<0.05 and **p<0.01.

To study the impact of serum on the particle uptake, we incubated nanoparticles with non heat-inactivated human serum and studied the uptake using flow cytometry. Remarkably, we found that nanoparticles up to 200 nm size had a tremendous reduction in the total uptake, as indicated by mean fluorescent intensities, compared to that of serum-free condition (Figure 4 vs Figure 3). In contrast, 500 and 1000 nm sized particles had either similar or higher uptake in both cell types compared to serum-free condition (Figure 4 vs Figure 3). Interestingly, we observed a significant higher uptake of nanoparticles (200 to 1000 nm) by M2 than M1, which was opposite to the observations at the serum-free condition. Representative flow cytometry histograms of uptake with serum are shown in Figure S3.

Furthermore, the fluorescent microscopic images clearly show the localization of nanoparticles (cell association, close to cell membrane; cell uptake, next to the nucleus) (Figure 5 and Figure S4). These data

confirm that nanoparticles first attached to the cell membrane as visible at 0.5 h and subsequently internalized by the cells completely at t=6h. Figure S4 shows that 50 nm nanoparticles were rapidly internalized by both M1 and M2 than 1000 nm particles (Figure 5A) in the absence of serum. The microscopic images in Figure 5B confirm that in the presence of serum M2 macrophages had a rapid and higher uptake compared to M1 confirming the flow cytometry data (Figure 4). In contrast, in the presence of serum both M1 and M2 had very low uptake of 50 nm nanoparticles compared to 1000 nm particles (Figure 5B and Figure S4), which is line of the flow cytometry data (very low MFI with 50 nm in Figure 4).

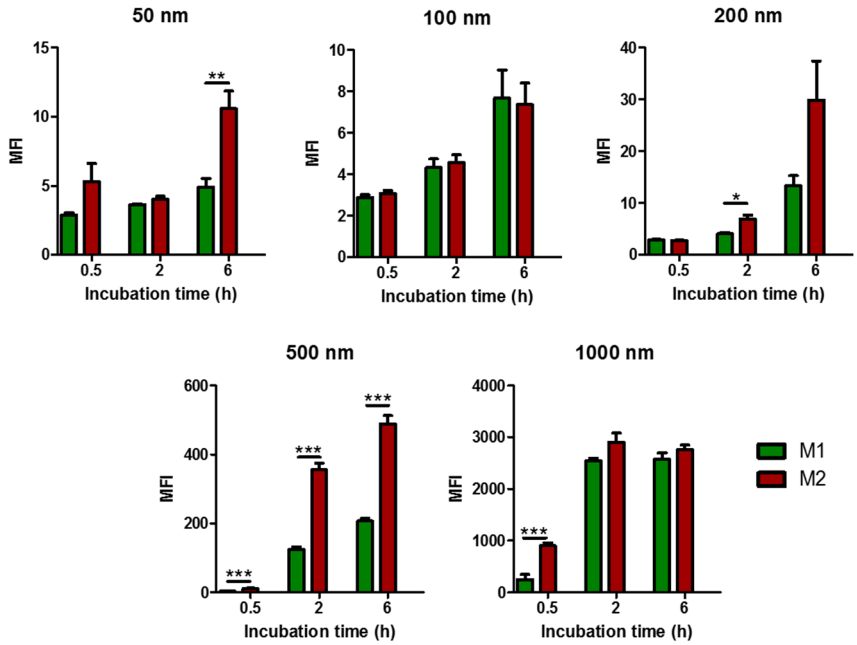

Figure 4: Quantitative uptake of differently sized nanoparticles by M1 and M2 macrophages with serum. (A) Quantitative analysis of the uptake of silica nanoparticles (50 – 1000 nm) by differentiated macrophages at different time points in the presence of serum, measured using flow cytometry. Identical settings were maintained at all time points. MFI: Mean Fluorescence Intensity. Values are shown as mean + SEM, of a minimum of 3 independent experiments. *p<0.05 and **p<0.01.

Since M2 macrophages, compared to M1, showed much higher uptake of 1000 nm particles at early time point (Figure 4), we attempted to capture the early events of interaction between 1000 nm particles and M1 and M2 macrophages using SEM analysis. The SEM images

revealed that the particles were associated much more with M2 macrophages than M1 macrophages after only 10 min of incubation time (Figure 6A and 6B). Furthermore, only M2 macrophages showed events of internalized particles, as indicated by an arrow in Figure 5B. These data further confirm that M2 macrophages have a higher interaction with large nanoparticles compared to M1 in the presence of serum.

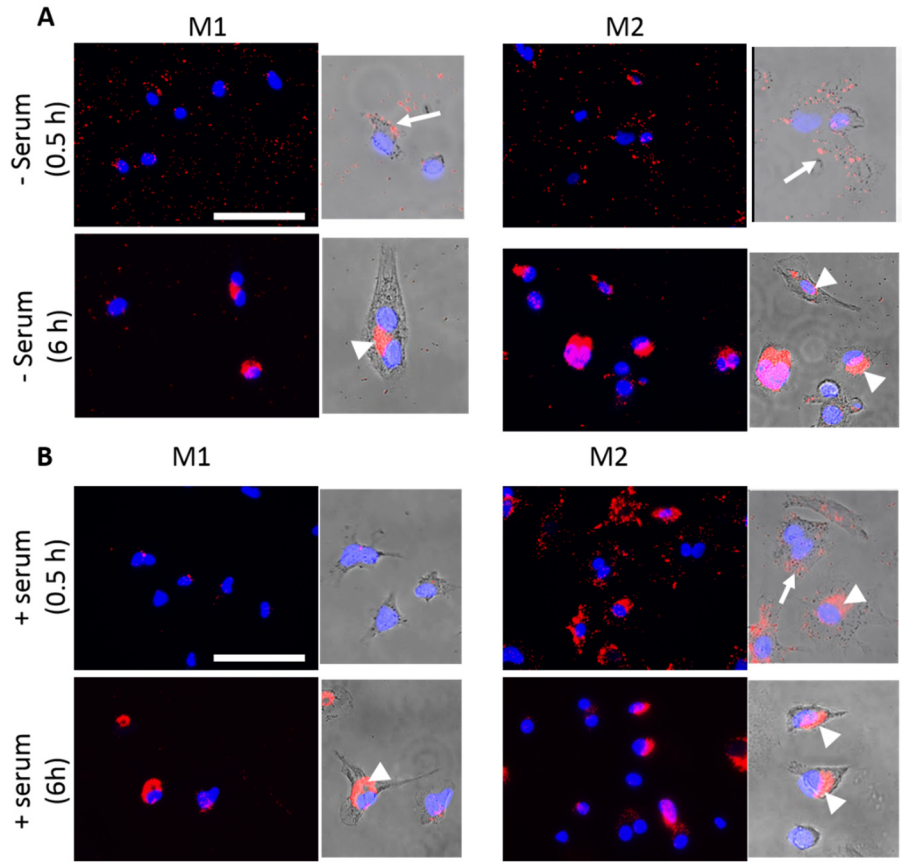

Figure 5: Fluorescent microscopy showing cellular uptake of nanoparticles by M1 and M2 macrophages (A) Microscopic pictures showing uptake of 1000 nm particles by M1 and M2 macrophages at 0.5h and 6h time points in the absence of serum (A) and in the presence of serum (B). Red color: silica nanoparticles, Blue: DAPI. Bar = 100 µm. The sublet of the images showing an overlay of the fluorescent microscopic picture with phase-contrast microscopic picture to show the cellular membrane association (indicated by arrows) and subsequently uptake (fluorescent signal next to nuclei; indicated by arrow heads).

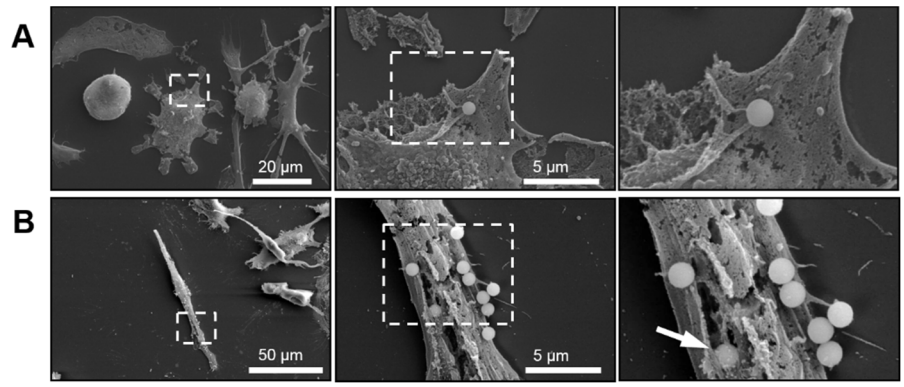

Figure 6: Scanning Electron Microscopic (SEM) images of 1000 nm sized particle interaction with M1 and M2 macrophages. Particles were incubated in the presence of 10% human serum for 10 min. (A) Typical M1 macrophage showed a little association of the particles without any event of uptake. (B) In contrast, typical M2 macrophage showed a large number of particles associated to the cell and events of particle internalization (indicated by arrow). The sequences of zoomed images are shown next to the main image depicted as dotted box within the images.

3.4 Effect of serum proteins on nanoparticle uptake by M1 and M2 macrophages.

To investigate the effect of serum proteins on the uptake of nanoparticles, we used only 50 nm and 1000 nm nanoparticles and studied their uptake in the presence of human non heat-inactivated serum, heat-inactivated serum and albumin. As expected, in view of Figure 3 and 4, the presence of human serum reduced the uptake of 50 nm nanoparticles in both macrophages (Figure 7A). Also, heat-inactivated serum or human albumin (4.5 mg/ml equivalent to the amount of albumin in 10% human serum) blocked their uptake. Interestingly, the serum-induced uptake of 1000 nm particles by M2, as also seen in Figure 4, did not appear in the presence of heat-inactivated serum (Figure 7B). These data indicated that adsorption of heat-sensitive serum proteins (for example complement factors and immunoglobulins (IgG)) played an important role in enhancing the uptake by M2 macrophages. Furthermore, when we changed the surface charge of 1000 nm particles to less negative (-7 mV versus -63 mV) by amination we found no serum-induced uptake, as it was observed with the highly negatively charged particles (Figure 7C). These data suggest that the surface charge played a crucial role in the

adsorption of specific serum proteins that are responsible for serum-induced uptake of particles.

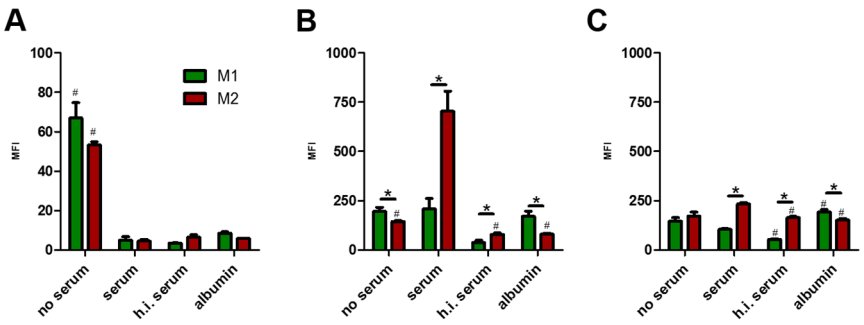

Figure 7: Effect of serum heat-inactivation and change in surface charge on M1 and M2 mediated uptake. Plain 50 nm (A) and 1000 nm (B) silica nanoparticles, and amine-functionalized 1000 nm particles (C) were incubated under different conditions (no serum; with 10% human serum; with 10% heat-inactivated human serum, h.i. serum; or 4.5 mg/ml of human albumin in culture medium for 30 minutes. The uptake of nanoparticles was determined using flow cytometry analyses, as explained in methods. Values are shown as mean + SEM, of a minimum of 3 independent experiments. * $p<0.05$ for M1 vs M2, # $p<0.05$ vs. same cell type in serum conditions.

3.5 Protein corona and phagocytosis gene array study

Since serum proteins affected the uptake of nanoparticles by M2 macrophages, we investigated the composition of the protein corona present on the silica nanoparticles using SDS-PAGE assay (Figure 8A and 8B). The hard protein corona was isolated after incubating the particles in 10% human serum and extensive washing, and proteins were then separated using SDS-PAGE. Interestingly, image analysis of the gel showed a correlation between protein size and particle size: for many smaller proteins, there was a downwards trend in percentage with increasing particle size, whereas percentages of large proteins (130 – 250 and > 250 kD) increased with increasing particle sizes. Proteins in these ranges are generally enriched with complement factors and IgGs, as shown somewhere else [25, 29-31].

To further explore whether M1 and M2 differentially express receptors and pathways which might explain their distinct uptake behavior, we conducted a phagocytosis gene array study in M1 and M2 cells. We analyzed the expression of a set of genes (84 genes) involved in the phagocytosis process including phagocytic receptors, recognition and

engulfment, phagosome maturation, phagosome processing and signal transduction. Interestingly, we found that there was a remarkable increase in the expression levels of the FCGR2B (26.7-fold), CD36 (8.9 fold), COLEC12 (7.8 fold) and ITGAM (7.1 fold) in M2 macrophages, compared to M1 macrophages, as shown in Figure 9. Of note, many of these receptors are the receptors for complement factors and IgGs, which explains that M2-induced receptors bind to the corona proteins (*i.e.* complement factors and IgGs) and induce their uptake by M2 but not by M1.

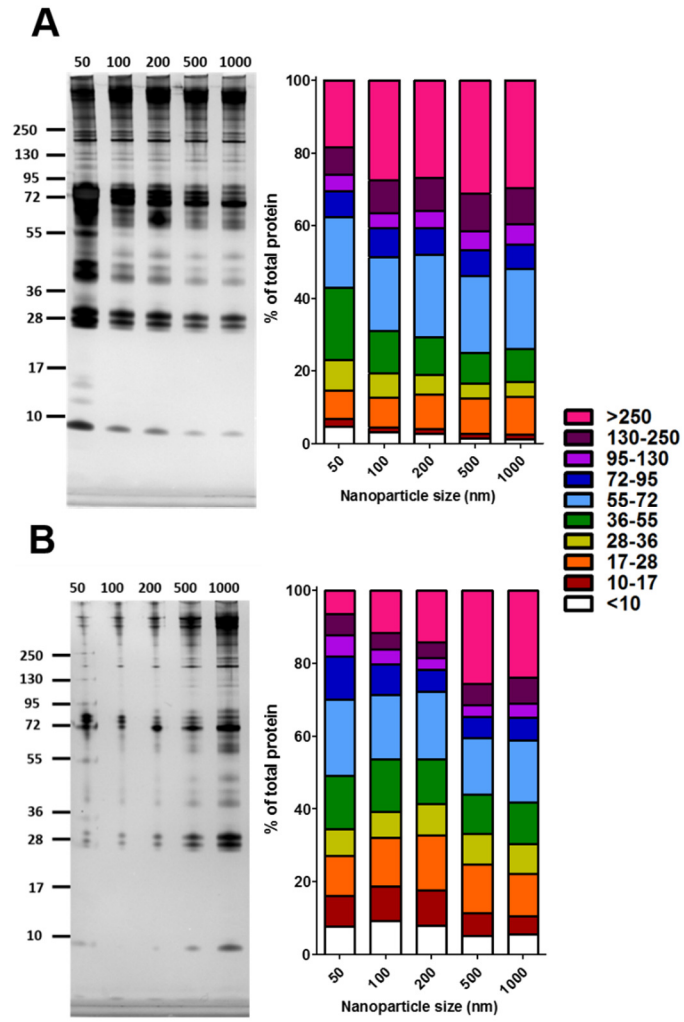

Figure 8: Protein corona analysis in silica nanoparticles. Silver staining of the SDS-PAGE (A) after loading lysates from equal particle amounts (in μg/ml) and (B) after

loading lysates corresponding to equal surface area of nanoparticles. Silica nanoparticles (25 µg/ml for each type of particle) were incubated with 10% human serum in culture medium for 30 min at 37 °C. Nanoparticles were washed and proteins originating from the hard protein corona were loaded onto a SDS-PAGE gel. The resulting gel was developed using silver staining. Left to right lanes show 50 to 1000 nm nanoparticles. Graphs shows analysis of protein bands, separated according to protein size per particle size. Total protein per particle was determined and size fractions of this total are shown.

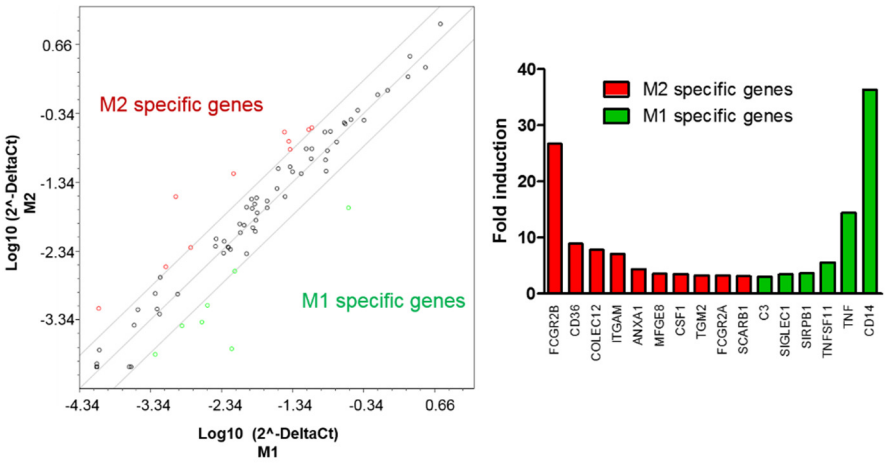

Figure 9: Gene expression array of human phagocytosis in M1 and M2 macrophages. Macrophages were differentiated into M1 and M2 phenotypes. Array was performed comparing M1 gene expression (x-axis) to M2 gene expression (y-axis). The bar graph at the right side shows genes which were upregulated in M2 and M1.

4 Discussion

The present study highlights the interaction of nanoparticles with M1 and M2 polarized macrophages, revealing the impact of particle size, charge and protein corona on the differential uptake. Under non-serum conditions, nanoparticles with a range of 50 to 1000 nm showed higher uptake by human M1 macrophages compared to M2 macrophages. Intriguingly, addition of human serum hindered the total uptake of the small sized (≤ 200 nm) nanoparticles but turned the uptake towards M2 for larger sizes. Our further investigation showed that adsorption of serum proteins (*e.g.* IgG and complement factors) on the nanoparticles was responsible for the higher uptake by M2 macrophages, as M2 macrophages expressed receptors against IgG and complement factors compared to M1 macrophages.

Although the interaction of general macrophages with nanoparticles has been extensively investigated [25, 29-32], the data showing the interaction of nanoparticles with M1 and M2 subpopulations is very limited [25]. Since M1 and M2 populations significantly vary in different disease conditions (M1 in inflammation and M2 in fibrosis and tumors), understanding of their interaction with nanoparticles is of paramount importance. In this study, we generated M1 and M2 polarized macrophages using human THP-1 monocytic cell line and proved their successful differentiation using well-defined parameters (specific genes and morphology) as reported in literature [33-35]. These data ensured us for a stable testing platform to study the interaction and uptake of nanoparticles with M1 and M2 macrophages.

To investigate the uptake of nanoparticles, we used fluorescently labeled silica nanoparticles, as they can be produced in a well-defined size range with low polydispersity [36, 37], which was confirmed by us herein. In the present study, we chose nanoparticle with the range of 50 to 1000 nm, since this range is considered important for cell nanoparticle interaction either due to *in vivo* applications or exposure as foreign particles [38, 39]. Since phagocytosis is a process which can last from minutes to several hours, we carried out a time course uptake study until 6 h. Considering the issues of the different dye content in different sized nanoparticles and differences in volume of small and large nanoparticles, we only compared the uptake of the same sized nanoparticle by M1 and M2 (different time points and with/without

serum) rather than among different sized nanoparticles. Our uptake study data in the absence of serum showed a higher uptake of all range of nanoparticle into M1 compared to M2, yet the uptake was more prominent with ≤ 200nm nanoparticles. We assume that the higher uptake by M1 might be attributed to their morphology. Since M1 macrophages are flatter and larger in size compared to M2 (Figure 1), they likely have higher unspecific interaction with nanoparticle and thereby higher uptake in serum-free conditions compared to M2.

However, when added human serum, we found that the total uptake of small particles (≤ 200 nm) was reduced, though we saw a slight increase in uptake by M2 compared to M1. The latter observation is in agreement with the study by Höppstadter et al [25]. These data indicated that adsorption of serum proteins on small sized nanoparticles block their unspecific uptake by both macrophages. To explain this, we performed uptake studies in the presence of albumin and found that albumin blocked the uptake of 50 nm sized nanoparticles but did not affect 1000 nm particle uptake (Figure 7). Furthermore, we found a strong induction of uptake of nanoparticles (200 to 1000 nm) by M2 compared to M1 in the presence of serum. These data suggested that adsorption of serum proteins (opsonization) enhanced the uptake of nanoparticles by M2 and this enhancement was more prominent with bigger nanoparticles.

Opsonization is process in which serum components such as complement proteins and IgGs bind to foreign bodies or nanoparticles, and induce their phagocytosis [40, 41]. To investigate the possible role of complements and IgGs, we performed uptake studies with heat-inactivated serum, as it is known that the heat-inactivation process inactivates these complements and aggregate IgGs complexes [42, 43]. Our data (Figure 7) showing inhibition of nanoparticles (both 50 and 1000 nm) uptake in the presence of heat-inactivated serum suggested the role of adsorbed complements and IgGs on nanoparticle in induction of M2-mediated phagocytosis. In line with these findings, human serum did not enhance the uptake of amine-conjugated 1000 nm particles, which might be explained by the data from Lundqvist et al, reporting that amine-conjugated polystyrene nanoparticles showed a decrease in complement factors and IgGs binding [44].

Furthermore, we investigated the protein corona on the different particle sizes to see whether they form different protein corona. Studies have already showed that the composition of the protein corona changed with the particle size [31]. In addition, a recent study by Fedeli et al. showed that nanoparticle concentration is a crucial parameter affecting the corona composition in human plasma and at low nanoparticles concentrations, the uptake by macrophages was prevented by the corona mainly formed by fibrinogen, kininogen and histidine rich glycoprotein (HRG) [45]. In contrast, at higher nanoparticles concentrations the recruitment of other proteins (fibrinogen, HDL, IgG, and other small proteins) allowed the uptake by macrophages, suggesting the importance of protein composition in macrophage uptake. Our data showed a trend of higher adsorption of large proteins on nanoparticles with an increase in size, while considering equal surface area into account (Figure 8B). This might be due to the large surface area allowing large proteins or protein aggregates to attach to a larger extent than small nanoparticles whose surface gets saturated by small proteins rapidly. Earlier studies have identified protein signatures on silica nanoparticle, showing that proteins above 130KDa include complement factor C3, complement factor H, and IgGs [31, 44]. These reports suggest that the protein corona in our samples was also enriched with complement factors and IgGs, likely responsible for higher uptake of large nanoparticles by M2 macrophages.

Since M2 macrophages internalized serum-incubated nanoparticles rapidly, we assumed that M2 might express specific receptors for corona proteins. A study by Shannahan et al also suggested that cellular uptake of nanoparticles by macrophages might be due to proteins in the corona however no specific proteins or receptors were identified [32]. In this study, to investigate whether M2 express receptors for complement factors, IgGs and other corona proteins, we performed a phagocytosis gene array in M1 and M2 macrophages. Interestingly, our data showed a strong induction of receptors for IgG (*i.e.* FCGR2B (CD32) [46, 47]), oxidized lipids (*i.e.* CD36 and COLEC12 [48, 49]) and complement factors (*i.e.* ITGAM or complement receptor 3 [50, 51]) in M2 macrophages compared to M1 macrophages. These data suggest that M2-expressing protein corona-binding receptors allowed these macrophages to strongly interact with nanoparticles in the presence of serum and thereby induced the nanoparticle uptake.

5 Conclusion

The present study demonstrates that M1 and M2 have different behavior for interacting and internalizing nanoparticles. Without serum, M1 had more interaction and uptake of nanoparticles, likely due to their flat morphology. In contrast, with serum M2 became dominant in internalizing nanoparticles which was attributed to their overexpressed phagocytic receptors against protein corona of nanoparticles. Moreover, the protein corona altered in composition depending on the size of the particles, which altered the internalization by M2 macrophages. Altogether, this study implies that nanoparticles size and protein corona are key determinants for the differential uptake by M1 and M2 macrophages. The present study has important implications for the understanding of the behavior of nanoparticles in the body either in healthy or pathological conditions, where subpopulations of macrophages are involved.

References

1. Duncan R, Gaspar R. Nanomedicine(s) under the microscope. Mol. Pharmaceutics 8(6), 2101-2141 (2011).
2. Petros RA, Desimone JM. Strategies in the design of nanoparticles for therapeutic applications. Nat. Rev. Drug Discov. 9(8), 615-627 (2010).
3. Waite CL, Roth CM. Nanoscale drug delivery systems for enhanced drug penetration into solid tumors: current progress and opportunities. Crit. Rev. Biomed. Eng. 40(1), 21-41 (2012).
4. Flannagan RS, Jaumouille V, Grinstein S. The cell biology of phagocytosis. Annu. Rev. Pathol.: Mech. Dis. 7 61-98 (2012).
5. Owens DE, 3rd, Peppas NA. Opsonization, biodistribution, and pharmacokinetics of polymeric nanoparticles. Int. J. Pharm. 307(1), 93-102 (2006).
6. Liu T, Choi H, Zhou R, Chen IW. Quantitative evaluation of the reticuloendothelial system function with dynamic MRI. PloS one 9(8), e103576 (2014).
7. Alexis F, Pridgen E, Molnar LK, Farokhzad OC. Factors affecting the clearance and biodistribution of polymeric nanoparticles. Mol. Pharmaceutics 5(4), 505-515 (2008).
8. Haniffa M, Bigley V, Collin M. Human mononuclear phagocyte system reunited. Semin. Cell Dev. Biol. doi:10.1016/j.semcdb.2015.05.004 (2015).
9. Podila R, Brown JM. Toxicity of engineered nanomaterials: a physicochemical perspective. J Biochem Mol Toxicol 27(1), 50-55 (2013).
10. Verma A, Stellacci F. Effect of surface properties on nanoparticle-cell interactions. Small 6(1), 12-21 (2010).
11. Lewis JS, Roy K, Keselowsky BG. Materials that harness and modulate the immune system. MRS Bull 39(1), 25-34 (2014).
12. Edwards DA, Hanes J, Caponetti G et al. Large porous particles for pulmonary drug delivery. Science 276(5320), 1868-1871 (1997).
13. Champion JA, Mitragotri S. Role of target geometry in phagocytosis. Proc. Natl. Acad. Sci. U. S. A. 103(13), 4930-4934 (2006).
14. Frohlich E. The role of surface charge in cellular uptake and cytotoxicity of medical nanoparticles. Int. J. Nanomed. 7 5577-5591 (2012).
15. Bhattacharjee S, Ershov D, Fytianos K et al. Cytotoxicity and cellular uptake of tri-block copolymer nanoparticles with different size and surface characteristics. Part. Fibre Toxicol. 9 11 (2012).

16. Anselmo AC, Zhang M, Kumar S et al. Elasticity of nanoparticles influences their blood circulation, phagocytosis, endocytosis, and targeting. ACS nano 9(3), 3169-3177 (2015).
17. Gordon S, Taylor PR. Monocyte and macrophage heterogeneity. Nat. Rev. Immunol. 5(12), 953-964 (2005).
18. Allavena P, Mantovani A. Immunology in the clinic review series; focus on cancer: tumour-associated macrophages: undisputed stars of the inflammatory tumour microenvironment. Clin. Exp. Immunol. 167(2), 195-205 (2012).
19. Viola J, Soehnlein O. Atherosclerosis - A matter of unresolved inflammation. Semin. Immunol. doi:10.1016/j.smim.2015.03.013 (2015).
20. Bartneck M, Warzecha KT, Tacke F. Therapeutic targeting of liver inflammation and fibrosis by nanomedicine. Hepatobiliary Surg. Nutr. 3(6), 364-376 (2014).
21. Sica A, Larghi P, Mancino A et al. Macrophage polarization in tumour progression. Semin. Cancer Biol. 18(5), 349-355 (2008).
22. Biswas SK, Gangi L, Paul S et al. A distinct and unique transcriptional program expressed by tumor-associated macrophages (defective NF-kappaB and enhanced IRF-3/STAT1 activation). Blood 107(5), 2112-2122 (2006).
23. Schiffelers RM, Metselaar JM, Fens MH, Janssen AP, Molema G, Storm G. Liposome-encapsulated prednisolone phosphate inhibits growth of established tumors in mice. Neoplasia 7(2), 118-127 (2005).
24. Banciu M, Schiffelers RM, Fens MH, Metselaar JM, Storm G. Anti-angiogenic effects of liposomal prednisolone phosphate on B16 melanoma in mice. J. Controlled Release 113(1), 1-8 (2006).
25. Hoppstadter J, Seif M, Dembek A et al. M2 polarization enhances silica nanoparticle uptake by macrophages. Front. Pharmacol. 6 55 (2015).
26. Krysko O, Holtappels G, Zhang N et al. Alternatively activated macrophages and impaired phagocytosis of S. aureus in chronic rhinosinusitis. Allergy 66(3), 396-403 (2011).
27. Durafourt BA, Moore CS, Zammit DA et al. Comparison of polarization properties of human adult microglia and blood-derived macrophages. Glia 60(5), 717-727 (2012).
28. Chinetti-Gbaguidi G, Baron M, Bouhlel MA et al. Human atherosclerotic plaque alternative macrophages display low cholesterol handling but high phagocytosis because of distinct activities of the PPARgamma and LXRalpha pathways. Circ. Res. 108(8), 985-995 (2011).

29. Lesniak A, Fenaroli F, Monopoli MP, Aberg C, Dawson KA, Salvati A. Effects of the presence or absence of a protein corona on silica nanoparticle uptake and impact on cells. ACS nano 6(7), 5845-5857 (2012).
30. Lesniak A, Salvati A, Santos-Martinez MJ, Radomski MW, Dawson KA, Aberg C. Nanoparticle adhesion to the cell membrane and its effect on nanoparticle uptake efficiency. J. Am. Chem. Soc. 135(4), 1438-1444 (2013).
31. Tenzer S, Docter D, Rosfa S et al. Nanoparticle size is a critical physicochemical determinant of the human blood plasma corona: a comprehensive quantitative proteomic analysis. ACS nano 5(9), 7155-7167 (2011).
32. Shannahan JH, Podila R, Brown JM. A hyperspectral and toxicological analysis of protein corona impact on silver nanoparticle properties, intracellular modifications, and macrophage activation. Int J Nanomedicine 10 6509-6521 (2015).
33. Martinez FO, Gordon S, Locati M, Mantovani A. Transcriptional profiling of the human monocyte-to-macrophage differentiation and polarization: new molecules and patterns of gene expression. J. Immunol. 177(10), 7303-7311 (2006).
34. Relloso M, Puig-Kroger A, Pello OM et al. DC-SIGN (CD209) expression is IL-4 dependent and is negatively regulated by IFN, TGF-beta, and anti-inflammatory agents. J. Immunol. 168(6), 2634-2643 (2002).
35. Willment JA, Marshall AS, Reid DM et al. The human beta-glucan receptor is widely expressed and functionally equivalent to murine Dectin-1 on primary cells. Eur. J. Immunol. 35(5), 1539-1547 (2005).
36. Stöber W, Fink A, Bohn E. Controlled growth of monodisperse silica spheres in the micron size range. J. Colloid Interface Sci. 26(1), 62-69 (1968).
37. Hartlen KD, Athanasopoulos AP, Kitaev V. Facile preparation of highly monodisperse small silica spheres (15 to >200 nm) suitable for colloidal templating and formation of ordered arrays. Langmuir : the ACS journal of surfaces and colloids 24(5), 1714-1720 (2008).
38. Scalia S, Young PM, Traini D. Solid lipid microparticles as an approach to drug delivery. Expert opinion on drug delivery 12(4), 583-599 (2015).
39. De Jong WH, Borm PJ. Drug delivery and nanoparticles:applications and hazards. International journal of nanomedicine 3(2), 133-149 (2008).

40. Van Lookeren Campagne M, Wiesmann C, Brown EJ. Macrophage complement receptors and pathogen clearance. Cellular microbiology 9(9), 2095-2102 (2007).
41. Yang A, Liu W, Li Z, Jiang L, Xu H, Yang X. Influence of polyethyleneglycol modification on phagocytic uptake of polymeric nanoparticles mediated by immunoglobulin G and complement activation. J Nanosci Nanotechnol 10(1), 622-628 (2010).
42. Giard DJ. Routine heat inactivation of serum reduces its capacity to promote cell attachment. In Vitro Cell. Dev. Biol. 23(10), 691-697 (1987).
43. Soltis RD, Hasz D, Morris MJ, Wilson ID. The effect of heat inactivation of serum on aggregation of immunoglobulins. Immunology 36(1), 37-45 (1979).
44. Lundqvist M, Stigler J, Elia G, Lynch I, Cedervall T, Dawson KA. Nanoparticle size and surface properties determine the protein corona with possible implications for biological impacts. Proc. Natl. Acad. Sci. U. S. A. 105(38), 14265-14270 (2008).
45. Fedeli C, Segat D, Tavano R et al. The functional dissection of the plasma corona of SiO(2)-NPs spots histidine rich glycoprotein as a major player able to hamper nanoparticle capture by macrophages. Nanoscale 7(42), 17710-17728 (2015).
46. Van Lent P, Nabbe KC, Boross P et al. The inhibitory receptor FcgammaRII reduces joint inflammation and destruction in experimental immune complex-mediated arthritides not only by inhibition of FcgammaRI/III but also by efficient clearance and endocytosis of immune complexes. Am. J. Pathol. 163(5), 1839-1848 (2003).
47. Underhill DM, Ozinsky A. Phagocytosis of microbes: complexity in action. Annu. Rev. Immunol. 20 825-852 (2002).
48. Su X, Abumrad NA. Cellular fatty acid uptake: a pathway under construction. Trends Endocrinol. Metab. 20(2), 72-77 (2009).
49. Ohtani K, Suzuki Y, Eda S et al. The membrane-type collectin CL-P1 is a scavenger receptor on vascular endothelial cells. J. Biol. Chem. 276(47), 44222-44228 (2001).
50. Berton G, Lowell CA. Integrin signalling in neutrophils and macrophages. Cell. Signal. 11(9), 621-635 (1999).
51. Fuentes AL, Millis L, Vapenik J, Sigola L. Lipopolysaccharide-mediated enhancement of zymosan phagocytosis by RAW 264.7 macrophages is independent of opsonins, laminarin, mannan, and complement receptor 3. J. Surg. Res. 189(2), 304-312 (2014).

Appendix: Supplementary data

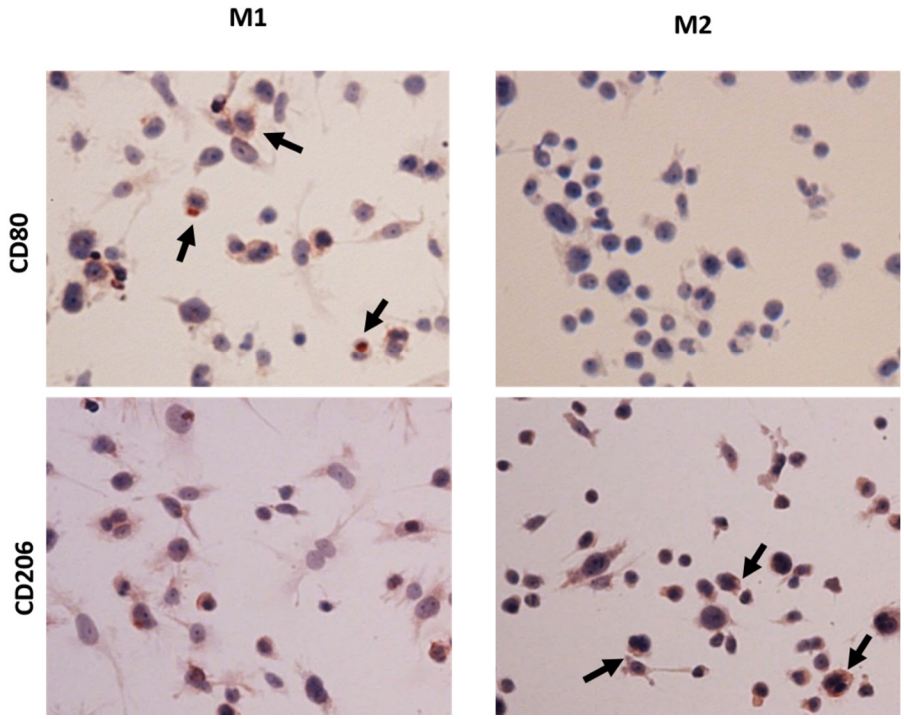

Figure S1: Immunocytochemical staining showing polarization of M1 and M2 macrophages. Immunostaining for CD80 (a marker for M1) and CD206 (a marker for M2) was performed after 96h of the incubation with differentiating cytokines, as mentioned in the materials and methods. Primary antibodies against CD80 (source: Biolegend) and CD206 (source: Bioss) were added to the acetone/methanol fixed cells for 1h and then secondary antibodies labeled with HRP were incubated for 1h. Subsequently, the red color was developed by adding 3-Amino-9-ethylcarbazole for 15 min. These data show that CD80 is only expressed by M1 but not by M2 whereas CD206 is strongly expressed by M2 compared to M1. Arrows indicate to the positive stained cells

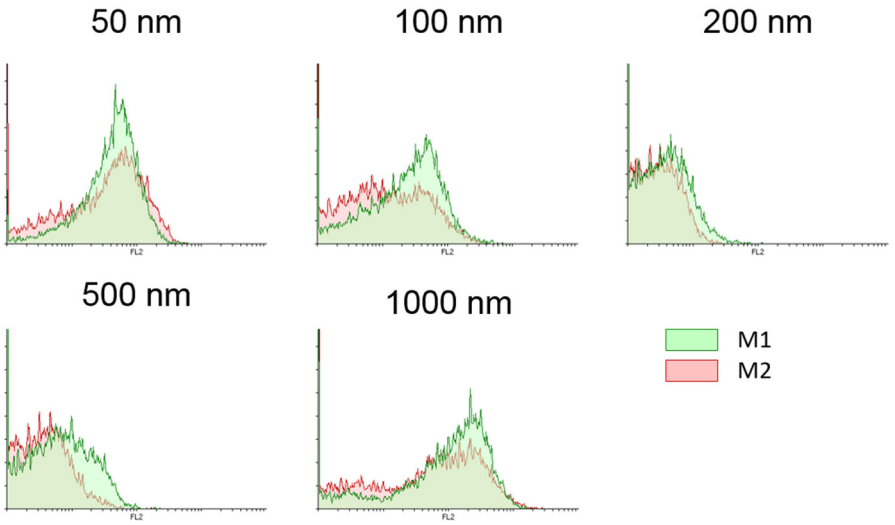

Figure S2: Flow cytometry histograms of nanoparticle uptake by differentiated macrophages without serum. Representative histograms are shown for different sized nanoparticles incubated for 30 min with M1 or M2 macrophages in the absence of serum.

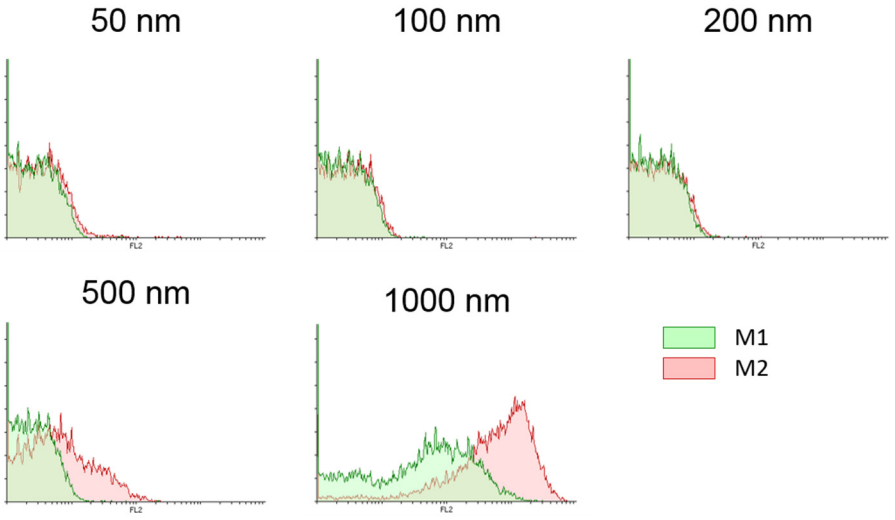

Figure S3: Flow cytometry histograms of nanoparticle uptake by differentiated macrophages with serum. Representative histograms are shown for different sized nanoparticles incubated for 30 min with M1 or M2 macrophages in the presence of serum.

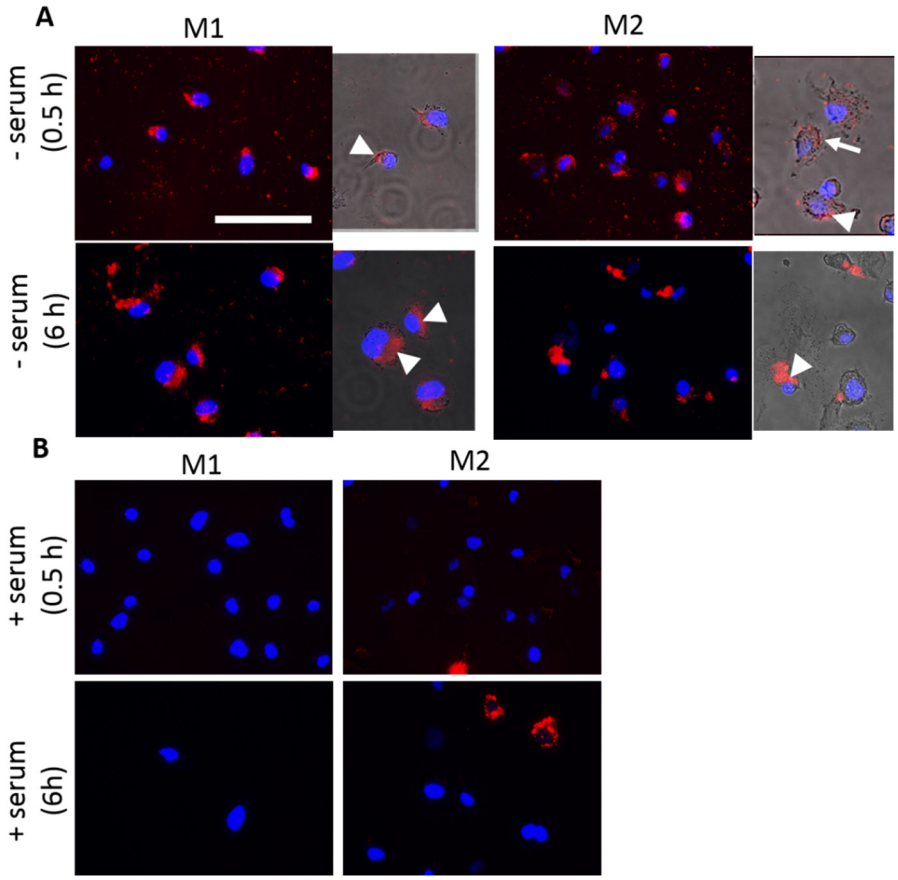

Figure S4: Fluorescent microscopy showing cellular uptake of nanoparticles by M1 and M2 macrophages (A) Microscopic pictures showing uptake of 50 nm particles by M1 and M2 macrophages at 0.5h and 6h time points in the absence of serum (A) and in the presence of serum (B). Red color: silica nanoparticles, Blue: DAPI. Bar = 100 µm. The sublet of the images showing an overlay of the fluorescent microscopic picture with phase-contrast microscopic picture to show the uptake (fluorescent next to nuclei; indicated by arrow head).

CHAPTER 4

TARGETING OF TUMOR-ASSOCIATED MACROPHAGES USING CARBOXYLATED-LIPID CONTAINING LIPOSOMES

Abstract

Tumor-associated macrophages (TAM) play a detrimental role in the growth and survival of many solid tumors. To treat these macrophages, we designed a novel liposomal carrier containing carboxylated lipids to target TAM. Several formulations containing PAzPC or PGPC liposomes were prepared. This study showed that carboxylated phosphatidylcholine (CyPC) present in the carboxylated lipids is able to bind to M2 surface receptors. However, the non-carboxylated form of PC did not show this binding. Moreover, *in vivo*, CyPC-containing liposomes accumulated more in tumor tissues, and less in organs such as the liver and spleen. Upregulated scavenger receptors Scarb1, Colec12 and to a smaller extent CD36, present on M2 macrophages, proved to be responsible for this M2-specific uptake of carboxylated-lipid containing liposomes. The tested liposomes did not show any toxicity or effect on macrophage differentiation. In conclusion, our results indicate we were able to specifically target TAM using a liposomal carrier containing carboxylated lipids.

1 Introduction

The tumor microenvironment (TME) contains a variety of nonmalignant cell types in addition to malignant tumors cells. The majority of the nonmalignant cells include stromal cells such as tumor-associated macrophages (TAMs), fibroblasts, and tumor vasculature cells. TAMs promote key processes in tumor progression, like angiogenesis, immunosuppression, invasion, and metastasis [1]. In tumors, M2 macrophages are the activated form of macrophages, which compose most of the TAMs. They promote angiogenesis, suppress the immune system, and enhance chemoresistance, thus limiting efficacy of chemotherapy [2]. Therefore, specific inhibition of pro-tumoral activities of M2 macrophages within the TME represents a promising strategy contributing to the fight against cancer.

Liposomes are the most commonly used drug carrier to deliver drugs to tumors. Many liposomal formulations such as Myocet® (non-PEGylated formulation of doxorubicin), Doxil® (Pegylated liposomal formulation of doxorubicin), DaunoXome® (Pegylated liposomal formulation of daunorubicin) and Marqibo® (liposomal formulation of vincristine sulfate) have been used clinically for the treatment of different cancer types. Liposome-enabled tumor targeting is mainly based on the principal of passive targeting that relies on the phenomenon called the Enhanced Permeability and Retention (EPR) effect.

Macrophages express different phagocytosis receptors such as pattern-recognizing receptors (*e.g.* mannose receptor), opsonic receptors and scavenger receptors (*e.g.* CD36) [3]. To target some of these receptors, many approaches such as surface modifications with mannose sugar, targeting peptides or monoclonal antibodies have been proposed to induce uptake of nanoparticles by macrophages [4, 5]. Oxidized phospholipids have been shown to interact with macrophages through CD36 receptor [6]. In order to target M2 macrophages specifically, it is important to understand the differences in uptake behavior by these cell types. In our previous studies, we have identified specific phagocytosis receptors which are upregulated in M2 macrophages [7]. By investigating their endogenous ligands, we were able to identify three different receptors involved in the recognition of oxidized lipids: the scavenger receptor class B member 1 (Scarb1), collectin subfamily

member 12 (Colec12) and the already mentioned CD36 receptor [7]. All three receptors belong to the class of scavenger receptors [8].

Unsaturated lipids are unstable and may oxidize into different derivatives [9, 10]. Moreover, oxidized lipids may result in toxicity or activation of macrophages [11-16]. Therefore, we selected saturated phospholipids, which are carboxylated at one chain, here called carboxylated phospholipids. The aim of the project is to design M2 macrophage-targeted liposomes using carboxylated phosphatidylcholine (CyPC) in their lipid composition, which can be potentially used for drug delivery purposes. We prepared unilamellar liposomes using a carrier lipid *i.e.* phosphatidylcholine in combination with the carboxylated forms of lipids. Different amounts of CyPC lipids were incorporated into the liposomes to optimize their binding to and uptake into M2 macrophages. We evaluated their toxicity and effect on gene expression of macrophages. Their macrophage specificity was tested *in vitro*, *in vivo* we evaluated their tumor accumulation and organ distribution. Finally, we investigated the role of the overexpressed receptors in the specific uptake of carboxylated-lipid containing liposomes by M2 macrophages.

2 Materials & Methods

2.1 Preparation of liposomes

Liposomes were prepared using the ethanol injection technique [17]. Briefly, hydrogenated soy phosphatidylcholine (HSPC, Lipoid GMBH, Germany), carboxylated lipids 1-palmitoyl-2-azelaoyl-sn-glycero-3-phosphocholine (PAzPC, Cayman chemicals, Ann Arbor, MI) or 1-palmitoyl-2-glutaryl phosphatidylcholine (PGPC, Cayman chemicals), cholesterol (Sigma Aldrich) and the lipophilic fluorescent label 1,1′-Dioctadecyl-3,3,3′,3′-tetramethylindocarbocyanine perchlorate (DiI, Sigma Aldrich, St Louis, MO) at a molar ratio of 0.1 of total lipid were dissolved in ethanol and heated at 70 °C. The heated lipid solution was injected into PBS to create a crude liposomal formulation with a concentration of 10 mM total lipid which was then diluted to 2.5 mM total lipid. The crude liposomal formulation was extruded using the Avestin Liposofast extruder. After preparation, liposomes were dialyzed against PBS using 10 kD cutoff slide-A-lyzers (Thermo Fisher Scientific, Waltham, MA). Liposomal size (in PBS) and zeta potential (in 0.1 mM KCl) were measured using Zetasizer Nano ZS (Malvern, Malvern, UK). Liposomes were prepared using different molar ratios of CyPC:HSPC:Cholesterol.

2.2 Liposome analysis

Concentration and composition of the liposomes were analyzed using the UltiMate® 3000 UHPLC with Charged Aerosol Detector (Dionex™ Corona™; Thermo Scientific) using an Acquity UPLC BEH C18 column (130Å, 1.7 µm, 2.1 mm X 50 mm). The binary mobile phase consisted of (A) methanol with 0.05% TFA, and (B) methanol:water (80:20 v/v) with 0.05% TFA, and a constant flow rate of 0.2 ml/min. Data was analyzed using Chromeleon® Chromatography Data System. Calibration curves were prepared in the range 6 – 200 µg/ml for all lipids. Before analysis, liposomes were diluted ten times in methanol and placed in an ultrasonic waterbath for 30 min.

2.3 Liposome stability

Liposomes were diluted ten times in cell culture medium without serum and incubated at 37 °C for 24 h. Size was determined using the Zetasizer Nano ZS (Malvern). For loss of fluorescence, undiluted samples were incubated in Amicon Ultra tubes (Mw cut-off 30 kD,

Sigma Aldrich) in a container containing cell culture medium without serum. Fluorescence of samples was determined before and after incubation using the Tecan Infinite 200 Pro (Männedorf, Switzerland).

2.4 Cell culture

Monocytic human THP-1 cells (ATCC, Rockville, MD) were cultured in suspension in RPMI-1640 medium supplemented with 10% FBS (Lonza, Basel, Switzerland), 100 U/ml penicillin, 0.1 mg/ml streptomycin (Sigma Aldrich, St Louis, MO) and 2 mM L-glutamine (GE Healthcare, Little Chalfont, UK) in a CO_2 incubator at 37°C. Murine bone marrow derived macrophages (BMDMs) were isolated from male C57BL6 mice by flushing the femur and tibia with PBS under sterile conditions. The bone marrow cells were then resuspended in RPMI-1640 medium supplemented with 1% L-glutamine, 1% Penicillin and streptomycin , 20% FBS and 20% 3T3-conditioned medium (filter-sterilized). The cells were then incubated for 10 days at 37 °C and 5% CO2 with medium change every 3–4 day. 4T1 tumor cells were cultured in RPMI-1640 medium supplemented with 10% FBS, 100 U/ml penicillin, 0.1 mg/ml streptomycin and 2 mM L-glutamine in a CO_2 incubator at 37°C.

2.5 Macrophage differentiation

Macrophages were differentiated as reported previously [7]. Briefly, THP-1 cells were treated for 24 h with 100 ng/ml of phorbol 12-myristate 13-acetate (PMA, Cayman Chemicals) to allow their attachment. The medium was replaced by medium containing 20 ng/ml IL-4 and IL-13 (Peprotech, London, UK) for M2 differentiation, or 20 ng/ml IFNγ (Peprotech) and 100 ng/ml LPS (Sigma Aldrich) for M1 differentiation. Cells were incubated with cytokines for 24 h (gene expression on differentiation), and 72 h (liposome uptake experiments). BMDMs were plated overnight with a density of 50,000 cells/ml. After 24 h, medium was aspirated. Cells were incubated for 24 h in complete RPMI medium containing IL-4 and IL-13 at 10 ng/ml (M2 differentiation) or LPS and IFN-γ at 100 and 10 ng/ml.

2.6 Macrophage transfection

0.25 x 10^6 cells were plated in a 24-well plate and activated as described above. siRNA (CD36, Colec12, Scarb1, Thermo Fisher Scientific) complexes using HiPerfect Transfection reagent (Qiagen, Venlo, The

Netherlands) were prepared as per manufacturer's instructions. siRNA was added to the cells at a concentration of 150 nM for 4 h, after which complexes were removed and cells were differentiated as described above. Cells were lysed 6 and 24 h after cytokine differentiation for PCR analysis. For quantitative liposome uptake experiments, cells were used 44 h after cytokine differentiation.

2.7 Quantitative Real Time PCR

0.5 x 10^6 THP-1 cells were plated in 12-well plates and activated using PMA. Cells were then incubated with different liposomal preparations (50 μM) or differentiation cytokines for 24 h. BMDM were differentiated as described above. After differentiation, cells were washed with PBS and then lysed using lysis buffer and total RNA was isolated using SV Total RNA Isolation System (Promega, Madison, WI). cDNA was prepared by using iScript cDNA synthesis kit (Bio-Rad, Hercules, CA) and qRT-PCR was performed with 10 ng of cDNA per reaction mixture using SYBR green assay (Bioline, London, UK). Primer sequences are listed in Table 1. Reactions were measured using the CFX384 Real-Time PCR detection system (Bio-Rad). The threshold cycles (Ct) values were calculated and relative gene expression (ddCt method) was analyzed after normalization using the *Rsp18* (THP-1) or *Gapdh* (BMDM) house-keeping gene.

Gene	Forward (5'→ 3')	Reverse (3'→ 5')	Accession
Arg-1 (m)	*GTGAAGAACCCACGGTCTGT*	*CTGGTTGTCAGGGGAGTGTT*	*NM_007482.3*
Cd36 (h)	TGGCAACAAACCACACACTG	AAGTCCTACACTGCAGTCCTC	NM_000072.3
Colec12 (h)	AGGTCGAGGTTAGACACTGAAG	GATCCTCTGTCACCTCTTGGAC	NM_130386.2
Dc-sign (h)	GAACTGGCACGACTCCATCA	CTGGAAGACTGCTCCTCAGC	NM_001144897.1
Dectin-1 (h)	ATGGCTCTGGGAGGATGGAT	GGGCACACTACACAGTTGGT	NM_197947.2
Gapdh (m)	*ACAGTCCATGCCATCACTGC*	*GATCCACGACGGACACATTG*	*XM_001476707.3, XM_001479371.4, XM_003946114.1, NM_008084.2*
Il-1β (h)	CAGAAGTACCTGAGCTCGCC	AGATTCGTAGCTGGATGCCG	NM_000576.2
Il-6 (h)	TGCAATAACCACCCCTGACC	ATTTGCCGAAGAGCCCTCAG	NM_000600.3
Il-6 (m)	*TGATGCTGGTGACAACCACGGC*	*TAAGCCTCCGACTTGTGAAGTGGTA*	*NM_031168.1*
Rps18 (h)	TGAGGTGGAACGTGTGATCA	CCTCTATGGGCCCGAATCTT	NM_022551.2
Scarb1 (h)	AAGATTGAGCCTGTGGTCCTG	CCTCCTTATCCTTTGAGCCCT	NM_005505.4
Tnf-α (h)	CTTCTGCCTGCTGCACTTTG	GTCACTCGGGGTTCGAGAAG	NM_000594.3

Table 1: Primer sequences of selected human (h) and murine (m) genes.

2.8 Microscopy analysis of liposome uptake

0.5 x 10^6 THP-1 cells per well were seeded in a 12-well plate and differentiated as described above. Fluorescence of different liposomes was measured in PBS, using the Victor3 multilabel fluorescence plate reader (Perkin Elmer, Waltham, MA). Liposomes were diluted to equal

fluorescence at a maximum concentration of 250 μM lipid in culture medium without serum and incubated for 2 h. After incubation, cells were vigorously washed and fixed during 20 minutes using 4% formalin. Cells were washed 2 times in PBS and mounted in mounting medium with DAPI. Uptake of liposomes was visualized using the inverted fluorescent microscope EVOS (Applied Biosystems). Images were taken at 40x magnification using identical settings.

2.9 Quantitative liposome uptake

Liposomes were diluted to equal fluorescence at a maximum concentration of 250 μM lipid (THP-1) or 125 μM (BMDM) in culture medium without serum and added to differentiated macrophages and incubated at 37°C for 2 h (THP-1) or 30 min (BMDM). After incubation, cells were vigorously washed, immediately placed on ice and then detached using Accutase cell detachment solution (Sigma Aldrich) and gentle scraping. Cells were then collected and particle uptake was assessed by measuring mean fluorescence intensities in the FL-2 channel for at least 10,000 gated cells, using flow cytometry (BD FACSCalibur, Becton Dickinson, Franklin Lakes, NJ). Gates were set in the FSC vs SSC plot, using untreated control cell populations. For all experiments, identical settings were used. Data was analyzed using Flowing Software 2.5.0.

2.10 Toxicity of CyPC liposomes

5×10^4 THP-1 cells per well were seeded in a 96-well plate and activated using PMA as described above. Cells were then incubated in the absence of serum for 24 h with different liposomal preparations (50 μM). After 24 h, medium was removed, cells were washed once with PBS, and a 10% 110 μg/ml Resazurin sodium salt solution (Sigma Aldrich) was added. Cells were allowed to incubate for an additional 75 minutes, after which the Resazurin solution was transferred to a black 96-well plate and fluorescence was measured using the Victor3 plate reader.

2.11 Liposome distribution in the 4T1 mouse tumor model

7 week old female Balb/c mice were injected with 0.1×10^6 4T1 tumor cells into the mammary fat pad. Tumors were allowed to develop until tumor size reached 500 mm^3. Liposomal formulations (HSPC 0:8:2, PazPC and PGPC 3:5:2) containing fluorescent label DiI were injected

i.v. Liposomal formulations were corrected to equal fluorescence before injections. Mice were sacrificed after 1 h. Organs and tumors were isolated.

2.12 Quantification of organ and tumor accumulation

Approximately equal amounts of frozen tissue from tumors, livers and spleens were lysed using RIPA buffer (Thermo Fischer). Tissues were homogenized thoroughly. Fluorescence in lysates was determined using the Victor 3 fluorescent plate reader. Fluorescence was corrected for protein content, determined using BCA kit (Thermo Fisher).

2.13 Cellular localization

Sections were cut from isolated organs and tumors and stained for macrophage marker F4/80 (Bio-rad) or CD206 (Santa Cruz) overnight. Secondary antibodies Rabbit anti Rat and Rabbit anti Goat (Dako) were used. Alexa 488 Donkey anti Rabbit (Thermo Fisher) antibodies were used for visualization. Sections were scanned using the Hamamatsu NanoZoomer Digital slide scanner 2.0HT (Hamamatsu Photonics, Bridgewater NJ).

2.14 Statistical analysis

Data are presented as mean + standard error of the mean (SEM). All graphs were created and statistical analysis were performed using Graphpad Prism (Graphpad, La Jolla, CA) using two-sided unpaired student's T-test, unless otherwise specified. Statistical tests were performed with a minimum significance level of $p<0.05$.

3 Results

3.1 CyPC liposomes preparation and characterization

Two different forms of carboxylated lipids (CyPCs) were selected and tested in this study: PAzPC and PGPC (Figure 1A). These lipids were incorporated into liposomes at different molar ratios. Size, polydispersity index (PDI) and zeta potential were determined, as shown in Table 1. The prepared liposomal preparations ranged from 80 (PGPC 2:6:2) to approximately 105 - 116 nm (other formulations) in mean size, with a small size distribution (Figure 1C). To quantify the incorporated amount of carboxylated lipid into these liposomes, we developed a uHPLC method using a corona CAD detector. Typical chromatograms showing lipid mixtures of liposome components are shown in Figure 1B. Using this method, the total amounts and molar ratios of CyPC in the prepared liposomes was investigated (Table 2). We found that the molar ratios for HSPC and PAzPC were comparable to the starting ratio, whereas the observed ratio PGPC-containing liposomes slightly deviated from the input ratio.

Formulations	**Size (nm ± SD)**	**PDI (± SD)**	**Zeta potential (mV ± SD)**
HSPC (0:8:2)	115.9 ± 6.2	0.12 ± 0.05	-22.6 ± 4.8
PAzPC (2:6:2)	107.9 ± 0.7	0.19 ± 0.06	-25.1 ± 4.9
PAzPC (3:5:2)	105.9 ± 15.7	0.22 ± 0.04	-27.8 ± 4.6
PGPC (2:6:2)	80.1 ± 0.9	0.20 ± 0.10	-17.0 ± 6.0
PGPC (3:5:2)	113.5 ± 16.5	0.2 ± 0.08	-21.1 ± 2.8

Table 2: Size, Polydispersity index (both measured in PBS) and zeta potential (in 0.1 mM KCl solution) of different compositions of liposomes. Molar ratios are shown between brackets. Results are shown from 2 – 5 different batches of liposomes, mean + SD.

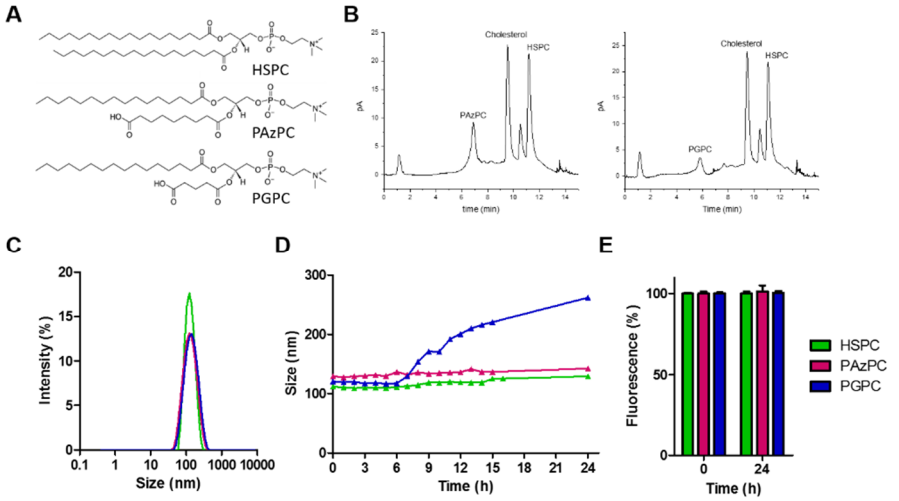

Figure 1: Preparation and analysis of CyPC-containing liposomes. (A) Structure of selected lipids (B) Typical chromatogram of lipid mixtures analyzed using uHPLC separation with corona CAD. (C) Representative DLS graphs showing size distribution of different liposomal preparations (D) Stability of liposomes in culture medium at 37 °C for 24 h. (E) Fluorescence of liposomes before and after incubation in culture medium at 37 °C for 24 h. Molar ratio CyPC:HSPC:Cholesterol 0:8:2 (HSPC) and 5:3:2 (PAzPC and PGPC) were used in panels C-E.

3.2 Stability of liposomes

Stability of the prepared liposomes was investigated at 37 °C for up to 24 h in culture medium. Results are shown in Figure 1D. HSPC and PAzPC liposomes remained stable over the course of 24 h, PGPC liposomes increased in size starting after 7 h of incubation. To verify the fluorescent label DiI did not degrade or leak from the liposomal preparations, we dialyzed samples at 37 °C in culture medium for 24 h (Figure 1E). We could not detect any loss of fluorescence, indicating the label remained inside the lipid bilayer of the liposomes during this time.

One batch of liposomes was tested in long term stability. We checked the size of liposomes after 3 weeks of storage in PBS at 4 °C and found little change in size, and a slight increase in PDI (Table 3). These results indicate the liposomes remained stable during this time.

	CyPC (mM)	HSPC (mM)	Choles-terol (mM)	Molar ratio
HSPC (0:8:2)	-	1.6 (2)	0.4 (0.5)	8 : 2
PAzPC (2:6:2)	0.4 (0.5)	1.15 (1.5)	0.5 (0.5)	2 : 5.6 : 2.4
PAzPC (3:5:2)	0.6 (0.75)	1.0 (1.25)	0.4 (0.5)	3 : 5 : 2
PGPC (2:6:2)	0.7 (0.5)	1.5 (1.5)	0.7 (0.5)	2.4 : 5 : 2.4
PGPC (3:5:2)	0.4 (0.75)	0.9 (1.25)	0.4 (0.5)	2.4 : 5.3 : 2.4

Table 3: uHPLC analysis of lipid content of CyPC-containing liposomes. Values are shown in mM, with theoretical amounts between brackets. The calculated molar ratio according to uHPLC analysis is shown in the last column.

	Size (nm ± SD) Start	PDI (± SD) Start	Size (nm ± SD) 3 weeks	PDI (± SD) 3 weeks
HSPC (0:8:2)	116.1 ± 3.36	0.06 ± 0.01	118.0 ± 0.36	0.12 ± 0.01
PAzPC (3:5:2)	83.34 ± 3.34	0.17 ± .003	87.23 ± 2.94	0.22 ± 0.01
PGPC (3:5:2)	96.79 ± 2.57	0.14 ±1.5	91.9 ± 0.44	0.16 ± 0.03

Table 4: Size and PDI of one batch of different CyPC-containing liposomal formulations, stored at 4 °C for 3 weeks. Mean ± SD.

3.3 Effect of CyPC-containing liposomes on the viability and differentiation state of macrophages

In order to examine the effects of the prepared nanoparticles on macrophages, we first determined their toxicity and effect on differentiation on macrophages. In the PMA-activated macrophages, CyPC-containing liposomes were incubated for 24 h. Results are shown in figure 2A. We found that all tested formulations showed no effect on the macrophage viability. Next to toxicity, the effect of liposomes on macrophage differentiation was investigated using the same method. After 24 h incubation, we could not detect changes in gene expression of M1 (*Tumor necrosis factor α* (*Tnf-α*) and *Interleukin 6* (*Il-6*)) and M2 (*Dc-sign* (*Cd209*) and *Dectin-1* (*Clec7a*)) related genes, indicating that the liposomes did not differentiate the macrophages into either the M1 or the M2 phenotype.

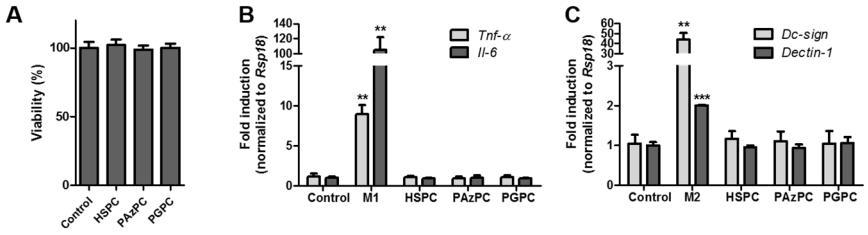

Figure 2: Viability and gene expression of macrophages treated with CyPC-containing liposomes. (A) Viability of PMA-differentiated macrophages, treated with CyPC-containing liposomes (0:8:2 or 3:5:2 CyPC:HSPC:Cholesterol molar ratio at 50 μM) for 24 h. (B and C) Gene expression data on M1 macrophage associated genes (*Tnf-α, Il-6*, B) and M2 macrophage associated genes (*Dc-sign, Dectin-1*, C) of PMA-differentiated macrophages, treated with CyPC-containing liposomes (50 μM) for 24 h. All experiments n=3, mean + SEM, **p<0.01, ***p<0.001 vs control

3.4 Uptake of CyPC by differentiated macrophages

To evaluate the uptake of CyPC-containing liposomes by M1 and M2 differentiated macrophages, liposomes with CyPC:HSPC:Cholesterol molar ratio 3:5:2 were incubated with differentiated macrophages (Figure 3A) and examined using fluorescent microscopic. HSPC liposomes were taken up in low and similar amounts and by both types of macrophages. A striking difference in uptake between M1 and M2 cells was seen using PAzPC-containing liposomes. Highest uptake was achieved using PGPC-containing liposomes, however, the difference between M1 and M2 cellular uptake was smaller. We then quantified the cellular uptake using flow cytometry and confirmed our observation that PAzPC were taken up much more by M2 compared to M1, while differences in case of PGPC were smaller, yet statistically significant (Figure 3B and C). Next to human cells, the specific uptake of PAzPC-containing liposomes was also confirmed in murine bone marrow derived macrophages (BMDM). BMDM were first differentiated into M1 and M2 phenotypes. Gene expression analysis confirmed differentiation (Figure S1A). Upon incubation with liposomes, M2 differentiated cells showed significantly higher uptake of PAzPC-containing liposomes, compared to M1 cells (Figure S1B and C).

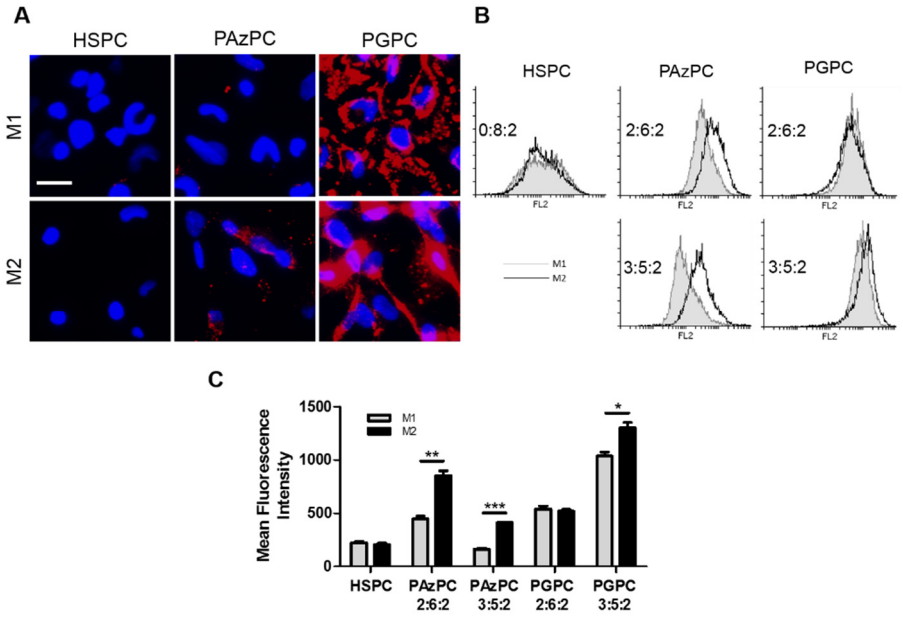

Figure 3: Uptake of CyPC-containing liposomes by differentiated macrophages. (A) Representative fluorescent images of cellular uptake of CyPC-containing liposomes by differentiated M1 and M2 macrophages, incubated for 2 h. Blue: DAPI, Red: CyPC-containing liposomes (3:5:2; CyPC:HSPC:Cholesterol molar ratio) labeled with DiI, bar = 25 µm). (B) Representative flow cytometry histograms of M1 and M2 differentiated macrophages, incubated with CyPC-containing liposomes (different ratios) for 2 h. (C) Quantification of flow cytometry data. All experiments n=3, mean + SEM, *p<0.05, **p<0.01, ***p<0.001 vs M1

3.5 *In vivo* distribution and uptake of CyPC-containing liposomes into tumor tissues and organs

To evaluate the effects of CyPC-containing liposomes on tissue distribution *in vivo*, mice were injected with 4T1 breast cancer tumor cells into the mammary fat pad. When tumors reached 500 mm^3, mice were injected with CyPC-containing liposomes via the tail vein and sacrificed after 1 h. Tumors and organs were isolated. Upon examination of tumor tissues using the microscope, clear differences in tumor accumulation between normal and CyPC-containing liposomes could be seen (Figure 4A). Both types of CyPC-containing liposomes showed increased tumor accumulation, compared to normal liposomes. This was confirmed by quantification of tumor fluorescence using tissue lysates (Figure 4B). Co-localization of liposomes and

TAMs (CD206, green) is shown in Figures 4C. As can be seen, although all liposomes show some co-localization with TAMs, it was the most pronounced in PAzPC liposomes.

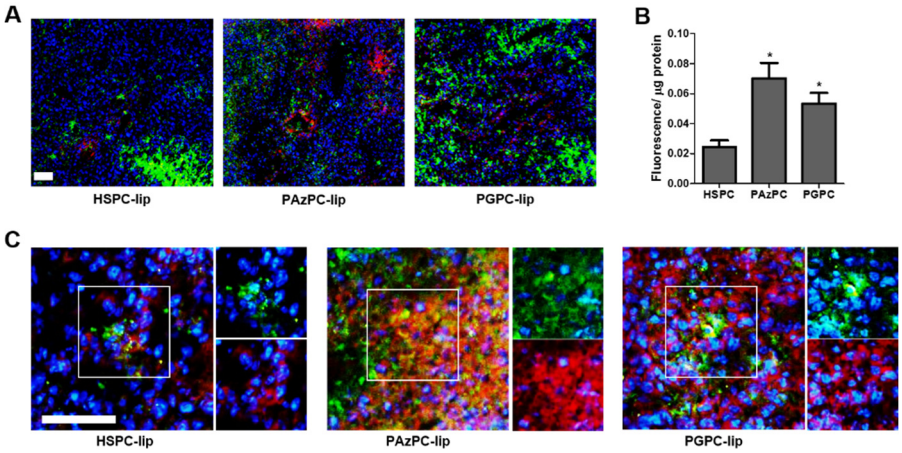

Figure 4: Tumor distribution of liposomes in 4T1 tumor-bearing mice. (A) Representative images of liposome distribution (0:8:2 or 3:5:2 CyPC:HSPC:Cholesterol molar ratio) in tumor tissues, 1 h after injection. Red: liposomes labeled with DiI, green: macrophage marker F4/80, blue: DAPI (B) Quantification of fluorescence in tumor homogenates. (C) Fluorescent images of macrophage-liposome co-localization within tumor tissues. Red: liposomes labeled with DiI, green: M2 macrophage marker CD206, blue: DAPI. Bar = 50 µm. All experiments n=3, mean + SEM, *p<0.05 vs HSPC.

Uptake of liposomes in other organs was also examined (Figure 5). PAzPC-containing liposomes showed significantly less uptake in liver tissues, compared to normal and PGPC-containing liposomes. Furthermore, both PAzPC- and PGPC-containing liposomes accumulated significantly less in spleen tissues.

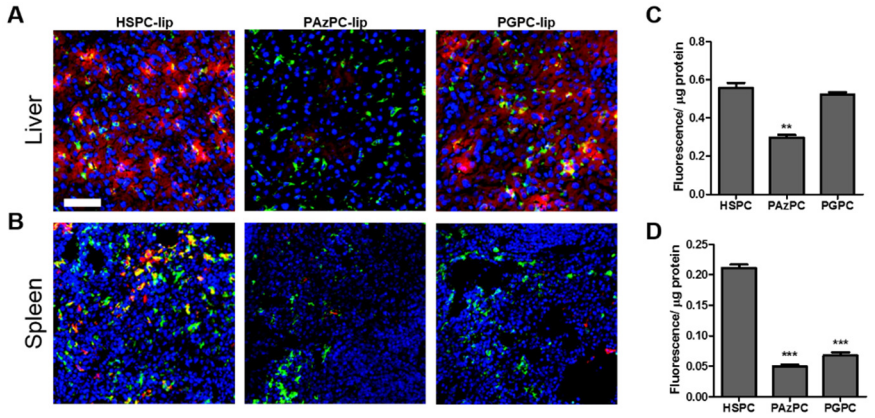

Figure 5: Liver and spleen organ distribution of liposomes in 4T1 tumor-bearing mice. (A and B) Representative fluorescent images of liposome (0:8:2 or 3:5:2 CyPC:HSPC:Cholesterol molar ratio) distribution within the liver (A) and spleen (B), 1 h after injection. Red: liposomes labeled with DiI, green: macrophage marker F4/80, blue: DAPI. Bar = 50 µm (C and D) Quantification of organ fluorescence of tissue homogenates. All experiments n=3, mean + SEM, **p<0.01, ***p<0.001 vs HSPC.

3.6 Mechanism of specific M2 uptake

In previous research, we investigated the differences in phagocytosis related genes in M1 and M2 cells [7]. From this research, we selected 3 different receptors, involved in oxidized lipid uptake; cluster of differentiation 36 (CD36), scavenger receptor class B member 1 (Scarb1) and collectin subfamily member 12 (Colec12) and reconfirmed their upregulation in M2 cells (Figure 6A). To study the role of these receptors in uptake, we used siRNA to silence these receptors in M2 differentiated macrophages (Figure 6B) and subsequently investigated the uptake of normal and PAzPC-containing liposomes. We found that silencing of the mentioned receptors did not affect HSPC liposome uptake (Figure 6C). In contrast, PAzPC liposomes showed a significant reduction in the uptake upon silencing the investigated genes in the following order (Cd36<Colec12<Scarb1). These data indicate that amongst the investigated receptors, Colec12 and Scarb1, and Cd36, are responsible for the M2-specific uptake of CyPC-containing liposomes.

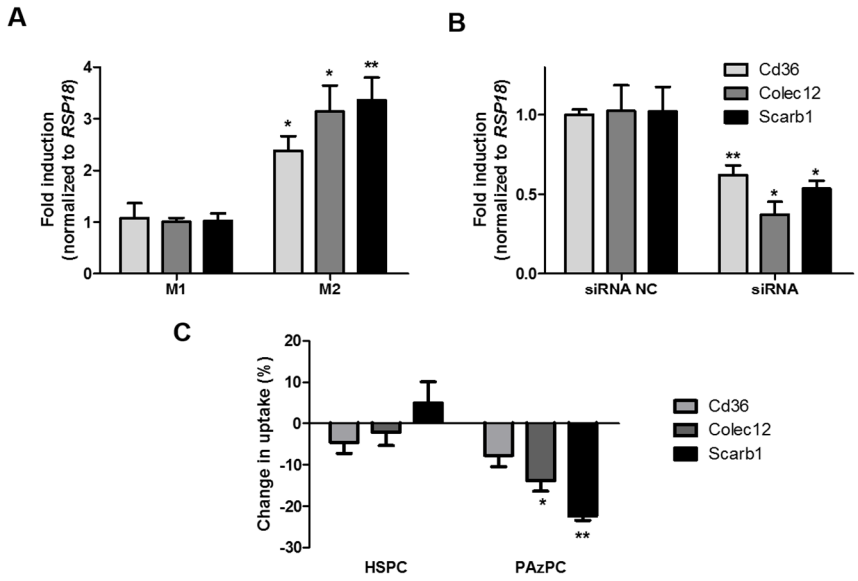

Figure 6: Mechanism of action of specific uptake of CyPC-containing liposomes by M2 macrophages. (A) Gene expression data on M2 specific surface receptors Cd36, Colec12 and Scarb1. (B) Treatment with siRNA complexes reduces the gene expression of Cd36, Colec12 and Scarb1 in M2 differentiated macrophages. (C) Quantification of flow cytometry analysis of change in uptake after silencing of M2-specific surface receptors using HSPC liposomes (0:8:2 CyPC:HSPC:Cholesterol molar ratio) or PAzPC (3:5:2 CyPC:HSPC:Cholesterol molar ratio) after 2 h of incubation. All experiments n=3-4, mean + SEM, *p<0.05, **p<0.01 vs M1 (A), siRNA NC (B) or HSPC (C).

4 Discussion

Macrophage targeting and depletion has been described extensively in literature [5, 18]. Additionally, macrophage polarization in disease conditions is a growing field of research [19-22]. Moreover, the functions of differentiated macrophages are becoming more and more clear. As M1 macrophages may be beneficial in cancer immunity, the specific targeting of TAM subpopulation in the treatment of cancer may be an effective way to treat these macrophages [5, 23, 24]. In this study, we aim to specifically target tumor-promoting macrophages (*i.e.* M2 macrophages/TAMs), through M2-induced surface receptors CD36, Collectin subfamily member 12 and Scavenger receptor class B member 1. Carboxylated lipids, which are the natural ligands for these receptors [10, 25-27], were incorporated into small unilamellar liposomes. We selected the well-characterized, stable carboxylated lipids PAzPC and PGPC and incorporated them at several ratios into liposomes composed of the carrier lipid HSPC and cholesterol.

Size stability was investigated over a period of 24 h at 37 ºC in culture medium, since these liposomes were not pegylated they are expected to circulate only for a few hours. During this period of time, HSPC and PAzPC liposomes remained stable while PGPC-containing liposomes increased in size after 7 h of incubation, indicating these liposomes were less stable (Figure 1C). Studies have shown that the shorter oxidatively truncated tail of PGPC flips to the outside of the lipid bilayer, whereas the somewhat longer tail of PAzPC is able to reside in the bilayer as well [9, 28]. This might result in a more stable liposome. At 4 ºC, these formulations remained stable for up to 3 weeks with no change in their size (table 3). To rule out the possibility of leakage or transfer of the fluorescent dye out of the bilayer, which might cause false positive results during uptake studies, we investigated the retention of the dye in the lipid bilayer under similar conditions as *in vitro* experiments. Although there was an increase in size, no leakage of the dye was seen indicating that the dye was well retained due to its high lipophilic nature.

Recent reports have shown that liposomes or lipids may modulate the macrophage phenotype [11-15]. The application of pegylated liposomes in a murine cancer model promoted tumor growth and angiogenesis, while suppressing the anti-tumor immune response. Further

investigation showed a decrease in Interferon-γ secreting (associated with M1) macrophages [14]. On the other hand, several studies have shown specifically oxidized lipids to induce inflammatory gene expression, most likely due to the interaction with Toll-like receptors (TLRs) [11-13, 15] or via transcription factor Nrf2 mediated gene expression [29]. As the aim of our study is to design a targeting strategy for the treatment of TAM, thereby reducing their tumor-promoting properties, we investigated the effect of our carriers on macrophage differentiation. We analyzed the gene expression profiles of liposome-treated macrophages for well-known genes associated with M1 (*Tnf-α* and *Il-6*) and M2 (*Dc-sign* and *Dectin-1*) macrophage differentiation [7, 30-32]. Macrophages were treated with M1 inducing (Lipopolysaccharide (LPS) and Interferon γ (IFN-γ)) and M2 inducing (IL-4 and IL-13) cytokines to provide positive controls. As can be seen in Figure 2B and C, treatment of macrophages with our liposomal preparations did not affect macrophage differentiation. Furthermore, no effect on cell viability was observed, suggesting these liposomes are not toxic and do not alter their phenotype. Based on these results, these liposomes may be applied for the targeting of TAM, without inducing cell death or macrophage differentiation.

Using fluorescent microscopy and flow cytometry, we delineated the differences between the liposomal uptake by M1 and M2 macrophages both microscopically and quantitatively (Figure 2). The most striking difference in M1 and M2 was seen using PAzPC liposomes at 3:5:2 molar ratio at which the liposomes became more specific to M2. The higher specificity of PAzPC compared to PGPC might be attributed to its longer tail with carboxylic group, which is likely to flip out to the surface and interact with cell surface receptors. However, the mechanism for its preference to M2-like cells is not known. Tumor accumulation and organ distribution of both types of carboxylated lipid liposomes were tested in the 4T1 murine breast cancer model. Most interestingly, using carboxylated-lipid containing liposomes, we found 2- (PGPC) to 3-fold (PAzPC) increase in tumor fluorescence. Most importantly, we were able to show the co-localization of PAzPC-containing liposomes with M2 macrophages (CD206 positive, Figure 4C). In HSPC and PGPC-containing liposomes the co-localization of liposomes and M2 macrophages was not as pronounced. In the liver and spleen, organs which play a major role in the clearance of nanoparticles [33], PAzPC-containing liposomes showed an almost 2-

fold reduction in uptake in the liver (Figure 5C), while both CyPC-containing liposomes showed a huge reduction (3- and 4-fold for PGPC and PAzPC respectively) in uptake by the spleen (Figure 5D). As tissue macrophages have varying phenotypes [34], we stained these macrophages using the general macrophage marker F4/80. Liposomes and macrophage (F4/80 positive) co-localization seemed to be absent in livers for PAzPC-containing liposomes and in the spleen for both types of CyPC-containing liposomes. HSPC-containing liposomes are mostly clustered around macrophages in both organs. This indicates HSPC liposomes are rapidly cleared from circulation, due to liver and spleen uptake, while CyPC-containing liposomes avoid this uptake. Greater tumor accumulation for these liposomes may therefore be achieved via higher availability of the liposomes and due to active uptake by TAM in tumor tissues.

Due to the superior effects PAzPC-containing liposomes have shown in M2-macrophage specificity, tumor accumulation and organ distribution, we chose these liposomes at a molar ratio of 3:5:2 to continue investigating the mechanism of action causing this specificity. In previous studies, we investigated differences in phagocytic receptors in M1 and M2 differentiated cells [7]. In this study, we found a number of upregulated phagocytosis receptors in M2 differentiated cells. Of those receptors, we selected the ones which are involved in oxidized lipid recognition and uptake.

CD36 is a member of the scavenger receptor class B family [8, 35]. It has been shown to play a role in accumulation of cholesterol in atherosclerotic plaques, via uptake of oxidized lipoproteins [36, 37]. Furthermore, oxidized phosphatidylserine (OxPS), expressed by apoptotic cells, is recognized by CD36, resulting in recognition and engulfment of apoptotic cells [38]. Other types of oxidized lipids, including PAzPC and PGPC have been identified to interact with CD36 as well [10].

Of the same class as CD36 is Scarb1 [8]. Its major function is the selective uptake of cholesteryl esters from high density lipoprotein (HDL) and the initial steps of reverse cholesterol transport [39, 40]. Moreover, Scarb1 binds oxidized low density lipoproteins (OxLDL) with high affinity. Since this binding is inhibited via competition of free oxidized lipoproteins from LDL and E06, a selective antibody against

oxidized phospholipids [41], this receptor is thought to play an important role in the binding of OxLDL by macrophages, mainly through the presence of oxidized phospholipids [25].

Colec12 is a member of the scavenger class A family [8]. This cell surface glycoprotein plays a role in host defense, due to its carbohydrate recognizing domain (CRD) [42]. Moreover, Ohtani *et al* have shown this receptor to recognize, bind and internalize oxLDL [27].

Using gene expression analysis on differentiated M1 and M2 macrophages, we were able to confirm these receptors to be upregulated in the M2 macrophage phenotype (Figure 6A). To study the role of these receptors in the specific uptake of carboxylated-lipid containing liposomes by M2 macrophages, we selectively silenced the genes for these receptors. Using siRNA complexes, we were able to reduce their gene expression profiles significantly (Figure 6B). Subsequently, we examined the effect of this silencing on the uptake of normal and PazPC-containing liposomes. Surprisingly, when using normal liposomes, silencing of the M2 specific uptake receptors did not affect liposome uptake at all (Figure 6C), suggesting these receptors do not play a role in the recognition and internalization of HSPC liposomes by M2 macrophages. However, when using PAzPC-containing liposomes, the liposomal uptake was reduced in Colec12 and Scarb1-silenced cells. Cd36-silenced cells showed a small non-significant reduction in uptake (Figure 6C). This suggests that Colec12 and Scarb1 play a major role in the recognition and uptake of PAzPC-containing liposomes by M2 macrophages.

5 Conclusion

In this study, we have shown that carboxylated-lipid containing liposomes may be employed in the specific targeting of TAM (*i.e.* M2 macrophages). As the detrimental role of TAM in the progression of cancer is becoming more and more clear [22], the specific targeting and treatment of these immune cells has become an active topic of investigation [5]. Recently, several compounds have been shown to inhibit TAM polarization, thereby reducing tumor growth and metastasis [43-46]. Liposomes are versatile, biodegradable and generally well-tolerated [47-49]. Carboxylated lipids are well-defined lipid molecules and can therefore be applied for the development of clinical products. Moreover, carboxylated lipids have been tested clinically [50] which may facilitate their clinical application for liposomal delivery. Therefore, the combination of liposomes and carboxylated lipids as a nanocarrier represents a very suitable candidate for drug encapsulation and delivery in a clinical setting.

References

1. Hanahan, D. and R.A. Weinberg, *Hallmarks of cancer: the next generation*. Cell, 2011. **144**(5): p. 646-74.
2. Schooley, A.M., et al., *beta 1 integrin is required for anchorage-independent growth and invasion of tumor cells in a context dependent manner*. Cancer Letters, 2012. **316**(2): p. 157-167.
3. Lander, A.D., et al., *What does the concept of the stem cell niche really mean today?* Bmc Biology, 2012. **10**.
4. Valastyan, S. and R.A. Weinberg, *Tumor Metastasis: Molecular Insights and Evolving Paradigms*. Cell, 2011. **147**(2): p. 275-292.
5. Binnemars-Postma, K., G. Storm, and J. Prakash, *Nanomedicine Strategies to Target Tumor-Associated Macrophages*. Int J Mol Sci, 2017. **18**(5).
6. Boullier, A., et al., *Phosphocholine as a pattern recognition ligand for CD36*. Journal of lipid research, 2005. **46**(5): p. 969-76.
7. Binnemars-Postma, K.A., et al., *Differential uptake of nanoparticles by human M1 and M2 polarized macrophages: protein corona as a critical determinant*. Nanomedicine (Lond), 2016. **11**(22): p. 2889-2902.
8. Murphy, J.E., et al., *Biochemistry and cell biology of mammalian scavenger receptors*. Atherosclerosis, 2005. **182**(1): p. 1-15.
9. Beranova, L., et al., *Oxidation changes physical properties of phospholipid bilayers: fluorescence spectroscopy and molecular simulations*. Langmuir, 2010. **26**(9): p. 6140-4.
10. Serbulea, V., D. DeWeese, and N. Leitinger, *The effect of oxidized phospholipids on phenotypic polarization and function of macrophages*. Free Radic Biol Med, 2017. **111**: p. 156-168.
11. Cruz, D., et al., *Host-derived oxidized phospholipids and HDL regulate innate immunity in human leprosy*. J Clin Invest, 2008. **118**(8): p. 2917-28.
12. Imai, Y., et al., *Identification of oxidative stress and Toll-like receptor 4 signaling as a key pathway of acute lung injury*. Cell, 2008. **133**(2): p. 235-49.
13. Oskolkova, O.V., et al., *Oxidized phospholipids are more potent antagonists of lipopolysaccharide than inducers of inflammation*. J Immunol, 2010. **185**(12): p. 7706-12.
14. Sabnani, M.K., et al., *Liposome promotion of tumor growth is associated with angiogenesis and inhibition of antitumor immune responses*. Nanomedicine, 2015. **11**(2): p. 259-62.

15. Walton, K.A., et al., *Receptors involved in the oxidized 1-palmitoyl-2-arachidonoyl-sn-glycero-3-phosphorylcholine-mediated synthesis of interleukin-8. A role for Toll-like receptor 4 and a glycosylphosphatidylinositol-anchored protein*. J Biol Chem, 2003. **278**(32): p. 29661-6.
16. Stemmer, U., et al., *Toxicity of oxidized phospholipids in cultured macrophages*. Lipids Health Dis, 2012. **11**: p. 110.
17. Batzri, S. and E.D. Korn, *Single bilayer liposomes prepared without sonication*. Biochim Biophys Acta, 1973. **298**(4): p. 1015-9.
18. Tang, X., et al., *Anti-tumour Strategies Aiming to Target Tumour-associated Macrophages*. Immunology, 2012.
19. Beljaars, L., et al., *Hepatic Localization of Macrophage Phenotypes during Fibrogenesis and Resolution of Fibrosis in Mice and Humans*. Front Immunol, 2014. **5**: p. 430.
20. Sica, A., et al., *Tumour-associated macrophages are a distinct M2 polarised population promoting tumour progression: potential targets of anti-cancer therapy*. Eur J Cancer, 2006. **42**(6): p. 717-27.
21. Colin, S., G. Chinetti-Gbaguidi, and B. Staels, *Macrophage phenotypes in atherosclerosis*. Immunol Rev, 2014. **262**(1): p. 153-66.
22. Mantovani, A., et al., *Tumour-associated macrophages as treatment targets in oncology*. Nat Rev Clin Oncol, 2017. **14**(7): p. 399-416.
23. Allavena, P. and A. Mantovani, *Immunology in the clinic review series; focus on cancer: tumour-associated macrophages: undisputed stars of the inflammatory tumour microenvironment*. Clin Exp Immunol, 2012. **167**(2): p. 195-205.
24. Biswas, S.K. and A. Mantovani, *Macrophage plasticity and interaction with lymphocyte subsets: cancer as a paradigm*. Nat Immunol, 2010. **11**(10): p. 889-96.
25. Gillotte-Taylor, K., et al., *Scavenger receptor class B type I as a receptor for oxidized low density lipoprotein*. J Lipid Res, 2001. **42**(9): p. 1474-82.
26. Nelms, K., et al., *The IL-4 receptor: signaling mechanisms and biologic functions*. Annu Rev Immunol, 1999. **17**: p. 701-38.
27. Ohtani, K., et al., *The membrane-type collectin CL-P1 is a scavenger receptor on vascular endothelial cells*. J Biol Chem, 2001. **276**(47): p. 44222-8.
28. Amirkavei, M. and P.K. Kinnunen, *Interactions and dynamics of two extended conformation adapting phosphatidylcholines in model biomembranes*. Biochim Biophys Acta, 2016. **1858**(2): p. 264-73.

29. Kadl, A., et al., *Identification of a novel macrophage phenotype that develops in response to atherogenic phospholipids via Nrf2*. Circ Res, 2010. **107**(6): p. 737-46.
30. Martinez, F.O., et al., *Transcriptional profiling of the human monocyte-to-macrophage differentiation and polarization: new molecules and patterns of gene expression.* Journal of Immunology, 2006. **177**(10): p. 7303-11.
31. Relloso, M., et al., *DC-SIGN (CD209) expression is IL-4 dependent and is negatively regulated by IFN, TGF-beta, and anti-inflammatory agents*. Journal of Immunology, 2002. **168**(6): p. 2634-43.
32. Willment, J.A., et al., *The human beta-glucan receptor is widely expressed and functionally equivalent to murine Dectin-1 on primary cells*. European Journal of Immunology, 2005. **35**(5): p. 1539-47.
33. Alexis, F., et al., *Factors affecting the clearance and biodistribution of polymeric nanoparticles*. Mol Pharm, 2008. **5**(4): p. 505-15.
34. Haldar, M. and K.M. Murphy, *Origin, development, and homeostasis of tissue-resident macrophages*. Immunol Rev, 2014. **262**(1): p. 25-35.
35. Suzuki, H., et al., *A role for macrophage scavenger receptors in atherosclerosis and susceptibility to infection*. Nature, 1997. **386**(6622): p. 292-6.
36. Endemann, G., et al., *CD36 is a receptor for oxidized low density lipoprotein*. J Biol Chem, 1993. **268**(16): p. 11811-6.
37. Febbraio, M., et al., *Targeted disruption of the class B scavenger receptor CD36 protects against atherosclerotic lesion development in mice*. J Clin Invest, 2000. **105**(8): p. 1049-56.
38. Greenberg, M.E., et al., *Oxidized phosphatidylserine-CD36 interactions play an essential role in macrophage-dependent phagocytosis of apoptotic cells*. J Exp Med, 2006. **203**(12): p. 2613-25.
39. Acton, S., et al., *Identification of scavenger receptor SR-BI as a high density lipoprotein receptor*. Science, 1996. **271**(5248): p. 518-20.
40. Ji, Y., et al., *Scavenger receptor BI promotes high density lipoprotein-mediated cellular cholesterol efflux*. J Biol Chem, 1997. **272**(34): p. 20982-5.
41. Horkko, S., et al., *Monoclonal autoantibodies specific for oxidized phospholipids or oxidized phospholipid-protein adducts inhibit macrophage uptake of oxidized low-density lipoproteins*. J Clin Invest, 1999. **103**(1): p. 117-28.

42. Nakamura, K., et al., *Molecular cloning and functional characterization of a human scavenger receptor with C-type lectin (SRCL), a novel member of a scavenger receptor family*. Biochem Biophys Res Commun, 2001. **280**(4): p. 1028-35.
43. Xue, N., et al., *Chlorogenic acid inhibits glioblastoma growth through repolarizating macrophage from M2 to M1 phenotype*. Sci Rep, 2017. **7**: p. 39011.
44. Jia, X., et al., *Emodin suppresses pulmonary metastasis of breast cancer accompanied with decreased macrophage recruitment and M2 polarization in the lungs*. Breast Cancer Res Treat, 2014. **148**(2): p. 291-302.
45. Pyonteck, S.M., et al., *CSF-1R inhibition alters macrophage polarization and blocks glioma progression*. Nat Med, 2013. **19**(10): p. 1264-72.
46. Binnemars-Postma, K., et al., *Targeting the Stat6 pathway in tumor-associated macrophages reduces tumor growth and metastatic niche formation in breast cancer*. FASEB Journal, 2017: p. In press.
47. Elizondo, E., et al., *Liposomes and other vesicular systems: structural characteristics, methods of preparation, and use in nanomedicine*. Prog Mol Biol Transl Sci, 2011. **104**: p. 1-52.
48. Sercombe, L., et al., *Advances and Challenges of Liposome Assisted Drug Delivery*. Front Pharmacol, 2015. **6**: p. 286.
49. Eloy, J.O., et al., *Liposomes as carriers of hydrophilic small molecule drugs: strategies to enhance encapsulation and delivery*. Colloids Surf B Biointerfaces, 2014. **123**: p. 345-63.
50. Feige, E., et al., *Modified phospholipids as anti-inflammatory compounds*. Current opinion in lipidology, 2010. **21**(6): p. 525-9.

Appendix: Supplementary data

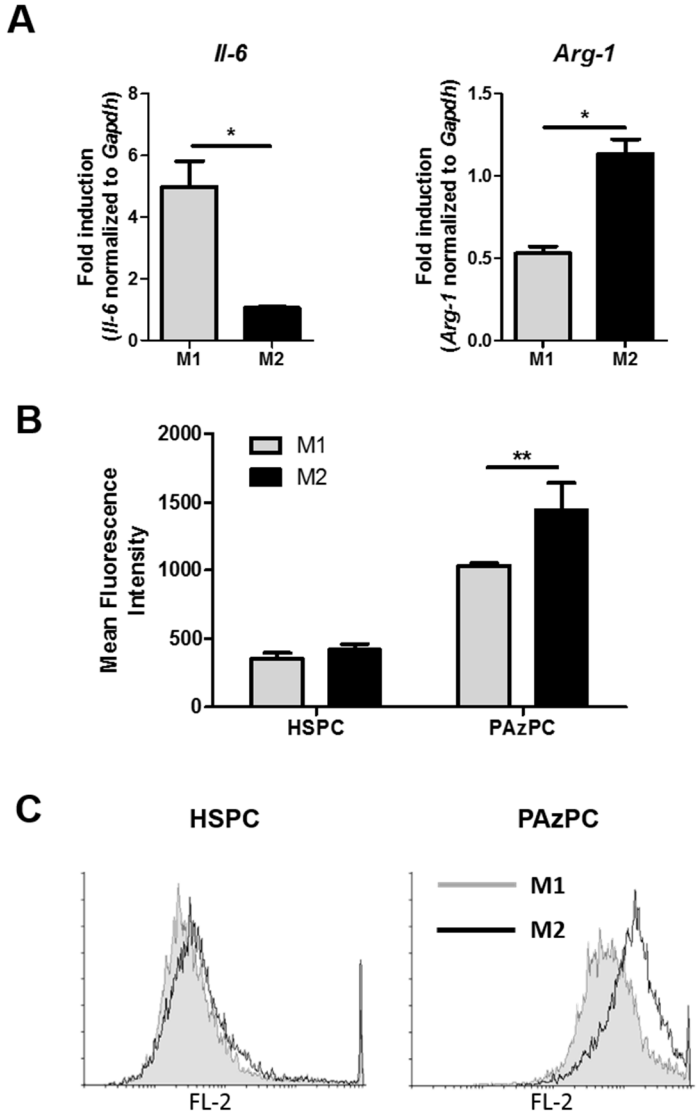

Figure S1: Differentiation and uptake of liposomes by BMDMs. (A) Gene expression analysis of M1 (Interleukin-6 (Il-6)) and M2 (Arginase-1 (Arg-1)). *p<0.05, students t-test (B) Quantification of flow cytometry data on uptake of normal- (8:2 HSPC:Chol) and CyPC- (1:7:2 PAzPC:HSPC:Chol) containing liposomes by differentiated BMDMs. *p<0.05, 2-way ANOVA (C) Representative flow cytometry histograms of uptake of normal and CyPC-containing liposomes by BMDMs. All data n=3, mean + SEM.

CHAPTER 5

TARGETING THE STAT6 PATHWAY IN TUMOR-ASSOCIATED MACROPHAGES REDUCES TUMOR GROWTH AND METASTATIC NICHE FORMATION IN BREAST CANCER

Accepted: FASEB Journal. 2017 Oct 10. In press

Abstract

Tumor-associated macrophages (TAMs) are the key effector cells in the tumor microenvironment, inducing neo-angiogenesis, matrix-remodeling, metastasis while suppressing the tumor immune system. These pro-tumoral macrophages display a M2 phenotype induced by IL-4 and IL-13 cytokines. In this study, we hypothesized that inhibition of the Stat6 pathway, a common downstream signaling pathway of IL-4 and IL-13, might be an interesting strategy to inhibit TAM differentiation and thereby their pro-tumorigenic activities. *In vitro*, inhibition of Stat6 pathway using siRNA or a pharmacological inhibitor AS1517499 inhibited differentiation of mouse RAW264.7 macrophages into M2 phenotype, as shown with reduction of *Arg-1* and *Mrc-1* expression and arginase activity. *In vivo*, AS1517499 significantly attenuated the tumor growth and early liver metastasis in orthotopic 4T1 mammary carcinoma mouse model. Furthermore, in another experiment, we found an increase in the intrahepatic mRNA expression of *F4/80* (total macrophages) and M2 macrophage markers (*Ym-1*, *Mrc-1*) and metastatic niche markers (*Mmp-2*, *Postn*, *Cd34*) in mice with increasing growth of primary tumors. Interestingly, these markers were found to be reduced after the treatment with AS1517499. In conclusion, inhibition of the Stat6 pathway in TAMs is a vital therapeutic approach to attenuate tumor growth and metastasis by inhibiting TAM-induced pro-tumorigenic and pro-metastatic activities.

1 Introduction

With almost 1.7 million new diagnoses and over half a million deaths in 2012, breast cancer is the most common type of cancer in woman worldwide (1). Increasing evidence shows the relation between a high degree of macrophage infiltration and poor prognosis in human breast cancer and other malignancies, suggesting that macrophages play an important role in tumor progression and metastasis in cancer (2-5). Macrophages are myeloid cells which show a high degree of plasticity, commonly defined as two distinct phenotypes: 'classically activated' M1 macrophages, that have pro-inflammatory and anti-tumoral effects and 'alternatively activated' M2 macrophages, which display immunosuppressive, wound-healing and pro-tumoral characteristics (6-8). Macrophage polarization state is determined by the external stimuli, present within the tissue microenvironment (9). Tumor-associated macrophages (TAMs), displaying the M2 phenotype, play a critical role in tumor survival, growth and metastasis (10, 11). TAMs either originate from resident macrophages or infiltrated monocytes from circulation to the tumor site. Tumor cells secrete cytokines such as IL-4, IL-13, and IL-10, which are able to polarize the infiltrated macrophages into TAMs (7).

Upon acquisition of the TAM phenotype, these macrophages support the tumor growth and progression by performing numerous pro-tumoral activities: stimulation of neo-angiogenesis, matrix-remodeling, excretion of growth factors, and suppressing the immune system (7, 10, 12, 13). TAMs have therefore become a key target cell type for the development of anti-tumor therapies. Studies have demonstrated that the depletion of TAMs using bisphosphonate-loaded liposomes led to inhibition of tumor growth and metastasis (14, 15). However, non-selective depletion of macrophages may lead to worse overall outcome, as macrophages also display anti-tumor activities (16). Other strategies aimed at the treatment of TAMs include the targeting of the colony-stimulating factor-1 receptor (CSF-1R), which plays a critical role in the migration, differentiation and survival of macrophages (17). The recently investigated compound BLZ-945, a CSF-1R inhibitor, was shown to inhibit TAM differentiation and tumor growth in a murine model for glioblastoma (18). Quail *et al*, however, recently showed that following treatment with BLZ-945 resulted in resistance and 56% of mice showed tumor recurrence due to tumor

microenvironment derived factors (19). On one hand, these findings advance the knowledge on TAM-based therapies, while on the other hand trigger the need for developing new therapies in this direction.

The signal transducer and activator of transcription 6 (Stat6) pathway is a common signaling pathway for cytokines IL-4 and IL-13, the key cytokines for TAM polarization. These cytokines, secreted within the tumor microenvironment, bind to their receptor IL-4Rα and IL-13Rα1 and activate the Jak/stat pathway (phosphorylation of Stat6) which results in translocation of pStat6 to the nuclei (6, 20). Once located in the nucleus, Stat6 activates the transcription of target genes specific for M2 macrophages, such as mannose receptor 1 (*Mrc-1*), resistin-like α (*Retnla, Fizz1*), chitinase 3-like 3 (*Chi3l3) and Ym-1* (9, 21). Therefore, Stat6 inhibition in TAMs might inhibit their pro-tumorigenic phenotype. In addition, there is evidence that deletion of the Stat6 gene facilitates development of potent anti-tumor immunity via a CD4(+)-independent pathway in 4T1 mouse tumor model (22). Furthermore, Krüppel-like factor 4 (KLF4), a member of the subfamily of the zinc finger class of DNA-binding transcriptional regulators, upon activation by Stat6, inhibits the HIF-1α /NF-κB pathway, which plays an important role in the activation of M1 macrophages (23). Activation of Stat6 thus has dual effects on macrophage differentiation, via induction of M2-associated gene transcription and inhibition of M1-associated signaling pathways.

Since Stat6 plays an important role in the differentiation of TAM and in the regulation of tumor immunity, we hypothesize that Stat6 may represent an interesting therapeutic target to inhibit TAM-induced pro-tumorigenic activities. In the present study, we first examined the activation of the Stat6 pathway in human patient breast tumor tissue and mouse tumor model. Then, we investigated the effect of silencing of Stat6 in murine M2 macrophages *in vitro*. To investigate the effect of pharmacological inhibition of the Stat6 pathway, we used an inhibitor AS1517499, previously used in models for antigen-induced bronchial hyper-reactivity (24-26) and studied its effect on TAM differentiation *in vitro* and the effect on tumor growth and metastasis in 4T1 mammary carcinoma mouse model *in vivo*.

2 Materials & Methods

2.1 Cell culture

Mouse RAW264.7 macrophages were obtained from the American Type Culture Collection. 4T1-luc breast cancer cells were kindly provided by Dr. O. van Tellingen (Netherlands Cancer Institute, Amsterdam, The Netherlands). Both cell lines were cultured in RPMI-1640 medium, supplemented with 10% FBS, 2 mM L-glutamine (Lonza, Basel, Switzerland), 100 U/ml penicillin and 0.1 mg/ml streptomycin (Sigma Aldrich, St Louis, MO). Anonymous human breast tumor tissue was provided by Dr. van Baarlen from LabPON, Hengelo, The Netherlands.

2.2 Macrophage differentiation

M1 macrophages were differentiated using murine recombinant interferon-γ (IFN-γ) and lipopolysaccharide (LPS, 055:B5, Sigma), 10 ng/ml. M2 macrophages were differentiated using murine recombinant interleukin-4 (IL-4) and interleukin-13 (IL-13), 10 ng/ml. All cytokines were obtained from Peprotech, London, UK. M1 differentiation of macrophages was determined by measuring the accumulation of NO_2 nitrite in medium of differentiated cells. Cells were seeded in a 96-well plate. After starvation, the cells were incubated with differentiation medium. After 24 h, the NO_2 concentration was measured at 540 nm, using Griess reagent. M2 differentiation of macrophages was determined by measuring arginase-1 activity in cell lysates of differentiated cells. Briefly, cell lysate was activated by incubating for 10 min at 55°C using 10 mM MnCl2/50mM Tris-HCl, pH 7.5 solution. Activated lysate was mixed with 0.5M L-arginine pH 9.7 solution and incubated for 24 h at 37°C. The reaction was stopped by adding 8.7% H_2SO_4, 23.2% H_3PO_4 in water solution. Color was developed by incubating at 100°C for 1 h using 9% α-Isonitrosopropiophenone in ethanol solution and measuring absorbance at 545 nm.

2.3 Quantitative Real Time PCR

Cells were differentiated according to above-mentioned method. Stat6 inhibitor AS1517499 (4-(benzylamino)-2-(3-chloro-4-hydroxyphenethyl-mino)pyrimidine-5-carboxamide, Axon Medchem, Groningen, The Netherlands) was added in concentrations of 10, 100

and 250 nM and cells were incubated for 24 h. Total RNA was isolated using GenElute Mammalian Total RNA Miniprep Kit (Sigma Aldrich). RNA was isolated from mouse tumors and livers using the SV Total RNA isolation System (Promega, Madison, WI). cDNA was prepared by using iScript cDNA synthesis kit (Bio-Rad, Hercules, CA). Primer sequences are listed in Table 1. Reactions were measured using the CFX384 Real-Time PCR detection system (Bio-Rad). The threshold cycles (Ct) were calculated and relative gene expression was analyzed after normalization with the *Gapdh* housekeeping gene.

Gene	Forward (5'→ 3')	Reverse (3'→ 5')	Accession
Arg-1	GTGAAGAACCCACGGTCTGT	CTGGTTGTCAGGGGAGTGTT	NM_007482.3
Cd34	GGGTAGCTCTCTGCCTGATG	TCTCTGAGATGGCTGGTGTG	NM_133654.3
Cd4	TTCCCTCCCTCTGTTCCCAA	GCCCTCTCGTAAACTGTGCT	NM_013488.2
Cd8	CACAAATGATCAGCGCCCAC	CAGCAGTTCAAAGCAGGCAG	NM_009858.2
F4/80	TGCATCTAGCAATGGACAGC	GCCTTCTGGATCCATTTGAA	NM_010130.4
FoxP3	CCCAGGAAAGACAGCAACCTT	TTCTCACAACCAGGCCACTTG	NM_001199348.1
Gapdh	ACAGTCCATGCCATCACTGC	GATCCACGACGGACACATTG	XM_001476707.3, XM_001479371.4, XM_003946114.1, NM_008084.2
Il-1β	GCCAAGACAGGTCGCTCAGGG	CCCCCACACGTTGACAGCTAGG	NM_008361.3
Il-6	TGATGCTGGTGACAACCACGGC	TAAGCCTCCGACTTGTGAAGTGGTA	NM_031168.1
Mrc -1	GGGACGTTTCGGTGGACTGTGG	TTGTGGGCTCTGGTGGGCGA	NM_008625.2
Mmp-2	TTTCTATGGCTGCCCCAAGG	GTCAAGGTCACCTGTCTGGG	NM_008610.2
Postn	ATCCACGGAGAGCCAGTCAT	TGTTTCTCCACCTCCTGTGG	NM_001198766.1
Stat6	GTTTACAGTGAAGAAGGCCCG	CTGGGCTGGCCCTAAAAACT	NM_009284.2
Ym-1	ACTTTGATGGCCTCAACCTG	AATGATTCCTGCTCCTGTGG	NM_009892.2

Table 1: Sequences of primers used for gene expression using quantitative real-time PCR

2.4 Cell viability

RAW264.7 cells were grown under experimental conditions as mentioned above. 4T1-luc cells were seeded at a cell density of 5×10^4 cells/ml. After 24 h culturing, they were starved overnight and subsequently treated with increasing concentrations of AS1517499. After treatment with AS1517499 at different concentrations for 24 h, medium was aspirated and replaced with a 10% Resazurin sodium salt (Sigma) solution (110 µg/ml) in culture medium without FBS. Cells were cultured for 1-4 h more. Medium was collected and measured using the Victor3 multilabel platereader (Perkin Elmer, Waltham, MA).

2.5 Gene silencing

24 h after seeding, RAW 264.7 cells were transfected using Stat6 siRNA or scrambled control siRNA (Santa Cruz, Dallas, TX) at a concentration of 10 nM combined with HiPerFect (Qiagen, Venlo, The Netherlands) transfection reagent as per manufacturer's instructions. Post 24 h transfection, cells were differentiated and harvested for gene expression and arginase activity as described above.

2.6 Western Blotting

To determine the effect of AS15171499 on inhibition of Stat6 phosphorylation, cells were differentiated and treated with AS1517499, while 4T1-luc cells remained untreated. Western blot analysis was performed according to standard protocol. In brief, cells were lysed using lysis buffer and equal amounts of samples were loaded on 10% Tris-Glycine gel (Thermo Scientific) and transferred onto PVDF membranes (Thermo Scientific). The blots were probed with anti-Stat6 or anti-pStat6 antibody (Cell Signaling, Danvers, MA) by incubating overnight at 4°C, followed by incubation at RT for 1 h with species specific horseradish peroxidase (HRP) conjugated secondary antibody. The proteins were detected by Pierce™ ECL Plus Western Blotting Substrate kit (Thermo Scientific) and exposed to FluorChem™ M System (ProteinSimple, CA). Target protein levels were quantified by Image J Software (NIH, MD).

2.7 *In vitro* paracrine effects of treated differentiated macrophages on 4T1-luc breast cancer cells

Cells were differentiated and treated with AS1517499. After 24 h of differentiation, medium was removed and cells were washed thoroughly. New medium without cytokines was added and conditioned medium was collected after 24 h of incubation. For the wound healing assay, 4T1-luc cells were seeded in 24-well plates. Cells were starved overnight and a scratch was made in the middle of the well. The cells were washed and conditioned medium from the treated macrophages was added. After 24 h of incubation, migration of cells into the scratched area was assessed, by analyzing images of 0 h and 24 h time points using NIH ImageJ software (NIH, Bethesda, MD). Percentage of cell migration was calculated by subtracting the 24 h value from the 0 h value, then dividing by the total area of the picture.

2.8 *In vivo* effects of AS1517499 in 4T1 mammary carcinoma model

All animals (female, Balb/c, approx. 20 g) were purchased from Envigo Indianapolis, IN. The experimental protocols were approved by the Animal Ethical Committee of the Utrecht University, The Netherlands. Animals were fed *ad libitum* and kept at a 12 h light and 12 h dark cycle. 1 x 10^5 4T1-luc cells were injected into the mammary fat pad and tumors were allowed to develop. Tumor size was determined using Vernier caliper and tumor volume was calculated using length x $width^2$ x 0.52. Treatment with AS1517499 (20 mg/kg, intraperitoneal administrations, twice a week) was started when the tumor volume reached ±100 mm^3. Before sacrificing, mice were injected with 3 mg of D-luciferin (Perkin Elmer, Waltham, MA) and were imaged after 30 minutes using the IVIS system.

2.9 Immunofluorescence

Anonymous human breast tumor tissue sections (formalin fixed paraffin embedded) were anonymously provided by the Department of Pathology, Laboratory Pathology East Netherlands (LabPON), Enschede, The Netherlands Ethical approvals were approved by the local Medical Ethical Committee at LabPON. The use of human tissues for this study was approved by the Local Ethics Committee, University of Twente. All the experiments involving human tissues were performed in accordance with institutional guidelines and regulations. 4 µm sections were deparaffinized and antigens were retrieved by overnight incubation at 80°C in 0.1 M Tris-HCl pH 9. Murine 5 µm cryosections were fixed in 4% formaldehyde. Sections were permeabilized in methanol at -20°C for 10 minutes. Sections were incubated with primary antibodies pStat6, Stat6 (Cell Signaling) and CD206 (Santa Cruz) overnight at 4°C. Secondary antibodies labeled with Alexa Fluor 488 or Alexa Fluor 594 (Life Technologies, Carlsbad, CA) were incubated for 1 h. Stained sections were mounted using mounting medium containing DAPI anti-fade mounting medium (Sigma). Sections were subsequently scanned using Hamamatsu NanoZoomer Digital slide scanner 2.0HT (Hamamatsu Photonics, Bridgewater NJ).

2.10 Statistical analysis

Data are represented as the mean + standard error of the mean (SEM). The graphs and statistical analyses were performed using GraphPad Prism version 5.02 (GraphPad Prism Software, Inc., La Jolla, CA, USA). Data was analyzed using an unpaired, 2-tailed Student's t-test, unless otherwise specified. The differences were considered significant at $p<0.05$.

3 Results

3.1 pStat6 expression in human and mouse breast tumors

To determine the expression of the activated Stat6 *i.e.* phosphorylated Stat6 (pStat6), we performed co-localization immunofluorescent staining in human breast tumor tissue and 4T1 mammary carcinoma tissue. As can be seen in Figure 1A and 1B, the Stat6 signaling was activated in both human and mouse breast tumor tissues in TAMs, as shown by co-localization of pStat6 with $CD206^{+}$ macrophages, as shown in the "M" marked area. The tumors stained with pStat6 were positive for both estrogen and progesterone receptors. Of note, tumor cells did not express pStat6, as can be seen in the "T" marked area.

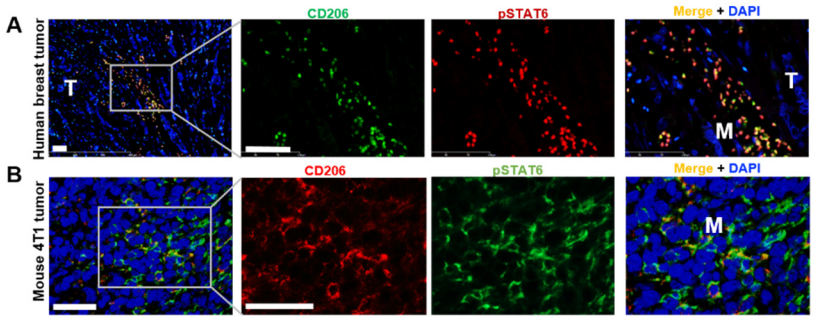

Figure 1: Representative fluorescent images showing co-immunostaining of pStat6 in human breast cancer and murine 4T1 breast tumor model. (A) pStat6 (red color) is co-localized mainly with CD206+ macrophages (green color). (B) pStat6 (green color) is co-localized with CD206+ macrophages (red color). "T" and "M" denote area with tumor cells and macrophage–rich area. Blue: DAPI. Scale bar 50 μm in all images. n=5

3.2 Macrophage differentiation and pStat6 expression

To study whether Stat6 pathway is specifically induced in M2 but not in M1, we first differentiated murine macrophages RAW 264.7 with IFNγ and LPS for M1 and with IL-4 and IL-13 for M2 macrophages (TAM) and examined their different phenotypes. Using qPCR, we confirmed the differentiation of M1 and M2 phenotypes with the induced M1 inflammatory markers (*Il-1β* and *Il-6)* and M2 markers (*Arg-1* and *Mrc-1)* (Figure 2A). Furthermore, we examined the enzymatic activity in the differentiated macrophages to confirm their distinct phenotypes (Figure 2B and C). The arginase activity, measured by the quantification of urea as a side product of the conversion of L-arginine into L-ornithine, showed higher activity in M2 macrophages

compared to M1 macrophages (Figure 2B). In contrast, NO_2^- production, as a result of induced NO synthase, was significantly increased in only M1 macrophages (Figure 2C). As expected, we found that the phosphorylation of Stat6 (pStat6) was highly induced in M2 macrophages specifically (Figure 2D). Although the undifferentiated or M1 macrophages had high expression levels of Stat6, no pStat6 expression was seen (Figure 2D). In addition, 4T1 murine breast cancer cells also expressed Stat6, but not pStat6, which is in line with the immunostaining data in human and mouse tumors (Figure 1).

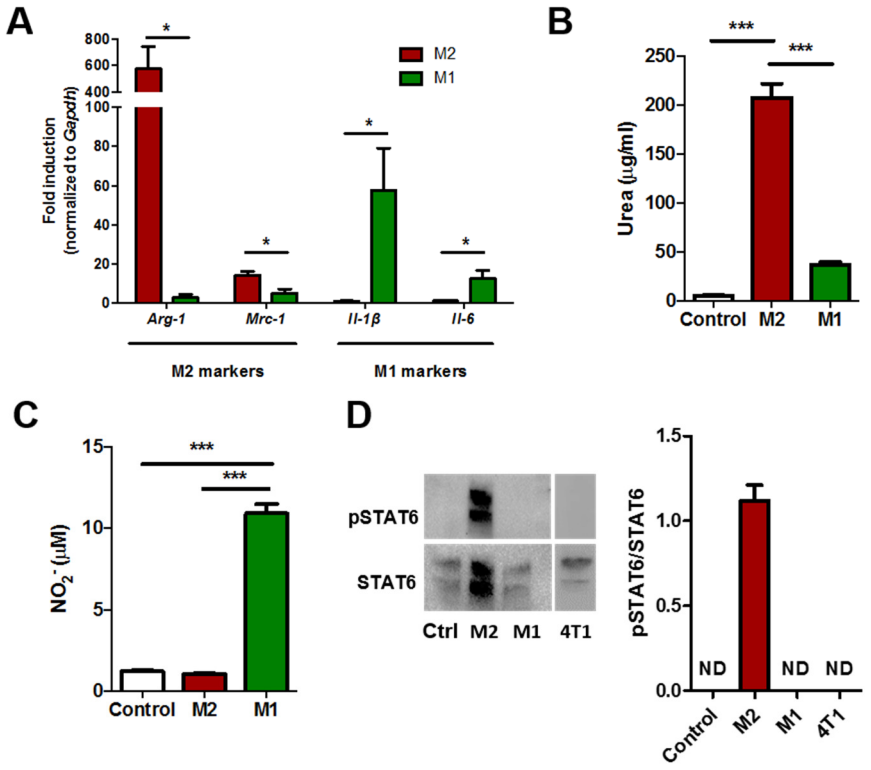

Figure 2: *In vitro* differentiation of murine macrophages into M2 and M1 macrophages. (A) Quantitative real-time PCR analysis of macrophage differentiation. (B) Arginase-1 activity in differentiated macrophages as measured by the amount of produced urea (expressed in µg/ml). (C) Nitrite release assay in supernatants of differentiated macrophages (expressed in µM). (D) Representative western blot results and quantification showing Stat6 phosphorylation is restricted to the M2 macrophage phenotype. Ctrl: undifferentiated control RAW 264.7 cells. Bars represent mean + SEM, n=3-4. *p<0.05, ***p<0.001.

3.3 *Stat6* gene silencing

To investigate whether Stat6 regulates M2 macrophage differentiation, we knocked down *Stat6* using siRNA approach. We found that transfection of si-Stat6 reduced the expression levels by 30% in M2 differentiated cells (Figure 3A). Interestingly, the reduction of Stat6 expression significantly inhibited the differentiation of macrophages into the M2 type, as shown with the reduced expression of Mrc-1 gene, a marker for M2 type, and arginase-1 activity, a biochemical assay for M2 specific activity (Figure 3A and 3B). Since arginase activity and *Mrc-1* gene expression are both elevated in M2 macrophages and have been established as reliable M2 markers, the decrease in these values after knocking down the *Stat6* gene confirms the crucial role of this transcription factor in M2 macrophage differentiation.

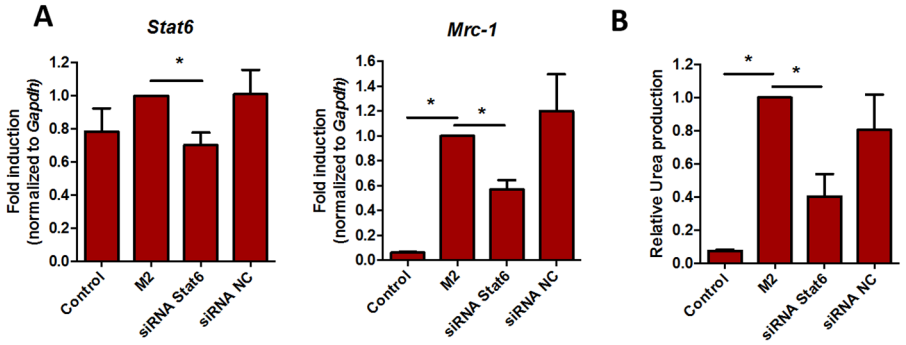

Figure 3: *In vitro* effects of *Stat6* gene silencing. (A) Quantitative gene expression analysis depicting inhibition of *Stat6* and *Mannose Receptor 1* (*Mrc-1*).(B) Inhibition of arginase activity using *Stat6* siRNA. Bars represent mean + SEM, n=3. *p<0.05.

3.4 Pharmacological inhibition of Stat6 phosphorylation using AS1517499

After confirming that Stat6 knockdown inhibits the differentiation of macrophages to the M2 type, we used a small drug molecule AS1517499 (Figure 4A) to study whether pharmacological inhibition of Stat6 is also able to inhibit macrophage differentiation. As confirmed with the WB analysis, treatment with AS1517499 inhibited the expression of pStat6 in M2 macrophages with increasing concentrations (Figure 4B). Also, AS1517499 inhibited M2 markers *Arg-1* and *Mrc-1* gene expression (Figure 4C), and arginase activity in these cells with increasing concentrations (Figure 4D). These data confirm that

pharmacological inhibition of Stat6 using AS1517499 can inhibit M2 macrophage differentiation. In contrast, treatment of M1 macrophages with AS1517499 did not show any inhibition of M1 macrophages, but instead slightly activated them towards M1 phenotype (Figure 4C). Since M1 macrophages are considered as anti-tumoral macrophages, differentiation to M1 type can be of interest to achieve anti-tumor effects. Of note, the used concentrations of AS1517499 also did not show any cytotoxicity to these cells (Figure E).

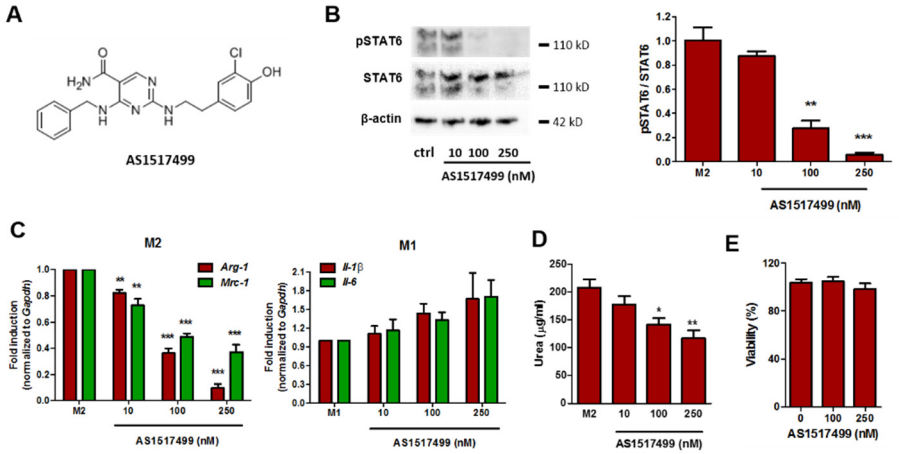

Figure 4: *In vitro* effects of Stat6 inhibitor AS1517499 in differentiated macrophages. (A) Structure of Stat6 inhibitor AS1517499. (B) Representative image and quantification of western blot results of Stat6 phosphorylation in differentiated RAW264.7 cells, treated with increasing concentrations of AS1517499. (C) Quantitative real-time PCR results of macrophage differentiation with increasing concentrations of AS1517499 for M2 markers *Arginase-1* (*Arg-1*) and *Mannose receptor-1* (*Mrc-1*) and M1 markers *Il-1β* and *Il-6*. (D) Inhibition of arginase activity using increasing concentrations of AS1517499. (E) Cell viability of RAW264.7 cells incubated with AS1517499. Bars represent mean + SEM, n=3 *p<0.05, **p<0.005, ***p<0.001.

3.5 AS1517499 inhibits tumor growth and metastasis in 4T1 mammary carcinoma model *in vivo*

To evaluate the effect of the Stat6 inhibitor AS1517499 *in vivo*, we treated 4T1-luc tumor bearing mice with 20 mg/kg of the inhibitor, *i.p.*, twice a week when the tumors became palpable. We found that the treatment with AS1517499 significantly reduced the tumor growth compared to the vehicle-treated control mice (Figure 5A). At the end of the experiment, we quantified the tumor mass and potential liver metastasis by imaging the luciferase activity using the IVIS system.

Interestingly, the AS1517499-treated mice showed a significant reduction in the tumor mass compared to the vehicle-treated group, as can be seen in intact tumors in Figure 5B and the quantification data in Figure 5C. To rule out direct cytotoxic effects of AS1517499 on 4T1 cells, we examined cell viability at much higher concentrations up to 4000 nM compared to the effective concentration of 250 nM in macrophages and observed no decrease in cell viability (Figure 5D). We examined the tumor gene expression of total and M2 macrophage markers (*F4/80, Arg-1 and Mrc-1*) but found no differences (data not shown). However, intratumoral T-cell population marker showed an increase in *CD8+* T cell gene expression and a slight increase in CD4 Treg marker *FoxP3*, whereas *CD4* remained unchanged in AS1517499 treated group compared to vehicle group (Figure 5E).

We also studied the potential metastasis in liver and found that the vehicle group (4/6 positive) had more luminescence signal than the AS1517499-treated group (2/6 positive), as indicated by the scoring shown in the Figure 5F. To determine whether M2 macrophages promote tumor cell migration and inhibition of Stat6 in these macrophages inhibit pro-migratory effect, we investigated the paracrine effects of M2 differentiated macrophages (with and without treatment with AS1517499) on tumor cell migration. We found that conditioned medium collected from M2 macrophages increased the tumor cell migration compared to undifferentiated macrophages (Figure 5G). Importantly, conditioned medium collected from M2 macrophages treated with AS1517499 completely inhibited this M2 macrophage-induced tumor cell migration (Figure 5G).

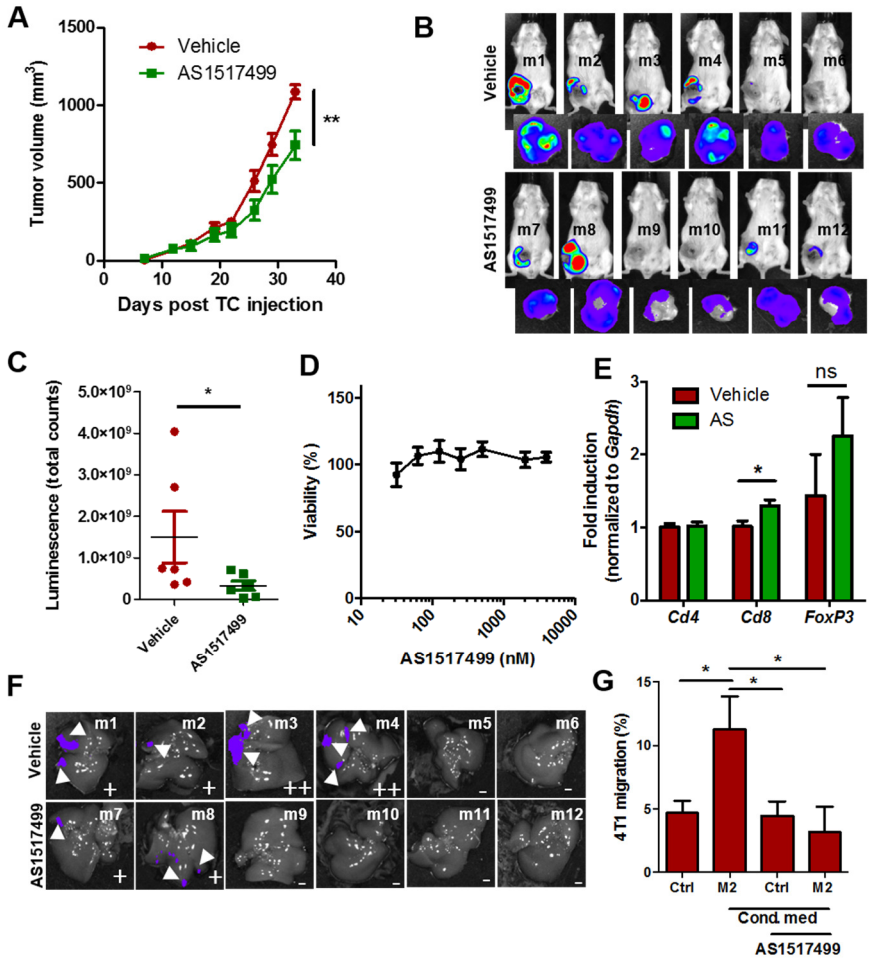

Figure 5: *In vivo* effect of AS1517499 treatment on tumor growth. (A) Tumor volume of vehicle- and AS1517499-treated animals (20 mg/kg i.p, twice weekly) in days post tumor cell (TC) injection (B) IVIS images of untreated and treated mice, prior to sacrificing, 15 min after luciferin injection. The isolated tumors are shown next to the respective mice. (C) Quantitative data showing ex-vivo tumor luminescence in the isolated tumors. (D) Cell viability of 4T1 cells incubated with AS1517499. (E) Quantitative real-time PCR results of T-cell markers (*Cd4*, *Cd8* and *FoxP3*) in untreated and treated animals. (F) Luminescence of livers after luciferin injection. Arrowheads indicate metastasis. Metastasis scoring (- no spots; + few spots of low intensity; ++ several spots) for livers is shown in the lower right corner of each image. (G) Quantification of migration of tumor cells, 24 h after making the scratch. *In vitro* experiments n=3-4, *in vivo* experiments n=6 per group. Data shown as mean + SEM, *p<0.05.

3.6 AS1517499 inhibits metastatic niche formation

Since we observed the inhibitory effect of AS1517499 on early metastasis, we became interested to investigate whether AS1517499 could also inhibit the metastatic niche formation in livers. We therefore set up a new experiment to track changes in macrophage phenotype and metastatic niche markers with the progression of breast tumor. In this experiment, we collected livers from normal mice and 4T1 tumor-bearing mice with increasing tumor sizes (Figure 6A). We found that the induction of tumors led to an increase of general macrophage marker *F4/80* at early stage, likely due to infiltrated macrophages (Figure 6B). The increase of the tumor size led to an increase of M2 macrophages markers (*Mrc-1*, *Ym-1*), metastatic niche markers matrix-metalloproteinase 2 (*Mmp-2*)), Periostin (*Postn*) and neo-angiogenesis marker *Cd34* in liver (Figure 6B). To examine whether Stat6 inhibition reduces the expression of metastatic niche markers in the liver, we examined these gene markers in the livers treated from AS1517499 from the experiment shown in Figure 5. Intriguingly, we found that treatment with AS1517499 significantly inhibited the expression of the metastatic niche markers (Figure 6C). These data suggest that AS1517499 not only attenuates the tumor growth but also the metastatic niche formation.

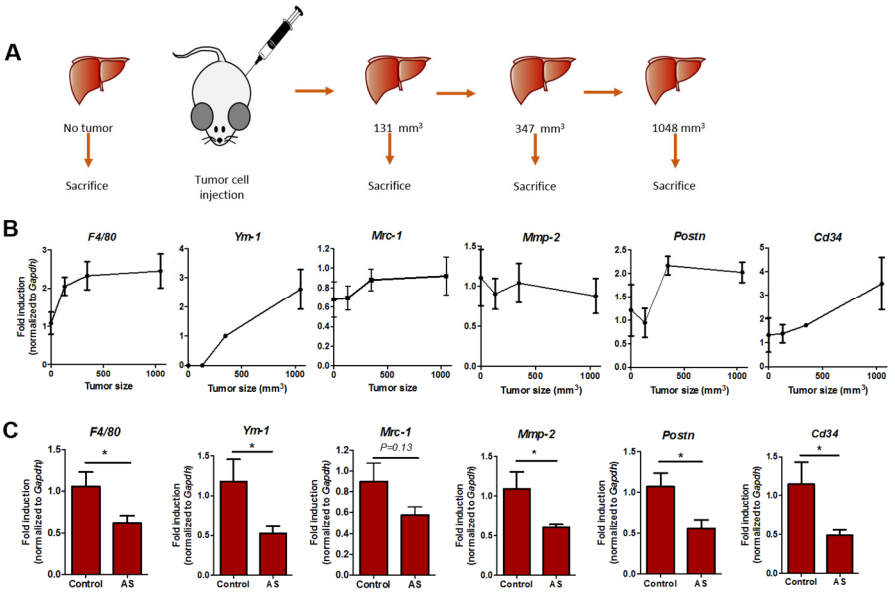

Figure 6: Macrophage and tumor progression markers measured in livers of mice bearing tumors of increasing sizes and in animals treated and untreated with AS1517499. (A) Experimental setup for tracking macrophage and metastatic markers in livers of mice bearing increasing tumor sizes. Mice were sacrificed before tumor development and when tumor reached the sizes of 131, 347 and 1048 mm3, n=3 per group (B) Gene expression analysis of macrophage (*F4/80, Ym-1* and *Mrc-1*) and tumor progression markers (*Mmp-2, Postn* and *Cd34*) in livers of mice bearing tumors during tumor development (C) Macrophage and tumor progression markers in control and AS1517499 treated animals. n=6 per group. Mean + SEM, *p<0.05.

4 Discussion

In this study, we for the first time demonstrates that the pharmacological inhibition of Stat6 in TAM using a specific inhibitor AS1517499 attenuates tumor growth and metastatic niche formation in breast cancer. We herein confirmed that Stat6 is expressed by TAM in human breast tumors and is essential for the differentiation of the TAM phenotype (M2 type macrophages). Inhibition of Stat6 using siRNA approach or AS1517499 inhibited M2 differentiation *in vitro*. Furthermore, treatment with AS1517499 not only attenuated the tumor growth but also early metastasis in syngeneic 4T1 mammary carcinoma model in mice. Subsequently, we demonstrated that several gene markers related to macrophage and metastatic niche were induced in liver with an increasing growth of the primary tumor in mice. Interestingly, treatment with AS1517499 significantly inhibited these metastatic niche markers in liver. This study underlines the importance of the Stat6 pathway in TAM differentiation and highlights that the inhibition of this pathway may be an interesting way to block TAM-induced pro-tumorigenic effects.

TAMs display a number of pro-tumoral functions, including extracellular matrix remodeling, neo-angiogenesis, suppression of adaptive immunity and facilitate tumor metastasis (12). Differentiation of infiltrated macrophages into the TAM phenotype through IL-4/IL-13 cytokines is well known and therefore their intrinsic pathway *i.e.* Stat6 pathway is a key target to intervene into TAM-induced tumor processes. In the present study, we showed that the phosphorylated Stat6 (activated form) was abundantly present in TAMs in both human breast tumor tissue and 4T1 tumors in mice, as shown with immunofluorescent stainings (Figure 1). Also, *in vitro*, the Stat6 pathway was specifically activated in M2 differentiated cells in contrast to M1. Earlier Jia *et al* have shown that activation of macrophages with 4T1 conditioned medium leads to induction of pStat6 pathway (27). Our data showing inhibition of differentiation of macrophages to M2 type after Stat6 silencing using siRNA confirmed that the Stat6 pathway is a key regulatory pathway in this process. To apply the Stat6 inhibition strategy pharmacologically *in vivo*, we used a Stat6 inhibitor AS1517499 which has been earlier reported as a potent Stat6 specific inhibitor in non-malignant diseases (24-26). In our study, AS1517499 showed a strong inhibition of Stat6 phosphorylation at nanomolar

concentrations and inhibited M2 differentiation, as shown with the inhibition of M2-related markers (*Arg-1* and *Mrc-1*) and enzyme activity.

In vivo, after treatment with AS1517499, tumor growth slowed down in 5/6 mice compared to the vehicle group. In the vehicle group, all mice had consistently high growth rate (Figure 5A). Since these tumors often become hypoxic and necrotic, we included 4T1-luciferase induced luminescence signal to represent the effect on the tumor mass and found a high reduction in the tumor mass. Although *in vitro* we showed that AS1517499 inhibited M2 differentiation, the *in vivo* effect might be because of cytotoxicity to tumor cells directly. The latter was ruled out when at much higher concentration AS1517499 showed no cytotoxicity to 4T1 cells (figure 5D). Moreover, pStat6 expression was also absent in 4T1 cells (Figure 2D), indicating the reduction in tumor growth after the treatment with AS1517499 was not due to direct effect of the inhibitor on tumor cells. To examine whether M2 macrophages induce tumor cell growth in a paracrine manner, we examined the effect of the conditioned medium collected from M2 macrophages on 4T1 cell growth and found no induction of the cell growth (data not shown). In tumors, we also found no change in the gene expression of M2 markers after the treatment with AS1517499. Earlier, Ostrand-Rosenberg *et al* demonstrated that when *Stat6*$^{-/-}$ mice were challenged with 4T1 tumor cells, the mice showed a delay in primary tumor growth and a reduction in metastasis (22). These effects were found independent of $CD4^+$ cells but due to elevated levels of $CD8^+$ cells in tumors. In line of the latter study, we also found that tumors treated with AS1517499 had an induced expression of CD8 but not of CD4, indicating that treatment with AS1517499 might have reduced the tumor growth by inhibiting TAM-induced immune-suppression.

A crucial finding of the present study is the reduction of liver metastasis as a result of the treatment with AS1517499, because most cancer-related mortalities occur due to metastasis. TAMs are known to induce tumor cell migration (28-30), which was also confirmed in this study. Furthermore, we showed that the inhibition of TAM (M2 macrophages) with AS1517499 inhibited tumor migration. To this end, we wondered whether AS1517499 only inhibited tumor cell migration or also metastatic niche formation at the metastatic site *i.e.* liver. Several studies summarized in a recent review by Peinado *et al* (31),

have demonstrated that tumor cells secrete extracellular vesicles and growth factors at the primary tumor site which migrate to the metastatic sites and establish pre-metastatic niche to harbor and nourish tumor cells. To examine the effect of AS1517499 on the metastatic niche in liver, we first examined which genes induce /alter in the liver during the 4T1 tumor development. Our data showed an increase in the gene expression of total (*F4/80*) and M2 macrophages (*Ym-1 and Mrc-1*) and other metastatic markers (*Mmp-2*, *Postn*, *Cd34*) in the liver (Figure 6B). Recruitment of infiltrated macrophages and activation of resident Kupffer cells are known to be the crucial processes of the pre-metastatic niche formation (31). MMP-2, a matrix-metalloproteinase, plays an important role in organizing the ECM of the metastatic niche (32). Periostin (Postn) is an extracellular matrix protein which has been shown to associated with pre-metastatic niche. Malanchi *et al* showed that periostin serves to concentrate and present Wnt ligands, and thereby induces and maintains stem-like metastasis founder cells (33). Recently, periostin was shown to be secreted by glioblastoma stem cells which resulted in an increased recruitment and differentiation of TAMs (34). During metastasis, bone marrow-derived cells are shown to infiltrate and express CD34 (35) and besides that, endothelial cells also express CD34 which is known to participate in establishing the metastatic niche. Interestingly, the AS1517499-treated mice showed a reduced expression of macrophage markers, suggesting a reduction in intrahepatic macrophage infiltration and an increased M2-driven macrophage polarization. Furthermore, AS1517499 also inhibited the expression of *Mmp-2*, *Postn* and *Cd34*, key genes in the metastasis formation. Nevertheless, it remains to be investigated whether the reduction of these key mediators with AS1517499 is a direct effect or a consequence of inhibition of primary tumor.

5 Conclusion

In conclusion, we demonstrate that the inhibition of Stat6 pathway in TAMs using AS1517499 leads to reduced tumor growth and metastasis. Since M2 macrophages induce pro-tumorigenic effects both at the primary tumor site and the metastatic site, inhibition of Stat6 pathway in these macrophages can provide dual effect to abrogate both tumor growth and metastasis development, as shown in this study. Furthermore, combination of AS1517499 with other anti-cancer agents (*e.g.* chemotherapy, immunotherapy) might be interesting to potentiate their therapeutic efficacy. Altogether, inhibition of Stat6 using AS1517499 is a promising approach to dampen the pro-tumorigenic effect of TAMs and is in potential to be explored as an adjuvant therapy for breast cancer.

References

1. Ferlay, J., Soerjomataram, I., Ervik, M., Dikshit, R., Eser, S., Mathers, C., Rebelo, M., Parkin, D.M., Forman, D., Bray, F. (2012) Breast Cancer, Estimated Incidence, Mortality and Prevalence Worldwide in 2012. In *GLOBOCAN 2012 v1.0, Cancer Incidence and Mortality Worldwide: IARC CancerBase No. 11 [Internet]* Vol. 2015, Lyon, France: International Agency for Research on Cancer; 2013
2. Tang, X. (2013) Tumor-associated macrophages as potential diagnostic and prognostic biomarkers in breast cancer. *Cancer Lett* **332**, 3-10
3. Oishi, K., Sakaguchi, T., Baba, S., Suzuki, S., and Konno, H. (2014) Macrophage density and macrophage colony-stimulating factor expression predict the postoperative prognosis in patients with intrahepatic cholangiocarcinoma. *Surg Today*
4. Ding, T., Xu, J., Wang, F., Shi, M., Zhang, Y., Li, S. P., and Zheng, L. (2009) High tumor-infiltrating macrophage density predicts poor prognosis in patients with primary hepatocellular carcinoma after resection. *Hum Pathol* **40**, 381-389
5. Mantovani, A., Allavena, P., and Sica, A. (2004) Tumour-associated macrophages as a prototypic type II polarised phagocyte population: role in tumour progression. *Eur J Cancer* **40**, 1660-1667
6. Wang, N., Liang, H., and Zen, K. (2014) Molecular mechanisms that influence the macrophage m1-m2 polarization balance. *Front Immunol* **5**, 614
7. Sica, A., Schioppa, T., Mantovani, A., and Allavena, P. (2006) Tumour-associated macrophages are a distinct M2 polarised population promoting tumour progression: potential targets of anti-cancer therapy. *Eur J Cancer* **42**, 717-727
8. Noy, R., and Pollard, J. W. (2014) Tumor-associated macrophages: from mechanisms to therapy. *Immunity* **41**, 49-61
9. Sica, A., and Mantovani, A. (2012) Macrophage plasticity and polarization: in vivo veritas. *J Clin Invest* **122**, 787-795
10. Sica, A., Allavena, P., and Mantovani, A. (2008) Cancer related inflammation: the macrophage connection. *Cancer Lett* **267**, 204-215
11. Mantovani, A., Marchesi, F., Malesci, A., Laghi, L., and Allavena, P. (2017) Tumour-associated macrophages as treatment targets in oncology. *Nat Rev Clin Oncol* **14**, 399-416
12. Allavena, P., and Mantovani, A. (2012) Immunology in the clinic review series; focus on cancer: tumour-associated

macrophages: undisputed stars of the inflammatory tumour microenvironment. *Clin Exp Immunol* **167**, 195-205
13. Biswas, S. K., Allavena, P., and Mantovani, A. (2013) Tumor-associated macrophages: functional diversity, clinical significance, and open questions. *Semin Immunopathol* **35**, 585-600
14. Brown, H. K., and Holen, I. (2009) Anti-tumour effects of bisphosphonates--what have we learned from in vivo models? *Curr Cancer Drug Targets* **9**, 807-823
15. Zeisberger, S. M., Odermatt, B., Marty, C., Zehnder-Fjallman, A. H., Ballmer-Hofer, K., and Schwendener, R. A. (2006) Clodronate-liposome-mediated depletion of tumour-associated macrophages: a new and highly effective antiangiogenic therapy approach. *Br J Cancer* **95**, 272-281
16. Ngambenjawong, C., Gustafson, H. H., and Pun, S. H. (2017) Progress in tumor-associated macrophage (TAM)-targeted therapeutics. *Adv Drug Deliv Rev*
17. Hume, D. A., and MacDonald, K. P. (2012) Therapeutic applications of macrophage colony-stimulating factor-1 (CSF-1) and antagonists of CSF-1 receptor (CSF-1R) signaling. *Blood* **119**, 1810-1820
18. Pyonteck, S. M., Akkari, L., Schuhmacher, A. J., Bowman, R. L., Sevenich, L., Quail, D. F., Olson, O. C., Quick, M. L., Huse, J. T., Teijeiro, V., Setty, M., Leslie, C. S., Oei, Y., Pedraza, A., Zhang, J., Brennan, C. W., Sutton, J. C., Holland, E. C., Daniel, D., and Joyce, J. A. (2013) CSF-1R inhibition alters macrophage polarization and blocks glioma progression. *Nat Med* **19**, 1264-1272
19. Quail, D. F., Bowman, R. L., Akkari, L., Quick, M. L., Schuhmacher, A. J., Huse, J. T., Holland, E. C., Sutton, J. C., and Joyce, J. A. (2016) The tumor microenvironment underlies acquired resistance to CSF-1R inhibition in gliomas. *Science* **352**, aad3018
20. Nelms, K., Keegan, A. D., Zamorano, J., Ryan, J. J., and Paul, W. E. (1999) The IL-4 receptor: signaling mechanisms and biologic functions. *Annu Rev Immunol* **17**, 701-738
21. Pauleau, A. L., Rutschman, R., Lang, R., Pernis, A., Watowich, S. S., and Murray, P. J. (2004) Enhancer-mediated control of macrophage-specific arginase I expression. *J Immunol* **172**, 7565-7573
22. Ostrand-Rosenberg, S., Grusby, M. J., and Clements, V. K. (2000) Cutting edge: STAT6-deficient mice have enhanced tumor immunity to primary and metastatic mammary carcinoma. *J Immunol* **165**, 6015-6019

23. Liao, X., Sharma, N., Kapadia, F., Zhou, G., Lu, Y., Hong, H., Paruchuri, K., Mahabeleshwar, G. H., Dalmas, E., Venteclef, N., Flask, C. A., Kim, J., Doreian, B. W., Lu, K. Q., Kaestner, K. H., Hamik, A., Clement, K., and Jain, M. K. (2011) Kruppel-like factor 4 regulates macrophage polarization. *J Clin Invest* **121**, 2736-2749
24. Nagashima, S., Yokota, M., Nakai, E., Kuromitsu, S., Ohga, K., Takeuchi, M., Tsukamoto, S., and Ohta, M. (2007) Synthesis and evaluation of 2-{[2-(4-hydroxyphenyl)-ethyl]amino}pyrimidine-5-carboxamide derivatives as novel STAT6 inhibitors. *Bioorg Med Chem* **15**, 1044-1055
25. Sakurai, M., Nishio, M., Yamamoto, K., Okuda, T., Kawano, K., and Ohnuki, T. (2003) TMC-264, a novel inhibitor of STAT6 activation produced by Phoma sp. TC 1674. *J Antibiot (Tokyo)* **56**, 513-519
26. Chiba, Y., Todoroki, M., Nishida, Y., Tanabe, M., and Misawa, M. (2009) A novel STAT6 inhibitor AS1517499 ameliorates antigen-induced bronchial hypercontractility in mice. *Am J Respir Cell Mol Biol* **41**, 516-524
27. Jia, X., Yu, F., Wang, J., Iwanowycz, S., Saaoud, F., Wang, Y., Hu, J., Wang, Q., and Fan, D. (2014) Emodin suppresses pulmonary metastasis of breast cancer accompanied with decreased macrophage recruitment and M2 polarization in the lungs. *Breast Cancer Res Treat* **148**, 291-302
28. Condeelis, J., and Pollard, J. W. (2006) Macrophages: obligate partners for tumor cell migration, invasion, and metastasis. *Cell* **124**, 263-266
29. Solinas, G., Schiarea, S., Liguori, M., Fabbri, M., Pesce, S., Zammataro, L., Pasqualini, F., Nebuloni, M., Chiabrando, C., Mantovani, A., and Allavena, P. (2010) Tumor-conditioned macrophages secrete migration-stimulating factor: a new marker for M2-polarization, influencing tumor cell motility. *J Immunol* **185**, 642-652
30. Guo, Q., Jin, Z., Yuan, Y., Liu, R., Xu, T., Wei, H., Xu, X., He, S., Chen, S., Shi, Z., Hou, W., and Hua, B. (2016) New Mechanisms of Tumor-Associated Macrophages on Promoting Tumor Progression: Recent Research Advances and Potential Targets for Tumor Immunotherapy. *J Immunol Res* **2016**, 9720912
31. Peinado, H., Zhang, H., Matei, I. R., Costa-Silva, B., Hoshino, A., Rodrigues, G., Psaila, B., Kaplan, R. N., Bromberg, J. F., Kang, Y., Bissell, M. J., Cox, T. R., Giaccia, A. J., Erler, J. T., Hiratsuka, S., Ghajar, C. M., and Lyden, D. (2017) Pre-metastatic niches: organ-specific homes for metastases. *Nat Rev Cancer* **17**, 302-317

32. Erler, J. T., Bennewith, K. L., Cox, T. R., Lang, G., Bird, D., Koong, A., Le, Q. T., and Giaccia, A. J. (2009) Hypoxia-induced lysyl oxidase is a critical mediator of bone marrow cell recruitment to form the premetastatic niche. *Cancer Cell* **15**, 35-44
33. Malanchi, I., Santamaria-Martinez, A., Susanto, E., Peng, H., Lehr, H. A., Delaloye, J. F., and Huelsken, J. (2011) Interactions between cancer stem cells and their niche govern metastatic colonization. *Nature* **481**, 85-89
34. Zhou, W., Ke, S. Q., Huang, Z., Flavahan, W., Fang, X., Paul, J., Wu, L., Sloan, A. E., McLendon, R. E., Li, X., Rich, J. N., and Bao, S. (2015) Periostin secreted by glioblastoma stem cells recruits M2 tumour-associated macrophages and promotes malignant growth. *Nat Cell Biol* **17**, 170-182
35. Kaplan, R. N., Riba, R. D., Zacharoulis, S., Bramley, A. H., Vincent, L., Costa, C., MacDonald, D. D., Jin, D. K., Shido, K., Kerns, S. A., Zhu, Z., Hicklin, D., Wu, Y., Port, J. L., Altorki, N., Port, E. R., Ruggero, D., Shmelkov, S. V., Jensen, K. K., Rafii, S., and Lyden, D. (2005) VEGFR1-positive haematopoietic bone marrow progenitors initiate the pre-metastatic niche. *Nature* **438**, 820-827

Appendix: Supplementary data

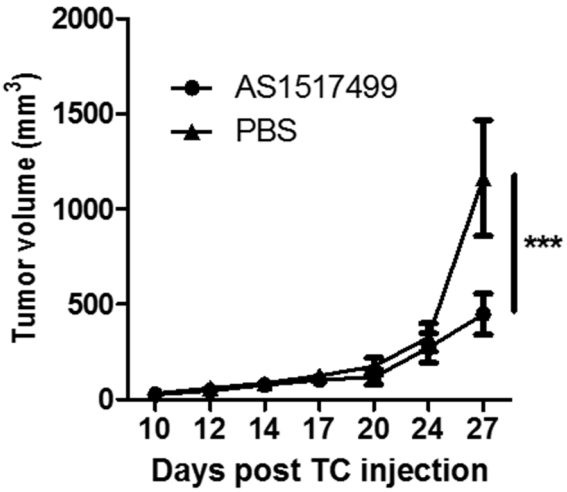

Figure S1: Tumor growth curves of animals treated with 10 mg/kg AS1517499. Animals were injected with 4T1-luc tumor cells as described in methods. Subsequently, at tumor size 100 mm^3, treatment was started using 10 mg/kg AS1517499 or PBS. Data shown as mean + SEM, n=6 per group, **p<0.001 at day 27.

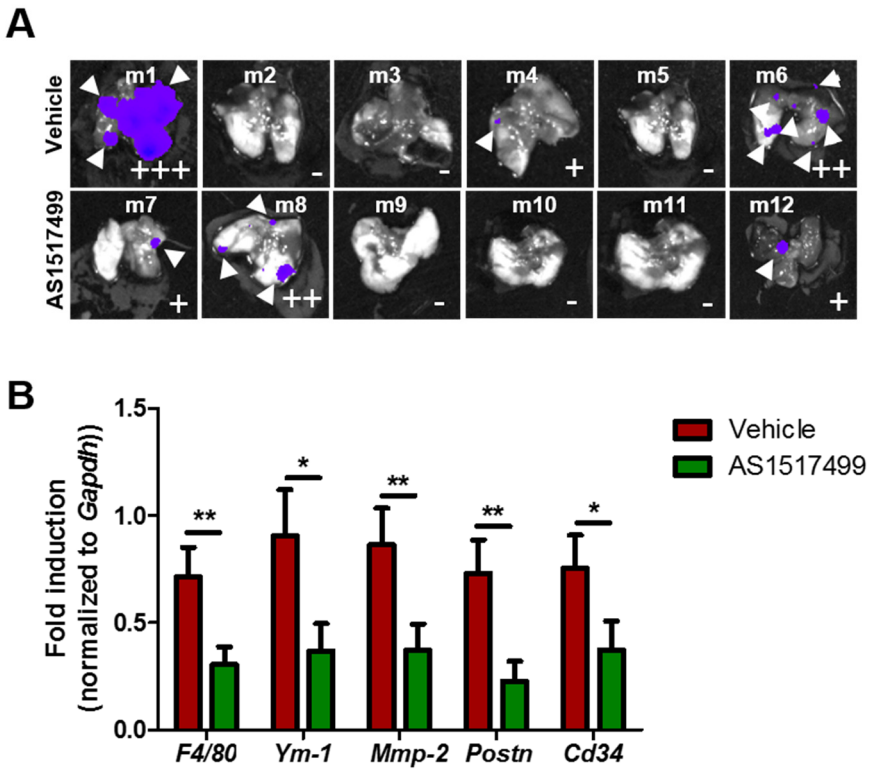

Figure S2: Lung metastasis and macrophage status of animals treated with AS1517499. Animals were treated and analysis was performed as for livers, as described in methods (A) Luminescence of lungs after luciferin injection. Arrowheads indicate metastasis. Metastasis scoring (- no spots; + few spots of low intensity; ++ several spots) for lungs is shown in the lower right corner of each image. (B) Gene expression analysis of macrophage (*F4/80, Ym-1*) and tumor progression markers (*Mmp-2, Postn* and *Cd34*) in lungs of mice bearing tumors during tumor development. Data are shown as mean + SEM, n=5-6 per group, *p<0.05, **p<0.01.

Chapter 6

Liposomal Delivery of AS1517499 for the Specific Targeting to Tumor-Associated Macrophages

Abstract

Tumor-associated macrophages (TAM) possess an M2-like phenotype and play an important role in tumor growth and progression. Current pre-clinical therapies aimed at the treatment of TAM show a lack of specific targeting or effect. We have earlier shown that the Stat6 pathway is activated in TAM and responsible for TAM-induced tumor growth and metastasis. In this research, we combine the specific Stat6 inhibitor AS1517499 into liposomes containing carboxylated lipids (CyPC) for the specific targeting and treatment of TAM. AS1517499 was successfully incorporated into these liposomes and showed adequate stability and release of the drug. We were able to inhibit M2-macrophage related gene expression by using our liposomal preparations. This research is the first step towards the specific targeting and treatment of TAM.

1 Introduction

Macrophages are important cells of the immune system, involved in acute inflammation and wound healing [1-3]. The phenotype of these highly plastic cells is regulated by the signals they receive from the local environment [1, 3]. 'Classically activated' M1 macrophages are present at sites of acute inflammation and show pro-inflammatory and anti-tumor activities [2, 4]. In contrast, 'alternatively activated' M2 macrophages, more involved in the wound healing process, display immunosuppressive and pro-tumoral effects [2-4]. Tumor-associated macrophages (TAMs), resembling the M2 macrophage phenotype, are present in the tumor micro-environment (TME), where they are responsible for immunosuppression, neo-angiogenesis, matrix remodeling and the excretion of growth factors, leading to increased tumor growth, survival and metastasis [5, 6].

Due to the damaging role of TAMs in tumor progression, different strategies, such as inhibition of recruitment and pro-tumoral effects of TAM, have been utilized in the treatment of these cells [7, 8]. Of interest is the pharmacological inhibition of TAM polarization. In previous research, Binnemars-Postma *et al* have shown the Stat6 pathway to be crucial in the differentiation of macrophages towards the M2 (*i.e.* TAM) phenotype [9]. By using the specific Stat6 inhibitor AS1517499, authors were able to inhibit TAM polarization *in vitro*. *In vivo*, the inhibitor reduced tumor growth by approximately 30%. Gene expression analysis of tumors revealed induced levels of CD8 expression, but not of CD4, indicating the reduced tumor growth might be caused by lifting the intra-tumoral immunosuppressive environment. Moreover, metastasis to the livers was decreased in treated animals. Upon investigation of this mechanism, the authors found that markers for macrophages/TAM (*F4/80*, *Mrc-1*, *Ym-1*) and metastasis (*Mmp-2*, *Postn*, *Cd34*) increased during tumor development in livers of untreated animals, but were significantly downregulated in treated animals. These results suggested that inhibition of the Stat6 pathway led to modulation of the pre-metastatic niche, thereby reducing the number of metastasis [9].

Other strategies are aimed at the specific targeting of macrophages. One of the most described methods of inhibiting TAM is the total depletion of TAM using liposomal bisphosphonates [10, 11]. However,

since this method depletes macrophages in general, subpopulations of macrophages, which might be beneficial against tumor growth, such as M1 macrophages are also eliminated. It is therefore crucial to specifically treat TAM, while leaving other macrophage populations intact. By using nanoparticles, functionalized with targeting ligands, this problem may be addressed.

Previous research has shown that TAM display a number of upregulated phagocytic receptors: Cd36, Collectin subfamily member 12 and Scavenger receptor B1. All three receptors are involved in the recognition of oxidized lipids [12-15]. In research performed by Binnemars-Postma *et al*, authors incorporated carboxylated lipids (PAzPC and PGPC) into liposomes and used them to specifically target M2 macrophages. *In vitro* results showed high specificity of PAzPC-containing liposomes for M2 macrophages. *In vivo*, these liposomes displayed superior tumor accumulation (4T1 mouse breast tumor model) and an astounding decrease in liver and spleen accumulation. The authors were able to confirm the involvement of Colec12 and Scarb1, and to a smaller degree Cd36 in this specific M2 macrophage uptake of carboxylated lipids (Chapter 4).

Since these liposomes have been well-characterized and show superior M2 macrophage specificity, they show great promise for TAM-targeted drug delivery. The specific Stat6 inhibitor showed significant reduction in tumor growth, but the effects may be limited due to rapid clearance and low tissue accumulation [16-18]. By incorporating this inhibitor into nanoparticles, we aim to address these challenges. In this chapter, we combine our previous findings about AS1517499 and PAzPC-containing liposomes to develop a new therapeutic strategy for the targeting and inhibition of TAM.

2 Materials & Methods

2.1 Preparation of liposomes

Liposomes were prepared using the ethanol injection technique [19]. Briefly, hydrogenated soy phosphatidylcholine (HSPC, Lipoid GMBH, Germany), carboxylated lipid 1-palmitoyl-2-azelaoyl-sn-glycero-3-phosphocholine (PAzPC, Cayman chemicals, Ann Arbor, MI), cholesterol (Sigma Aldrich) (molar ratio 8:2 HSPC:Cholesterol for HSPC liposomes, 1:7:2 PAzPC:HSPC:Cholesterol for PAzPC liposomes) and where necessary, the lipophilic fluorescent label 1,1′-Dioctadecyl-3,3,3′,3′-tetramethylindocarbocyanine perchlorate (DiI, Sigma Aldrich, St Louis, MO) at a molar ratio of 0.1 of total lipids were dissolved in ethanol and heated at 70 °C. AS1517499 (Axxon Medchem, Groningen, The Netherlands) was dissolved in DMSO, and subsequently dissolved in a 10% 2-hydroxypropyl-β-cyclodextrin (Sigma Aldrich) solution. The heated lipid solution was injected into this 10%/2.2% cyclodextrin/DMSO solution in PBS containing 0.5 mg AS1517499 to create a crude liposomal formulation with a concentration of 8 mM total lipid. The crude liposomal formulation was extruded using the Avestin Liposofast extruder. After preparation, liposomes were dialyzed against PBS using 10 kD cutoff slide-A-lyzers (Thermo Fisher Scientific, Waltham, MA). Liposomal size and PDI (in PBS) were measured using Zetasizer Nano ZS (Malvern, Malvern, UK).

2.2 Analysis of liposomal drug content

Liposomes were prepared as described above. After dialysis, moisture from 50 µl of liposomes was evaporated under nitrogen. Liposomes were dissolved in methanol and vortexed thoroughly. Subsequently, samples were centrifuged at 20.000 rcf for 5 min. Samples were then measured at 261 and 306 nm using ND-1000 Spectrophotometer (NanoDrop, Thermo Fisher Scientific). Sample concentration was determined using AS1517499 calibration curves.

2.3 Liposome stability

Liposomes were diluted 10 times in cell culture medium without serum and incubated at 37 °C for 24 h. Size was determined using the Zetasizer Nano ZS (Malvern). For loss of AS1517499, undiluted samples were incubated in Amicon Ultra tubes (Mw cut-off 30 kD, Sigma Aldrich) in a container containing serum free medium at 37 °C,

under continuous agitation. After 24 h, drug content was determined using UV-Vis as described above.

2.4 Cell culture

Murine RAW264.7 macrophages were obtained from the American Type Culture Collection. The cells were cultured in RPMI-1640 medium, supplemented with 10% FBS, 2 mM L-glutamine (Lonza, Basel, Switzerland), 100 U/ml penicillin and 0.1 mg/ml streptomycin (Sigma Aldrich, St Louis, MO) at 37 °C.

2.5 Macrophage differentiation and treatment

For AS1517499 treatment, 1 x 10^6 RAW264.7 cells/ml were plated in 24- and 96-well plates. After 24h, liposomes were added at a concentration of 1 μM AS1517499 in RPMI medium without FBS. After 16h of liposome incubation, 10 ng/ml IL-4 and IL-13 cytokines were added and liposomes were diluted to 0.5 μM. After 24 h of treatment, cells were lysed for PCR analysis or used in viability and nitric oxide release assays. For the uptake experiments, RAW264.7 cells were plated overnight. Medium was aspirated and cells were incubated for 24 h in complete RPMI medium containing IL-4 and IL-13 at 10 ng/ml (M2 differentiation), or Lipopolysaccharide (LPS, Sigma Aldrich) and IFN-γ (Peprotech) at 100 and 10 ng/ml (M1 differentiation). After incubation, cells were used in uptake experiments.

2.6 Phagocytosis gene array

For analysis of phagocytic receptors, recognition and engulfment, phagosome maturation, phagosome processing and signal transduction, RAW264.7 cells were cultured and differentiated as described in macrophage differentiation. After 24 h of cytokine incubation, cells were lysed and RNA was isolated as described above. Gene expression was analyzed using the RT2 Profiler PCR array for human phagocytosis (Qiagen, Venlo, The Netherlands). Samples were measured using the CFX96 Real-Time PCR detection system (Bio-Rad). Results were analyzed using software (SABioscience, MD, USA) specifically designed for the analysis of Qiagen PCR arrays. Results were normalized using *Gapdh* and expression threshold was set to 3.0.

2.7 Quantitative liposome uptake

RAW264.7 cells were differentiated as described above. DiI-containing liposomes were added at equal fluorescence at a maximum concentration of 125 μM. Cells were incubated for 2 h at 37 °C, after which cells were thoroughly washed. Cells were gently detached using scraping. Cells were then collected and particle uptake was assessed by measuring mean fluorescence intensities in the FL-2 channel for at least 10,000 gated cells, using flow cytometry (BD FACSCalibur, Becton Dickinson, Franklin Lakes, NJ). Gates were set in the FSC vs SSC plot, using untreated control cell populations. For all experiments, identical settings were used. Data was analyzed using Flowing Software 2.5.0.

2.8 Quantitative Real Time PCR

RAW264.7 cells were differentiated and treated as described above. Cells were washed with PBS and then lysed using lysis buffer and total RNA was isolated using GenElute™ Mammalian total RNA isolation kit (Sigma). cDNA was prepared by using iScript cDNA synthesis kit (Bio-Rad, Hercules, CA) and qRT-PCR was performed with 20 ng of cDNA per reaction mixture using SYBR green assay (Bioline, London, UK). Primer sequences are listed in Table 1. Reactions were measured using the CFX384 Real-Time PCR detection system (Bio-Rad). The threshold cycles (Ct) values were calculated and relative gene expression (ddCt method) was analyzed after normalization using the *Gapdh* house-keeping gene.

Gene	Forward (5'→ 3')	Reverse (3'→ 5')	Accession
Arg-1	GTGAAGAACCCACGGTCTGT	CTGGTTGTCAGGGGAGTGTT	NM_007482.3
Gapdh	ACAGTCCATGCCATCACTGC	GATCCACGACGGACACATTG	XM_001476707.3, XM_001479371.4, XM_003946114.1, NM_008084.2
Mrc -1	GGGACGTTTCGGTGGACTGTGG	TTGTGGGCTCTGGTGGGCGA	NM_008625.2

Table 1: Sequences of primers used for gene expression using quantitative real-time PCR.

2.9 Viability and Nitric oxide release

RAW264.7 cells were treated as described above. After liposome incubation, medium was collected for nitric oxide release assay. Briefly, 90 μl of medium was mixed with 180 μl Griess reagent and color was measured at 540 nm. For viability, cells were washed and incubated for 2 h at 37 °C with 10% 110 ug/ml resazurin sodium salt in PBS solution

in RPMI medium without FBS. After incubation, medium was collected and measured using the Victor3 multilabel fluorescence plate reader.

2.10 Statistical analysis

Data are presented as mean + standard error of the mean (SEM). All graphs were created and statistical analysis were performed using Graphpad Prism (Graphpad, La Jolla, CA) using two-sided unpaired student's T-test, unless otherwise specified. Statistical tests were performed with a minimum significance level of $p<0.05$.

3 Results

3.1 Encapsulation of AS1517499 into CyPC-liposomes

In order to target the macrophage modulating drug AS1517499 to TAM, we incorporated this drug into normal and PAzPC-containing liposomes. Since AS1517499 is poorly soluble in water, 2-hydroxypropyl-β-cyclodextrin was used to facilitate its dissolution in water. Figure 1A shows a schematic representation of cyclodextrin-AS1517499 complex in the aqueous core of a liposome. The prepared liposomes all showed a small size (approximately 130 nm) and narrow size distribution (Figure 1B and Table 2). The stability of the liposomal preparations was tested at 37 °C in culture medium for 24 h. We found the HSPC, HSPC-AS and PAzPC formulations to be stable. PAzPC-AS seemed to slightly fluctuate in size. Release of AS1517499 from the liposomal preparations was also investigated (Figure 1D). HSPC-AS liposomes showed a 13% release of AS1517499 after 24 h of incubation at 37 °C in culture medium. PAzPC-AS liposomes showed a 36% release, indicating PAzPC-containing liposomes release drug more easily than normal liposomes.

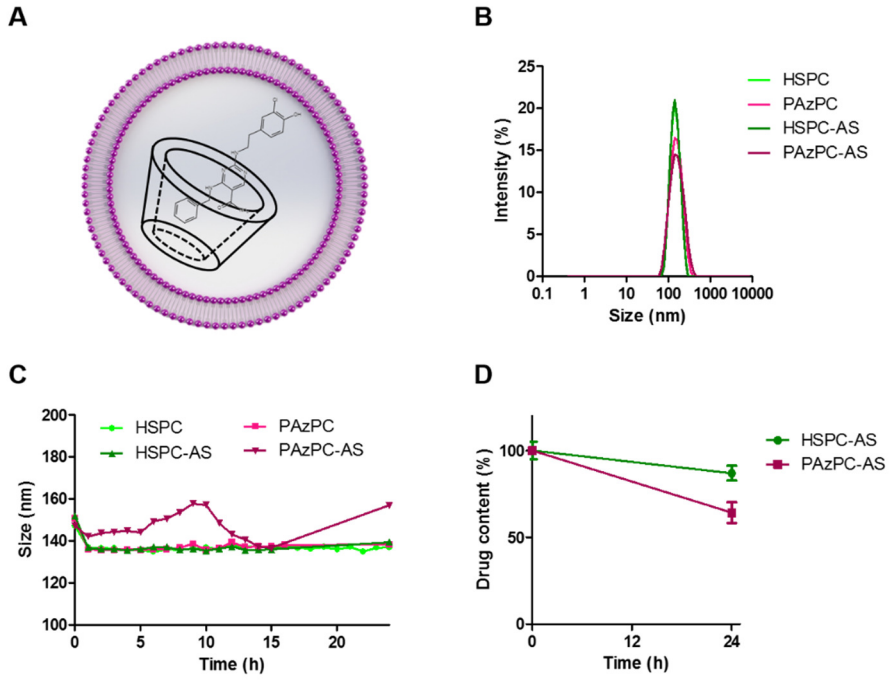

Figure 1: Encapsulation of AS1517499 into PAzPC-containing liposomes. (A) Graphical

representation of AS1517499 encapsulation into liposomes, facilitated by cyclodextrins. (B) Representative graphs of liposomal size distribution. (C) Size stability at 37 °C in medium. (D) AS1517499 content after 24 h of incubation at 37 °C in medium.

	Size (nm, ± SD)	PDI
HSPC	135.0 ± 1	0.07
PAzPC	129.8 ± 1.1	0.07
HSPC-AS	136.7 ± 1.9	0.07
PAzPC-AS	128.1 ± 0.9	0.09

Table 2: Size and Polydispersity Index (PDI) of liposomal preparations

3.2 Effects of AS1517499-containing liposomes on macrophages

To specifically target and treat TAM, we combined the M2-targeting liposomes containing PAzPC and AS1517499, a drug which inhibits M2 macrophage differentiation. To assess the effects of the liposomes and free drug on macrophage toxicity, we performed a cell viability assay after liposome and/or drug incubation. As shown in Figure 2A, none of the liposomal formulations, empty or containing AS1517499, showed any effect on cell viability. To assess whether these liposomes induced nitric oxide release (marker for M1 macrophage differentiation), we assessed its release in M2 differentiated cells (Figure 2B). We found the liposomes, with or without drug, to be unable to switch the differentiation towards the M1 phenotype in the presence of M2-inducing cytokines. When analyzing gene expression levels of M2-related genes (Arg-1 and Mrc-1), a significant decrease in gene expression, compared to empty liposomes, of both genes could be observed (Figure 2C). HSPC liposomes seemed to reduce Arg-1 gene expression slightly, while PAzPC liposomes induced its expression. No additional effects of PAzPC liposomes compared to HSPC liposomes could be detected.

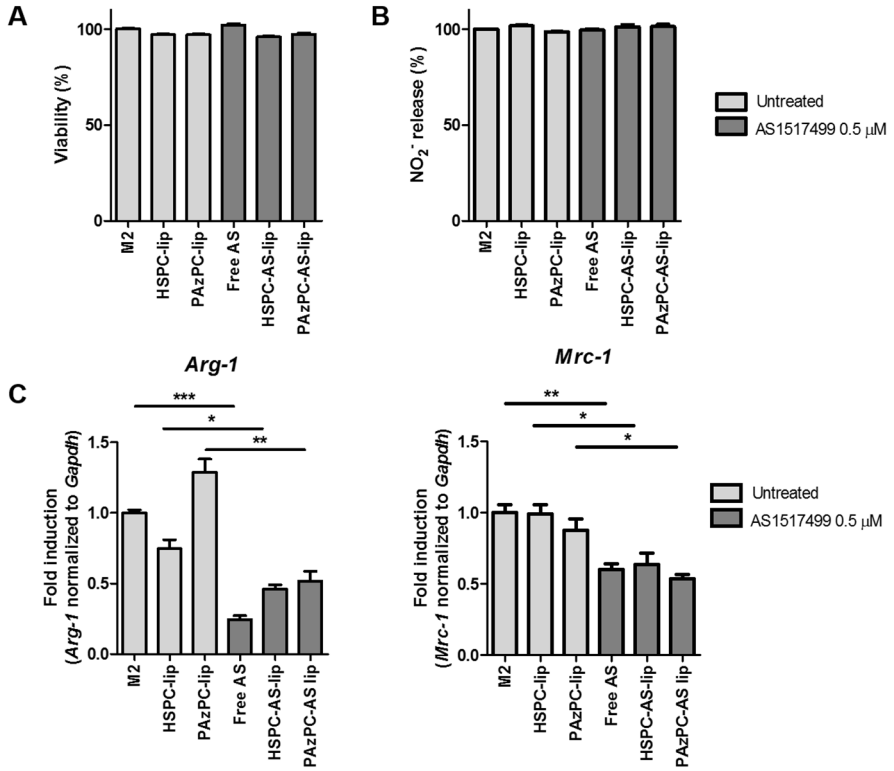

Figure 2: Effect of liposomes on M2 differentiated macrophages. (A) Viability of M2 macrophages, incubated with empty (light grey) or AS1517499-containing (dark grey) liposomes. (B) Nitric oxide release of M2 macrophages, incubated with empty (light grey) or AS1517499-containing (dark grey) liposomes. (C) Gene expression analysis of M2 marker Arg-1 and Mrc-1, when treated with empty (light grey) or AS1517499-containing (dark grey) liposomes. All experiments mean + SEM, n=3.

3.3 Uptake of liposomes by RAW264.7 cells

Since we could not show increased effectiveness of PAzPC-AS liposomes, compared to HSPC-AS liposomes, in order to determine the specificity of HSPC and PAzPC liposomes in differentiated RAW264.7 cells, we incubated the liposomes containing DiI as a fluorescent label at equal fluorescence and measured liposomal uptake using flow cytometry. Quantification of liposomal uptake is shown in Figure 3A and B. HSPC liposomes show low, but equal uptake in M1 and M2 cells. PAzPC liposomes were taken up to much greater extent, but no specificity by M2 cells could be detected. Analysis of phagocytosis-related genes (Figure 4A-C) revealed there were no relevant upregulated phagocytosis receptors in M2 macrophages. M1

macrophages showed some upregulated receptors (*Fas*, *FcγR1*, *Pla2γ4a*, *Siglec1*, *Syk*), unrelated to lipid recognition. These results indicate the RAW264.7 cell line is not suitable to show the differential uptake of carboxylated lipid containing liposomes.

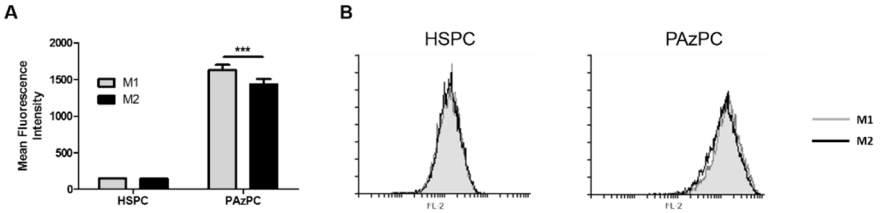

Figure 3: Uptake of liposomes and gene expression of RAW264.7 cells. (A) Uptake of normal (HSPC) and CyPC-containing (PAzPC) liposomes by differentiated RAW264.7 cells. (B) Respresentative FACS histograms of liposomal uptake by M1 and M2 cells. Data are shown as mean + SEM, n=3, ***p<0.001.

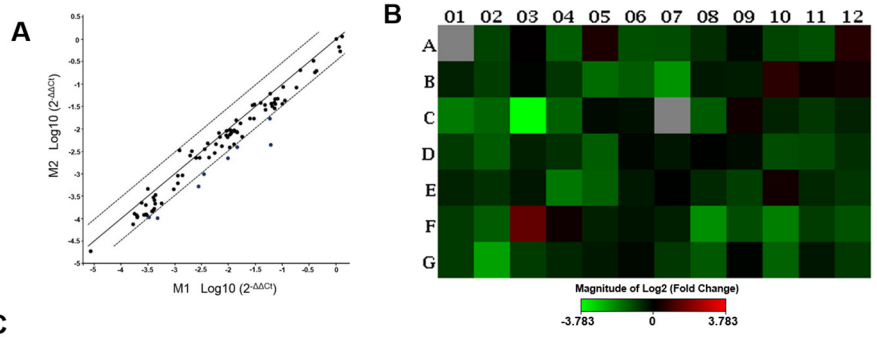

C

Layout	1	2	3	4	5	6	7	8	9	10	11	12
A	Adipoq -1.44	Ager -1.99	Anxa1 1.02	Axl -2.58	C3 1.32	Calr -2.22	Cd14 -2.19	Cd36 -1.58	Cd44 -1.06	Cd47 -2.02	Ceacam3 -2.23	Clec7a 1.47
B	Clic4 -1.39	Cnn2 -1.86	Colec12 -1.04	Crk -1.72	Crp -3.06	Csf1 -2.58	Csf2 -4.62	Csk -1.27	Cyp2s1 -1.34	Dock1 1.54	Dock2 1.13	Elmo1 1.23
C	Fas -3.54	Fcer1g -2.77	Fcgr1 -13.76	Fcgr2b -2.66	Fcgr3 -1.12	Fyn -1.18	Gulp1 -1.44	Ifng -2.53	Il1rl1 1.17	Iqsec1 -1.41	Itgam -1.74	Itgav -1.43
D	Itgb2 -1.83	Lyn -2.51	Mapk14 -1.39	Marco -1.62	Mbl2 -2.58	Mcoln3 -1.06	Mertk -1.25	Mfge8 -1.01	Mif -1.13	Msn -2.19	Myd88 -2.11	Nod1 -1.61
E	Pecam1 -1.43	Pik3cb -1.64	Pip5k1a -1.25	Pla2g4a -3.46	Pla2g5 -2.70	Pld1 -1.27	Pld2 -1.02	Prkce -1.50	Pros1 -1.89	Pten 1.21	Rab5a -1.46	Rab7 -1.70
F	Rac1 -1.82	Rac2 -2.60	Rala 2.71	Ralb 1.16	Rapgef3 -1.38	Rhoa -1.20	Scarb1 -1.37	Serpine1 -4.37	Sftpd -2.19	Siglec1 -3.67	Sirpb1a -1.85	Stab2 -2.32
G	Stx18 -1.82	Syk -5.26	Tgm2 -1.87	Ticam1 -1.47	Tlr3 -1.29	Tlr9 -1.09	Tnf -1.75	Tnfsf11 -2.49	Vamp7 -1.05	Vav1 -2.76	Was -1.25	Wnt5a -1.79

Figure 4: Gene expression analysis of phagocytosis related genes in differentiated M1 and M2 RAW264.7 cells (A) Phagocytosis gene array of differentiated RAW264.7 cells. (B and C) Phagocytosis array heat map (B) and numerical values (C), shown as fold change (M2 vs M1).

4 Discussion

This study combines the two modalities of effectively treating macrophages: on the one hand we utilize a targeting system, specifically designed to interact with TAM. On the other hand, we incorporate a drug into this targeting system, which inhibits the polarization of macrophages towards the TAM-phenotype.

The first step of this research involved the effect of the AS1517499-containing liposomes on the differentiation of macrophages. AS1517499 is a small molecular inhibitor of Stat6, which has been shown to inhibit M2 macrophage differentiation, tumor growth and metastasis [9]. Even though the effects of AS1517499 were clear, the effect on tumor growth and metastasis might be improved. Moreover, although we did not study the pharmacokinetics, Nagashima *et al* reported the effect of intravenous AS1517499 might be limited due to rapid clearance, by conjugation of its hydroxyl group [17, 18]. To increase the therapeutic efficacy of AS1517499 by increasing its circulation time and specifically target TAM, we incorporated the drug into TAM-targeting liposomes.

For encapsulation into liposomes, the physical properties of AS1517499 are unfavorable: it is hardly charged and has very low solubility at pH 7.4 (isoelectric point 7.01, Log P 3.74) [20]. Due to its hydrophobic nature, we first dissolved the drug in dimethylsulfoxide (DMSO) and then diluted this solution in a 10% 2-hydroxypropyl-β-cyclodextrin (2HPβCD) solution. Cyclodextrins (CDs) are water soluble conically shaped molecules, with a hydrophobic core and hydrophilic exterior [21]. Hydrophobic molecules preferentially reside inside the cone, while the drug-CD complex remains water soluble. Due to this dual nature, CDs are particularly suitable as solubility enhancing agents. Moreover, 2HPβCD displays low toxicity [22], and has been used as excipient in marketed pharmaceutical preparations for intravenous administration (Sporanox, MitoExtra) [21]. However, cyclodextrins may destabilize liposomes, by extracting lipids or cholesterol from the lipid bilayer, which replace the drug, resulting in premature release of drug from the liposomes [23]. In our studies, we tested the stability of liposomes and release of drug from the liposomes during 24 h at 37 °C (Figure 1C). Liposomes remained stable in size during this time, however, PAzPC-AS liposomes showed some fluctuation in size. We

found a reduction of 13% (HSPC) and 36% (PAzPC) in AS content (Figure 1D). These results indicate that PAzPC-liposomes are less stable with AS1517499 incorporated. This may account for the greater amount of leakage of AS1517499 from these liposomes, compared to normal liposomes. One possible explanation might be the transfer of AS1517499 between cyclodextrins and the lipid bilayer of liposomes, possibly disturbing and destabilizing the structure of PAzPC-containing bilayers more easily than full HSPC bilayers. Further optimization of AS1517499, cyclodextrin and CyPC content may be necessary to improve the stability of these liposomes.

To investigate the effects of liposomal AS1517499 on TAM differentiation, we incubated the cells with HSPC, PAzPC, HSPC-AS and PAzPC-AS liposomes (Figure 2). We found no effect on viability using any type of liposome, or the free drug (Figure 2A), indicating the liposomes and free drug are not toxic to the cells at the tested concentration. We also investigated the nitric oxide release upon incubation with liposomes (Figure 2B). Nitrite, a stable nitric oxide metabolite, which is used as an index for nitric oxide production [24], was measured using Griess reagent [25]. Nitric oxide release is associated with M1 macrophage differentiation [26], as M1 macrophages express nitric oxide synthase, which metabolizes arginine to nitric oxide and citrulline [27]. Using our liposomes, we found that the liposomes could not revert the M2 macrophages towards the M1 phenotype without any additional stimuli (Figure 2B). We evaluated the effects on M2 macrophage differentiation using gene expression analysis of known M2 markers *arginase-1* (*Arg-1*) and *mannose receptor-1* (*Mrc-1*) (Figure 2C). Here we found that liposomal AS1517499 had a comparable effect to free drug. Although we found the expected inhibition of M2 macrophage differentiation, we did not find increased effectiveness of PAzPC-AS liposomes, compared to HSPC-AS liposomes. Since we could not detect increased effectiveness of PAzPC-AS-containing liposomes, we investigated the uptake of these liposomes in our cell culture model (Figure 3). Although there was a large difference in uptake of HSPC- and PAzPC-containing liposomes (approximately 10-fold increase when using PAzPC-liposomes) using the RAW264.7 cell line, we did not observe the expected differences in uptake of CyPC-containing liposomes by M2 cells, compared to M1 cells, as previously seen in human THP-1 cells and murine bone marrow derived macrophages (BMDM) (Chapter 4). Most surprisingly,

M1 cells even seem to take up more PAzPC-liposomes than M2 cells. Since we have clearly seen the differences in tumor and organ distribution, and the co-localization of CyPC-containing liposomes with $CD206^+$ macrophages (Chapter 4) *in vivo*, we investigated the phagocytic gene expression profile of differentiated M1 and M2 RAW264.7 cells. As can be seen in Figure 4A-C, there are no upregulated phagocytic genes for M2 cells. M1 cells showed several upregulated phagocytosis genes, but none correspond to our previous findings, where the upregulated receptors specifically interacted with oxidized lipids. These results suggest there is a specific mechanism which is responsible for the increased uptake of PAzPC liposomes by M2 cells, which is not present in RAW264.7 cells. Since our previous studies have shown that the CyPC-containing liposomes were taken up to a higher extent by M2 differentiated THP-1 cells and murine BMDMs, the RAW264.7 cell line might not be suitable for these experiments. However, to confirm this, the phagocytic receptors on differentiated BMDM and their involvement in carboxylated lipid uptake remain to be investigated. Another method to confirm the effectiveness of PAzPC-AS-liposomes is to test the formulation *in vivo*.

Drug loading was not optimized in these experiments. In previous studies free drug was dosed at 10 and 20 mg/kg in mice [9]. Although nanoformulations may result in smaller effective dosages, further optimization of AS1517499 content in liposomes may be needed to reach these clinically effective dosages. Moreover, to ensure receptor-ligand interactions between carboxylated lipid tails protruding from the liposomes, we used unPEGylated liposomes, which are known to circulate much more briefly, as compared to PEGylated liposomes [28]. If PEGylation proves to be necessary, we recommend the use of carboxylated lipids conjugated to PEG chains, as to prevent the shielding of these tails by the PEG chains.

5 Conclusion

Although there are still factors to be investigated, this study shows that AS1517499 can be incorporated into PAzPC-containing liposomes and indicate these liposomes are effective in the inhibition of M2 macrophage differentiation. We have taken the first steps in effectively targeting and inhibiting TAM using CyPC-AS liposomes and hope this research may serve as a foundation for further research into this area.

References

1. Patel, U., et al., Macrophage polarization in response to epigenetic modifiers during infection and inflammation. Drug Discov Today, 2017. 22(1): p. 186-193.
2. Wang, N., H. Liang, and K. Zen, Molecular mechanisms that influence the macrophage m1-m2 polarization balance. Front Immunol, 2014. 5: p. 614.
3. Sica, A. and A. Mantovani, Macrophage plasticity and polarization: in vivo veritas. J Clin Invest, 2012. 122(3): p. 787-95.
4. Sica, A., et al., Macrophage polarization in pathology. Cell Mol Life Sci, 2015. 72(21): p. 4111-26.
5. Allavena, P. and A. Mantovani, Immunology in the clinic review series; focus on cancer: tumour-associated macrophages: undisputed stars of the inflammatory tumour microenvironment. Clin Exp Immunol, 2012. 167(2): p. 195-205.
6. Biswas, S.K., P. Allavena, and A. Mantovani, Tumor-associated macrophages: functional diversity, clinical significance, and open questions. Semin Immunopathol, 2013. 35(5): p. 585-600.
7. Binnemars-Postma, K., G. Storm, and J. Prakash, Nanomedicine Strategies to Target Tumor-Associated Macrophages. Int J Mol Sci, 2017. 18(5).
8. Tang, X., et al., Anti-tumour strategies aiming to target tumour-associated macrophages. Immunology, 2013. 138(2): p. 93-104.
9. Binnemars-Postma, K., et al., Targeting the Stat6 pathway in tumor-associated macrophages reduces tumor growth and metastatic niche formation in breast cancer. FASEB Journal, 2017: p. In press.
10. Brown, H.K. and I. Holen, Anti-tumour effects of bisphosphonates--what have we learned from in vivo models? Curr Cancer Drug Targets, 2009. 9(7): p. 807-23.
11. Zeisberger, S.M., et al., Clodronate-liposome-mediated depletion of tumour-associated macrophages: a new and highly effective antiangiogenic therapy approach. Br J Cancer, 2006. 95(3): p. 272-81.
12. Endemann, G., et al., CD36 is a receptor for oxidized low density lipoprotein. J Biol Chem, 1993. 268(16): p. 11811-6.
13. Febbraio, M., et al., Targeted disruption of the class B scavenger receptor CD36 protects against atherosclerotic lesion development in mice. J Clin Invest, 2000. 105(8): p. 1049-56.

14. Gillotte-Taylor, K., et al., Scavenger receptor class B type I as a receptor for oxidized low density lipoprotein. J Lipid Res, 2001. 42(9): p. 1474-82.
15. Ohtani, K., et al., The membrane-type collectin CL-P1 is a scavenger receptor on vascular endothelial cells. J Biol Chem, 2001. 276(47): p. 44222-8.
16. Binnemars-Postma, K.A., et al., Differential uptake of nanoparticles by human M1 and M2 polarized macrophages: protein corona as a critical determinant. Nanomedicine (Lond), 2016. 11(22): p. 2889-2902.
17. Mulder, G.J., Conjugation Reactions In Drug Metabolism: An Integrated Approach1990: Taylor & Francis.
18. Nagashima, S., et al., Synthesis and evaluation of 2-{[2-(4-hydroxyphenyl)-ethyl]amino}pyrimidine-5-carboxamide derivatives as novel STAT6 inhibitors. Bioorg Med Chem, 2007. 15(2): p. 1044-55.
19. Batzri, S. and E.D. Korn, Single bilayer liposomes prepared without sonication. Biochim Biophys Acta, 1973. 298(4): p. 1015-9.
20. ChemAxon. AS1517499 stucture and properties. [cited September 2017]; Available from: https://chemicalize.com.
21. Brewster, M.E. and T. Loftsson, Cyclodextrins as pharmaceutical solubilizers. Adv Drug Deliv Rev, 2007. 59(7): p. 645-66.
22. Gould, S. and R.C. Scott, 2-Hydroxypropyl-beta-cyclodextrin (HP-beta-CD): a toxicology review. Food Chem Toxicol, 2005. 43(10): p. 1451-9.
23. Piel, G., et al., Betamethasone-in-cyclodextrin-in-liposome: the effect of cyclodextrins on encapsulation efficiency and release kinetics. Int J Pharm, 2006. 312(1-2): p. 75-82.
24. Lancaster, J.R., Jr., Simulation of the diffusion and reaction of endogenously produced nitric oxide. Proc Natl Acad Sci U S A, 1994. 91(17): p. 8137-41.
25. Redente, E.F., et al., Lung tumor growth is stimulated in IFN-gamma-/- mice and inhibited in IL-4Ralpha-/- mice. Anticancer Res, 2009. 29(12): p. 5095-101.
26. Kalish, S.V., et al., Macrophages Reprogrammed In Vitro Towards the M1 Phenotype and Activated with LPS Extend Lifespan of Mice with Ehrlich Ascites Carcinoma. Med Sci Monit Basic Res, 2015. 21: p. 226-34.
27. Rath, M., et al., Metabolism via Arginase or Nitric Oxide Synthase: Two Competing Arginine Pathways in Macrophages. Front Immunol, 2014. 5: p. 532.

28. Harris, J.M., N.E. Martin, and M. Modi, Pegylation: a novel process for modifying pharmacokinetics. Clin Pharmacokinet, 2001. 40(7): p. 539-51.

Chapter 7

Summary and Future Perspectives

1 Summary

Breast cancer is a disease which affects 1 in 7 women during their lifetime. With 464.000 new cases and 131.000 deaths, it is the most occurring cancer type and leading cause of cancer related deaths in women in Europe [1]. As the overall age of the population is predicted to increase, these numbers will rise as well. Cytotoxic agents, hormone treatment, radiation and small molecule inhibitors are the current therapies used in the treatment of breast cancer [2]. Although these therapies work well towards the primary tumor, they do not affect the surrounding stromal cells. Tumor growth and survival depend greatly on the support of the tumor micro-environment (TME), where stromal cells promote neo-angiogenesis, matrix remodeling and cause suppression of the adaptive immune system [3, 4]. Macrophages play a major role in these processes. Tumor-associated macrophages (TAM), present in the TME, have been shown to play a crucial role in tumor growth and progression [5]. Therefore, effective treatment of TAM might prove to be a successful treatment strategy in breast cancer therapy. This thesis project aimed to develop a novel nanoparticle-based strategy to target TAM and inhibit their tumor growth promoting activities. A novel drug candidate was identified for such inhibition, and incorporated into a newly designed nanoparticle delivery system, which is able to selectively deliver TAM-modulating drugs to TAM.

In **Chapter 2**, the role of TAM in tumor development is discussed in detail. Different strategies for the modulation of TAM are discussed:

- Inhibiting macrophage recruitment
- Reprogramming TAM towards a more anti-tumoral phenotype
- Initiation of immune response
- Blocking the tumor-promoting functions of TAM
- Depletion of TAM

Often, drug candidates include cytotoxic agents, aimed at the depletion of macrophages. As these therapies are aimed to specifically remove pro-tumoral macrophages, other macrophage populations, which display anti-tumor properties, or perform other critical functions, should not be affected. In order to achieve this, this literature update confirms that TAM-targeted nanoparticles selectively delivering TAM-modulating drugs are an attractive option.

In **Chapter 3**, the functional and biological differences in phagocytosis displayed by M1 and M2 macrophages were investigated. Here, the innate ability of M1 and M2 macrophages to phagocytose different sizes of particles (silica, 50 – 1000 nm), under different conditions was studied. Serum proteins were found to greatly affect the uptake of nanoparticles by M2 macrophages, especially in the larger size range (200 – 1000 nm). Moreover, using gene expression analysis, distinct differences in expression of phagocytosis-related genes between M1 and M2 cells were found, where M2 cells displayed several receptors associated with the recognition of proteins present in the protein corona (Figure 1). From this study, we proposed that M2 macrophages showed higher uptake of silica nanoparticles due to increased expression of phagocytic receptors against protein corona ligands. The knowledge acquired about differential expression of phagocytic receptors expressed by M1 and M2 macrophages was used for the development of M2-targeted delivery system to target TAMs in the next chapter.

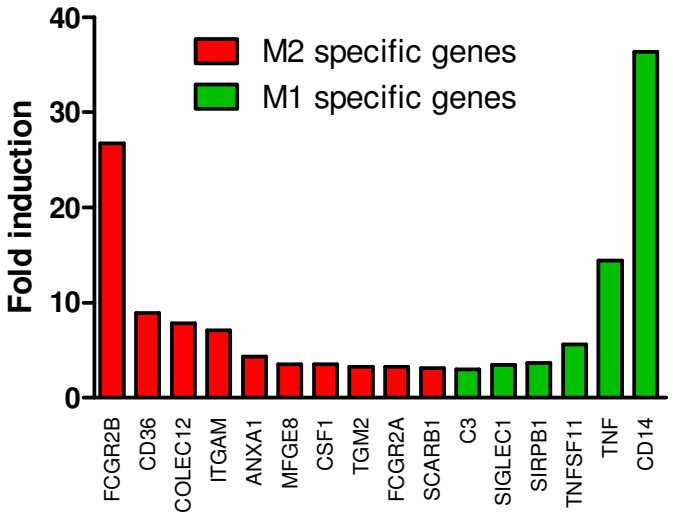

Figure 1: Upregulated phagocytosis-related genes in M2 and M1 cells.

In **Chapter 4**, we found that amongst the upregulated receptors identified in chapter 3 (Figure 1), cluster of differentiation 36 (CD36), scavenger receptor class B1 (Scarb1) and collectin subfamily member 12 (Colec12) are involved in the recognition of oxidized lipids [6-8]. We

explored the possibility of targeting these receptors by using the natural ligands to these receptors, namely carboxylated phosphatidylcholines (CyPC) and incorporated these into liposomes. *In vitro*, significantly more uptake of CyPC-containing liposomes by M2 macrophages, as compared to M1 macrophages was observed with human THP-1 cells and murine bone marrow derived macrophages (BMDM). *In vivo*, enhanced tumor and decreased liver and spleen accumulation were found. Analysis of tumor tissues revealed co-localization of liposomes with the M2 macrophage marker CD206. Analysis of the uptake mechanism revealed that Scarb1 and Colec12 were mainly responsible for the M2-specific uptake of CyPC-containing liposomes. In conclusion, CyPC-containing liposomes showed superior M2-macrophage uptake, increased tumor but decreased liver and spleen accumulation. This research suggests that these M2-targeted nanoparticles may serve as an effective nanoparticle delivery system for the specific delivery of drugs to TAM, given their M2 phenotype.

In **Chapter 5,** we investigated a novel drug for the treatment of TAM. Since TAM (or M2 macrophages) but not other macrophage populations show pro-tumoral effects, we aimed to target a pathway which is specifically upregulated in M2-macrophages. We identified such a pathway by exploring the mechanism of M2 differentiation. After binding of IL-4 and IL-13 (two major cytokines for M2 differentiation) to their common receptor, the signal transducer and activator of transcription 6 (Stat6) becomes activated and regulates the gene transcription of M2-associated genes [9-12]. We investigated the role of Stat6 in macrophage polarization. Stat6 was highly activated in M2 macrophages, while silencing of the *Stat6* gene led to inhibition of M2-macrophage polarization. Using the selective Stat6 inhibitor AS1517499, Stat6 activation and subsequently M2 macrophage differentiation was inhibited pharmacologically. When using this inhibitor *in vivo*, a significant reduction in tumor growth was found. Moreover, less liver metastasis was observed. Upon investigation of the mechanism of action, it was shown that treatment with AS1517499 led to a reduction in genes related to metastatic niche formation. From this study, we conclude that the Stat6 pathway plays an important role in M2-macrophage differentiation. Moreover, we were able to successfully inhibit this pathway, without affecting M1 macrophage populations. *In vivo*, this drug showed promising potential to reduce

tumor growth and metastasis. These data reveal that inhibition of the Stat6 pathways is a promising way to inhibit TAM-driven tumorigenesis and metastasis.

In **Chapter 6**, we combined the knowledge we obtained from the previous chapters, in which we developed CyPC-containing liposomes for M2 specific targeting of AS1517499, the selective M2 inhibitor. We encapsulated AS1517499 into CyPC-containing liposomes and tested the uptake in M2 macrophages *in vitro*. AS1517499-loaded CyPC-containing liposomes inhibited M2 differentiation successfully. However, drug loading and particle stability still need to be improved. Moreover, the effects of this nanoparticle delivery system need to be confirmed *in vivo*. Nevertheless, in this chapter we have taken the first steps towards targeting and inhibiting TAM using a novel nanoparticle drug delivery system.

In conclusion, this thesis has explored the design and development of a novel M2 macrophage targeting system to deliver therapeutic agents to TAM for the treatment of breast cancer. This research gives a better understanding of the interaction between macrophages and nanoparticles, the therapeutic role of the Stat6 pathway in modulating M2 macrophages, and we propose a novel liposome-based TAM-delivery system. Our data suggest that the targeted delivery of a Stat6 inhibitor represents a promising approach in the fight against breast cancer. Altogether, the research from this thesis opens up new opportunities to utilize the TME to achieve improved antitumor responses by targeting and modulate TAM.

2 Future perspectives

In the context of this thesis, we designed a novel nanoparticle-based delivery system which is able to specifically target the M2-inhibiting drug AS1517499 to M2 macrophages for the inhibition of TAM. The results suggest that CyPC-containing liposomes are attractive to reach our goal of inhibition of tumor growth and metastasis, but further optimization is needed.

Factors which remain to be investigated relate to optimization of pharmaceutical formulation properties (like encapsulation efficiency and storage stability)and to demonstration of *in vivo* effectiveness, toxicity and immunogenicity.

The observed *in vivo* results from Chapter 4 suggest the CyPC-containing liposomes may be utilized in the specific targeting of TAM. In chapter 6, our findings indicate that AS1517499-containing CyPC-liposomes are effective in inhibiting TAM differentiation *in vitro*. This should be tested and confirmed *in vivo*. Other models, such as the polyoma middle T oncoprotein murine breast cancer model, in which breast cancer spontaneously occurs, bear more resemblance to the human disease [13]. In such a model dose response and bio-distribution studies are needed to confirm our *in vitro* findings to achieve a better appreciation of the clinical relevance of our newly developed M2-targeted drug delivery system.

Immunogenicity is another important issue to be considered when a nanotherapeutic drug targeting formulation is being developed. Amongst others, hypersensitivity related reactions (referred to as complement activation-related pseudoallergy (CARPA)) have been observed using clinically approved pegylated liposomal formulations, even though pegylated lipids were originally thought to be immunologically inert [14, 15]. Fortunately, premedication and adjustment of infusion rate appear to be efficient ways to prevent such immune responses [16, 17].

Obviously, the drug encapsulation efficiency should be sufficient to allow the administration of clinically relevant doses. As with many nanoformulations, upscaling of the production may prove to be challenging. Long-term stability of the particles should be investigated. Methods such as freeze-drying may be needed to ensure adequate shelf-lifes.

Recently, by inhibiting the colony stimulating factor receptor 1 (CSF-R1), using the small molecular inhibitor BLZ945, Pyonteck *et al* were able to show altered macrophage polarization and inhibition of glioma progression [18]. However, further investigation revealed that in >50% of mice, tumors recurred due to drug resistance [19]. Authors revealed that continuous inhibition of CSF-1R led to increased activity of the phosphatidylinositol 3-kinase (PI3K) pathway, which was driven by upregulation of TAM-derived insulin-like growth factor 1 (IGF-1) and tumor cell IGF-1 receptor, leading to tumor growth and metastasis. By targeting multiple pathways, authors were able to significantly increase survival in mice with recurrent tumors mice. In our research (Chapter

5), we inhibited only a single pathway, by using the Stat6 inhibitor AS1517499. Though we have shown that Stat6 successfully suppresses protumoral TAM activity, it is likely that other mechanisms may also contribute to TAM activation. Moreover, compensation mechanisms, such as seen when inhibiting the CSF-1R might occur. Since all these are complicated processes, involving multiple pathways, *in vitro* results are not sufficient to draw definite conclusions yet.

Despite the early status of our research and the many aspects to be investigated, the encapsulation of TAM-modulating molecules into TAM-targeted nanoparticles deserves further future experimentation, as - shown in Chapter 5 -, tumor growth and metastasis were reduced in tumor-bearing animals. Since cancer related deaths mainly occur due to metastatic disease, preventing metastasis formation is of great benefit to cancer patients [20]. By inhibiting TAM through targeting of the Stat6 pathway, our results indicate that the modulation of the pre-metastatic niche results in reduced metastatic burden. Our novel nanoformulation may be applied in combination with chemotherapy, radiation therapy and primary tumor resection. In the future, combinatorial approaches involving nanoformulations targeting the TME may prove very useful in increasing patient survival. Moreover, next to breast cancer, the application of this therapy may be extended to other cancer types, in which TAM promote tumor growth and metastasis.

References

1. Ferlay, J., et al., *Cancer incidence and mortality patterns in Europe: estimates for 40 countries in 2012*. Eur J Cancer, 2013. **49**(6): p. 1374-403.
2. Robinson, A.G., C.M. Booth, and E.A. Eisenhauer, *Progression-free survival as an end-point in solid tumours--perspectives from clinical trials and clinical practice*. Eur J Cancer, 2014. **50**(13): p. 2303-8.
3. Mantovani, A., et al., *Cancer-related inflammation*. Nature, 2008. **454**(7203): p. 436-44.
4. Quail, D.F. and J.A. Joyce, *Microenvironmental regulation of tumor progression and metastasis*. Nat Med, 2013. **19**(11): p. 1423-37.
5. Allavena, P. and A. Mantovani, *Immunology in the clinic review series; focus on cancer: tumour-associated macrophages: undisputed stars of the inflammatory tumour microenvironment*. Clin Exp Immunol, 2012. **167**(2): p. 195-205.
6. Serbulea, V., D. DeWeese, and N. Leitinger, *The effect of oxidized phospholipids on phenotypic polarization and function of macrophages*. Free Radic Biol Med, 2017. **111**: p. 156-168.
7. Gillotte-Taylor, K., et al., *Scavenger receptor class B type I as a receptor for oxidized low density lipoprotein*. J Lipid Res, 2001. **42**(9): p. 1474-82.
8. Ohtani, K., et al., *The membrane-type collectin CL-P1 is a scavenger receptor on vascular endothelial cells*. J Biol Chem, 2001. **276**(47): p. 44222-8.
9. Sica, A. and A. Mantovani, *Macrophage plasticity and polarization: in vivo veritas*. J Clin Invest, 2012. **122**(3): p. 787-95.
10. Nelms, K., et al., *The IL-4 receptor: signaling mechanisms and biologic functions*. Annu Rev Immunol, 1999. **17**: p. 701-38.
11. Wang, N., H. Liang, and K. Zen, *Molecular mechanisms that influence the macrophage m1-m2 polarization balance*. Front Immunol, 2014. **5**: p. 614.
12. Pauleau, A.L., et al., *Enhancer-mediated control of macrophage-specific arginase I expression*. J Immunol, 2004. **172**(12): p. 7565-73.
13. Lin, E.Y., et al., *Progression to malignancy in the polyoma middle T oncoprotein mouse breast cancer model provides a reliable model for human diseases*. Am J Pathol, 2003. **163**(5): p. 2113-26.

14. Kohli, A.G., et al., *Designer lipids for drug delivery: from heads to tails*. J Control Release, 2014. **190**: p. 274-87.
15. Jiskoot, W., et al., *Immunological risk of injectable drug delivery systems*. Pharm Res, 2009. **26**(6): p. 1303-14.
16. Szebeni, J., et al., *Activation of complement by therapeutic liposomes and other lipid excipient-based therapeutic products: prediction and prevention*. Adv Drug Deliv Rev, 2011. **63**(12): p. 1020-30.
17. Szebeni, J. and G. Storm, *Complement activation as a bioequivalence issue relevant to the development of generic liposomes and other nanoparticulate drugs*. Biochem Biophys Res Commun, 2015. **468**(3): p. 490-7.
18. Pyonteck, S.M., et al., *CSF-1R inhibition alters macrophage polarization and blocks glioma progression*. Nat Med, 2013. **19**(10): p. 1264-72.
19. Quail, D.F., et al., *The tumor microenvironment underlies acquired resistance to CSF-1R inhibition in gliomas*. Science, 2016. **352**(6288): p. aad3018.
20. Gupta, G.P. and J. Massague, *Cancer metastasis: building a framework*. Cell, 2006. **127**(4): p. 679-95.

APPENDICES

NEDERLANDSE SAMENVATTING

DANKWOORD

PUBLICATIES

NEDERLANDSE SAMENVATTING

Borstkanker treft gedurende het leven 1 op de 7 vrouwen. Met 464.000 nieuwe diagnoses en 131.000 sterfgevallen, is het de meest voorkomende type kanker en de voornaamste kanker-gerelateerde doodsoorzaak bij vrouwen in Europa [1]. Omdat de gemiddelde leeftijd van de populatie de komende jaren zal stijgen, wordt verwacht dat de genoemde aantallen ook omhoog zullen gaan. De huidige therapieën die worden toegepast bij de behandeling van borstkanker zijn chemotherapie, hormoonbehandelingen, bestraling en toepassing van laag-moleculaire remmers [2]. Hoewel deze therapieën goed werken tegen de primaire tumor, hebben ze geen effect op de omliggende stroma cellen. Tumorgroei en metastase zijn zeer afhankelijk van de ondersteuning van de tumor micro-omgeving. Hierin bevorderen stromale cellen de groei van nieuwe bloedvaten, herstructurering van het weefsel en onderstukken het adaptieve immuunsysteem [3, 4]. Macrofagen spelen een belangrijke rol in deze processen. Van tumor geassocieerde macrofagen (TAM), die aanwezig zijn in de tumor micro-omgeving, is aangetoond dat ze een cruciale rol spelen in tumorgroei en metastase [5]. Hierdoor zou de effectieve behandeling van TAM een goede strategie zijn voor het behandelen van borstkanker. In dit proefschrift wordt geprobeerd om TAM te targeten en hun tumor-bevorderende eigenschappen te remmen door middel van een nieuwe, op nanodeeltjes gebaseerde methode. Een nieuw geneesmiddel is gevonden voor deze remming en is geïntegreerd in nieuw ontwikkelde nanodeeltjes die in staat zijn om selectief het geneesmiddel aan TAM te bezorgen.

In **Hoofdstuk 2** wordt de rol van TAM in de ontwikkeling van tumoren in detail besproken. Verschillende strategieën voor het moduleren van TAM worden besproken:

- Het remmen van de aantrekking van macrofagen
- Het reprogrammeren van TAM richting een meer anti-tumor fenotype
- Het initiëren van een immuunrespons
- Het blokkeren van tumor-bevorderende activiteiten van TAM
- Het verwijderen van TAM

Vaak bestaan geneesmiddelen uit chemotherapeutische middelen, die zich richten op het verwijderen van macrofagen. Omdat deze therapieën zijn bedoeld om specifiek TAM te verwijderen, moeten andere types macrofagen, die anti-tumor eigenschappen hebben of andere kritische processen uitvoeren niet worden beïnvloed. Om dit te behalen bevestigt dit literatuuroverzicht dat nanodeeltjes die specifiek TAM targeten en een TAM-inhiberend geneesmiddel afleveren een veelbelovende optie zijn.

In **Hoofdstuk 3** worden de functionele en biologische verschillen in fagocytose door M1 en M2 macrofagen onderzocht. Het vermogen van M1 en M2 macrofagen om deeltjes van verschillende groottes (silica nanodeeltjes 50 – 1000 nm) op te nemen onder verschillende omstandigheden is onderzocht. De aanwezigheid van eiwitten uit serum bleek een groot effect te hebben op de opname van deeltjes door M2 macrofagen, vooral voor de grotere deeltjes (200- 1000 nm). Door middel van genexpressie analyse werden duidelijke verschillen in fagocytose-gerelateerde genen gevonden tussen M1 en M2 cellen. M2 cellen lieten verschillende receptoren zien die geassocieerd zijn met de herkenning van eiwitten uit de eiwit corona die aanwezig is rondom nanodeeltjes. Door deze studie stellen we voor dat M2 macrofagen een grotere opname van silica nanodeeltjes laten zien door de verhoogde expressie van fagocytose receptoren die specifiek zijn voor de eiwitten uit de eiwit corona. De kennis die is opgedaan over de verschillende expressie van fagocytose-gerelateerde receptoren tussen M1 en M2 cellen is gebruikt bij de ontwikkeling van een tegen M2-gerichte nanodeeltjes systeem wat gebruikt wordt om TAM te targeten.

In **Hoofdstuk 4** vonden we tussen de geïdentificeerde receptoren uit het vorige hoofdstuk dat CD36, Scarb1 en Colec12 betrokken zijn bij de herkenning van geoxideerde lipiden [6-8]. We onderzochten of we deze receptoren konden targeten door middel van hun natuurlijke ligand, namelijk gecarboxyleerde fosfatidylcholines (CyPC) en hebben deze geïntegreerd in liposomen. *In vitro* werd er meer opname van CyPC-bevattende liposomen waargenomen bij M2 cellen, vergeleken met M1 cellen in humane THP-1 macrofagen en muizenmacrofagen afkomstig uit het beenmerg (BMDM). *In vivo* werd verhoogde tumor en verlaagde lever en milt opname van CyPC-bevattende liposomen waargenomen. Analyse van tumor weefsel liet zien dat de liposomen geco-lokaliseerd waren met macrofagen die positief waren voor de M2 marker CD206.

Analyse van het opname mechanisme liet zien dat de receptoren Scarb1 en Colec12 een voorname rol spelen in de specifieke M2 opname van CyPC-bevattende liposomen. Samenvattend lieten CyPC-bevattende liposomen een grotere opname door M2 cellen, een grotere tumor opname en een verlaagde lever en milt opname zien. Dit onderzoek suggereert dat deze M2 getargete nanodeeltjes een effectieve manier zijn om geneesmiddelen specifiek af te leveren aan TAM, door hun M2 fenotype.

In **Hoofdstuk 5** hebben we een nieuw geneesmiddel voor de behandeling van TAM onderzocht. Omdat TAM (of M2 macrofagen), maar niet andere types macrofagen pro-tumor effecten laten zien, hebben we geprobeerd een signaalpad te remmen wat specifiek is geactiveerd in M2 macrofagen. We hebben dit signaalpad gevonden door het mechanisme van differentiatie van M2 macrofagen te onderzoeken. Na het binden van IL-4 en IL-13 (twee belangrijke cytokines voor M2 differentiatie) aan hun gemeenschappelijke receptor, wordt signal transducer and activator of transcription 6 (Stat6) actief en reguleert het de gen transcriptie van M2-gerelateerde genen [9-12]. We onderzochten de rol van Stat6 in macrofaagdifferentiatie. Stat6 was zeer actief in M2 macrofagen, terwijl gene silencing van het Stat6 gen tot een inhibitie van M2-macrofaag differentiatie leidde. Door gebruik te maken van de laag-moleculaire remmer van Stat6 AS1517499 konden Stat6 activatie en vervolgens M2 macrofaagdifferentiatie farmacologisch worden geremd. Toen de inhibitor *in vivo* werd getest, vonden we een significante remming van tumorgroei. Daarnaast vonden we minder lever metastases. Bij onderzoek naar het werkingsmechanisme, lieten we zien dat de behandeling met AS1517499 leidde tot een vermindering van genen die gerelateerd zijn aan de metastatic niche formatie. Uit deze studie konden we concluderen dat Stat6 een belangrijke rol speelt in M2 macrofaagdifferentiatie. Daarnaast konden we dit signaalpad succesvol remmen, zonder dat het invloed had om M1 macrofagen. *In vivo* liet dit geneesmiddel veel potentie zien voor het verminderen van tumorgroei en metastase. Deze data laten zien dat het remmen van het Stat6 signaalpad een veelbelovende manier is om de M2-gedreven tumorgroei en metastase te remmen.

In **Hoofdstuk 6** combineren we de kennis die is opgedaan uit de vorige hoofdstukken. In dit hoofdstuk ontwikkelden we CyPC

liposomen voor het specifieke targeten van M2 macrofagen met AS1517499, de selectieve M2-remmer. We integreerden AS1517499 in deze liposomen en testten hun opname *in vitro*. AS1517499-geladen liposomen waren succesvol in het remmen van M2 macrofaagdifferentiatie. Echter, belading en de deeltjes stabiliteit moeten nog worden verbeterd. Daarnaast moeten de effecten van de beladen nanodeeltjes nog worden bevestigd *in vivo*. Desalniettemin nemen we in dit hoofdstuk de eerste stappen richting en targeten en remmen van TAM door middel van een nanodeeltjes systeem.

Samenvattend, in dit proefschrift onderzoeken we het ontwerp en de ontwikkeling van een nieuw M2-macrofaag getarget systeem voor het afleveren van therapeutische stoffen aan TAM voor de behandeling van borstkanker. Dit onderzoek geeft meer inzicht in de interactie van macrofagen met nanodeeltjes, de therapeutische rol van Stat6 bij het moduleren van M2 macrofagen en stellen we een nieuw op liposomen gebaseerd TAM getarget systeem voor. Onze data suggereren dat de gerichte bezorging van een Stat6 remmer een veelbelovende manier is om borstkanker te bestrijden. Alles samengenomen opent het onderzoek uit dit proefschrift nieuwe mogelijkheden voor het gebruiken van de tumor micro-omgeving om een verbeterde anti-tumor respons te bereiken voor middel van het remmen van TAM.

1. Ferlay, J., et al., *Cancer incidence and mortality patterns in Europe: estimates for 40 countries in 2012*. Eur J Cancer, 2013. **49**(6): p. 1374-403.
2. Robinson, A.G., C.M. Booth, and E.A. Eisenhauer, *Progression-free survival as an end-point in solid tumours--perspectives from clinical trials and clinical practice*. Eur J Cancer, 2014. **50**(13): p. 2303-8.
3. Mantovani, A., et al., *Cancer-related inflammation*. Nature, 2008. **454**(7203): p. 436-44.
4. Quail, D.F. and J.A. Joyce, *Microenvironmental regulation of tumor progression and metastasis*. Nat Med, 2013. **19**(11): p. 1423-37.
5. Allavena, P. and A. Mantovani, *Immunology in the clinic review series; focus on cancer: tumour-associated macrophages: undisputed stars of the inflammatory tumour microenvironment*. Clin Exp Immunol, 2012. **167**(2): p. 195-205.
6. Gillotte-Taylor, K., et al., *Scavenger receptor class B type I as a receptor for oxidized low density lipoprotein*. J Lipid Res, 2001. **42**(9): p. 1474-82.
7. Ohtani, K., et al., *The membrane-type collectin CL-P1 is a scavenger receptor on vascular endothelial cells*. J Biol Chem, 2001. **276**(47): p. 44222-8.
8. Serbulea, V., D. DeWeese, and N. Leitinger, *The effect of oxidized phospholipids on phenotypic polarization and function of macrophages*. Free Radic Biol Med, 2017. **111**: p. 156-168.
9. Nelms, K., et al., *The IL-4 receptor: signaling mechanisms and biologic functions*. Annu Rev Immunol, 1999. **17**: p. 701-38.
10. Pauleau, A.L., et al., *Enhancer-mediated control of macrophage-specific arginase I expression*. J Immunol, 2004. **172**(12): p. 7565-73.
11. Sica, A. and A. Mantovani, *Macrophage plasticity and polarization: in vivo veritas*. J Clin Invest, 2012. **122**(3): p. 787-95.
12. Wang, N., H. Liang, and K. Zen, *Molecular mechanisms that influence the macrophage m1-m2 polarization balance*. Front Immunol, 2014. **5**: p. 614.

DANKWOORD

Hoewel dit proefschrift mijn werk vertegenwoordigt, had ik het niet voor elkaar kunnen krijgen zonder de hulp en aanmoediging van vele personen. In dit dankwoord wil ik jullie dan ook graag persoonlijk bedanken.

Jai, ik was jouw eerste PhD student in het Targeted Therapeutics lab. Het starten van een nieuw lab was een leuke en spannende uitdaging! Niet alleen mocht ik meewerken aan het opzetten van het lab, maar ook alle experimenten mocht ik zelf bedenken en uitvoeren. Hoewel ik soms moe werd van 'het wiel (telkens opnieuw) uitvinden', heb ik ontzettend veel geleerd en ben ik dankbaar dat ik deel mocht uitmaken van dit bijzondere team. Ik bedank jou voor je begeleiding en steun tijdens dit mooie (en soms frustrerende) traject!

Gert, zonder jou was ik nooit in de bij UT en dus de Targeted Therapeutics vakgroep terecht gekomen. Dankzij jouw vak Nanomedicine, wat ik als student heb gevolgd aan de UU, ben ik in contact gekomen met jou en de wereld van nanomedicijnen. Daarnaast kon ik dankzij jou beginnen aan mijn promotietraject op de UT. Ik wil je heel erg bedanken voor jouw geloof in mij en de ondersteuning die je hebt geboden tijdens mijn promotie onderzoek.

I would like to thank my **committee members** Prof. Dr. H.B.J. Karperien, Prof. Dr. P.C.J.J. Passier, Prof. Dr. R. Schiffelers, Prof. Dr. M.P.J. de Winther, Dr. P. van Hoogevest and Dr. J.M. Metselaar for their willingness to read and approve my thesis and for participating in my defense ceremony.

Iris, wat ben ik blij dat jij er was. Ik heb genoten van je gezelschap, niet alleen tijdens werk, maar ook (en nog steeds) daarbuiten. Zonder jouw enthousiasme en vrolijkheid had mijn PhD er heel anders uitgezien! Ook al ga ik nu elders aan de slag, hoop ik dat we nog heel lang vrienden blijven!

Ruchi, thank you for being my friend and helping me out in the lab. Without your guidance, I would have made countless more mistakes and would have had to repeat experiments infinitely before getting them right. Your know-how has gotten me through this.

Hetty, ik heb ontzettend veel geluk gehad dat jij mij hebt geholpen met het maken en analyseren van de liposomen. Zonder jouw inzet en enthousiasme had ik het nooit af gekregen. Dankjewel!

Karin Roelofs, naast onze gezellige gesprekken wil ik je graag bedanken voor jouw hulp bij mijn eerste FACS experimenten en de injecties van liposomen bij muizen.

Karin Hendriks, ik wil jou graag bedanken voor alle ondersteuning die je me over de jaren, maar vooral tijdens het afronden van mijn promotie hebt gegeven. Op jou kan ik altijd vertrouwen!

Bart, ik wil jou graag bedanken voor jouw input, leuke discussies en spectaculaire reisverslagen tijdens de start van mijn PhD. Ik vond het altijd erg gezellig wanneer jij weer in Twente was!

Dwi, Praneeth, Jonas, Acarilia, Saleh, Tushar, Dhadhang and Deby, I want to thank you for the good times we have had in the TT-lab, during outings and conferences. I wish you all the best for the future and your careers!

Zlata, Lydia, Marc, Yvonne en Kirsten, bedankt voor alle hulp die jullie mij hebben geboden bij het uitvoeren van mijn experimenten en de zaken daaromheen!

I would like to thank all other **members of the BST group** for their enthusiasm and drive to make the BST group the BEST group at UT. I could not have wished for a more welcoming and helpful team and am glad for your support. Good luck to all of you!

I would like to thank my **paranimphs** Iris and Ruchi for their support and friendship during the last stages of my PhD and defense. I am thankful to you for sharing your experience with me and experiencing this event with you ☺

Ik wil graag mijn **familie en vrienden** bedanken voor jullie ondersteuning, gezelligheid en gezelschap. Jullie hielpen mij om even mijn gedachten te verzetten en met een frisse blik verder te gaan!

Stefan, zonder jouw liefde, ondersteuning en begrip had ik mijn PhD niet af kunnen maken. Je hebt me door moeilijke tijden heen geholpen en met me gevierd wanneer het goed ging. Jij stimuleerde me om door te gaan en het beste uit mezelf naar boven te halen. Samen hebben we

veel mooie dingen mogen meemaken in de afgelopen 5 jaar. Zo zijn we getrouwd, verhuisd en hebben we ons eerste kindje Thijs mogen verwelkomen. Ik ben ontzettend blij met jou in mijn leven en zou je voor geen goud willen missen!

Thijs, elke dag kijk ik weer uit naar jouw lieve lach en ondeugende streken. Ik kan niet wachten tot je weer naar me toe komt om even een knuffel te halen! Dankzij jou besef ik hoe kostbaar tijd is en kan ik van elk moment genieten!

Karin

PUBLICATIES

This thesis is based on the following publications:

1. K. Binnemars-Postma, G. Storm, and J. Prakash, *Nanomedicine Strategies to Target Tumor-Associated Macrophages*. Int J Mol Sci, 2017. **18**(5). **(Chapter 2)**

2. K. Binnemars-Postma, H.W. Ten Hoopen, G. Storm, and J. Prakash, *Differential uptake of nanoparticles by human M1 and M2 polarized macrophages: protein corona as a critical determinant*. Nanomedicine (Lond), 2016. **11**(22): 2889-2902. **(Chapter 3)**

3. K. Binnemars-Postma, R. Bansal, G. Storm, and J. Prakash, *Targeting the Stat6 pathway in tumor-associated macrophages reduces tumor growth and metastatic niche formation in breast cancer*. FASEB J, 2017. **(Chapter 5)**

CONFERENTIES

Work from this thesis was represented at the following conferences and meetings:

1. MIRA evaluation day 2013. Poster presentation: *Differential uptake of lipid nanoparticles by differentiated tumor-associated macrophages.*
2. Figon Dutch Medicine Days 2014. Poster and oral presentation: *Targeting the Stat6 pathway to inhibit tumor-associated macrophages.*
3. MIRA day 2014. Poster presentation: *Differential targeting and inhibition of tumor-associated macrophages.*
   Winner of poster prize.
4. European Cancer Congress 2015. Poster presentation: *Targeting the Stat6 pathway to inhibit tumor-associated macrophages-induced tumor growth and metastasis in breast cancer.*

5. Figon Dutch Medicine Days 2015. Poster presentation: *Targeting the Stat6 pathway to inhibit tumor-associated macrophages-induced tumor growth and metastasis in breast cancer*.
6. European Symposium on Controlled Drug Delivery 2016. Poster presentation: *Interaction of silica nanoparticles with human M1 and M2 polarized macrophages*.
7. 2nd EACR-OECI Conference 2017: Making it Personal. Poster presentation: *Targeting the Stat6 pathway to inhibit tumor-associated macrophages-induced tumor growth and metastasis in breast cancer*.